Technische Universität München

Lehrstuhl für Ökologische Chemie und Umweltanalytik

Novel tools and methods for the high resolution analysis of bacterial signalling molecules in complex matrices

Matthias Englmann

Vollständiger Abdruck der von der Fakultät Wissenschaftszentrum Weihenstephan für Ernährung, Landnutzung und Umwelt der Technischen Universität München zur Erlangung des akademischen Grades eines Doktors der Naturwissenschaften genehmigten Dissertation.

Vorsitzender: Univ.-Prof. Dr. W. Huber

Prüfer der Dissertation:
1. Priv.-Doz. Dr. (INPL Vandoevre-les-Nancy/Frankreich) Ph. Schmitt-Kopplin
2. Univ.-Prof. Dr. Dr. h. c. (Zonguldak Univ./Türkei) H. Parlar

Die Dissertation wurde am 08.11.2007 bei der Technischen Universität München eingereicht und durch die Fakultät Wissenschaftszentrum Weihenstephan für Ernährung, Landnutzung und Umwelt am 04.02.2008 angenommen.

I would like to thank…

… first of all Philippe Schmitt-Kopplin for the investment of time, his interest in my work, for many good ideas, an always open door and always open ears

… Istvan Gebefügi for building many bridges which were very helpful in many ways

… Agnes Fekete and Moritz Frommberger for the introduction into the analytical techniques, for their time, their patience and many good ideas

… the people without whom…: Heinz Frisch, Wolfgang Dietz and Peter Streitenberger not only for precise technical fabrications but also for their passion, good ideas and the investment of their wide experiences

… for successful cooperations: Prof. Anton Hartmann, Christina Kuttler, Christine Götz and everybody else in the GSF rhizosphere project, as well as Veronika Fekete and Prof. Jenoe Fekete

… my father, Helmut Englmann for some help with physics questions

… Prof. Wilfried Huber and Prof. Harun Parlar for their agreement to be part of the examination board

… all friends and colleagues in the working group for the good atmosphere during and after work as well as for their helpfulness. Heidi Neumeir is especially acknowledged for the transport of larger amounts of food over the years

… all artists featured on my mp3-player for mental support during routine work

… and last but not least Cornelia Hoffmann for her support and much more.

The dissertation was prepared from August, 1st 2004 to October 31st 2007 at the Institute of Ecological Chemistry at the GSF National Research Center for Environment and Health in the Helmholtz Association in Neuherberg.

Publications

Articles:

[I] **M. Englmann**, A. Fekete, I. Gebefügi Ph. Schmitt-Kopplin: The dosage of small volumes for chromatographic quantifications using a drop-on-demand dispenser system; *Analytical and Bioanalytical Chemistry* 2007, *388,* 1109-1116

[II] **M. Englmann**, A. Fekete, Ch. Kuttler, M. Frommberger, X. Li, I. Gebefügi, J. Fekete, Ph. Schmitt-Kopplin: The hydrolysis of unsubstituted N-acylhomoserine lactones to their homoserines metabolites. Analytical approaches using Ultra Performance Liquid Chromatography; *Journal of Chromatography A* 2007, *1160,* 184-193

[III] Ph. Schmitt-Kopplin, **M. Englmann**: Capillary electrophoresis – mass spectrometry: Survey on developments and applications 2003 – 2004; *Electrophoresis* 2005, *26*, 1209-1220

[IV] A. Gaspar, **M. Englmann,** A. Fekete, M. Harir, Ph. Schmitt-Kopplin: Trends in Capillary Electrophoresis – Mass Spectrometry 2005 – 2006; *Electrophoresis* 2008, *in press*

[V] X. Li, A. Fekete, **M. Englmann**, M. Frommberger, S. Lv, G. Chen, Ph. Schmitt-Kopplin: At-line coupling of UPLC to chip-electrospray-FTICR-MS; *Analytical and Bioanalytical Chemistry* 2007, *in press*

[VI] A. Fekete, M. Rothballer, M. Frommberger, X. Li, **M. Englmann**, J. Fekete, A. Hartmann, L. Eberl, Ph. Schmitt-Kopplin: Identification of bacterial N-acylhomoserine lactones (AHL) with a combination of ultra-performance liquid chromatography (UPLC), ultra-high-resolution mass spectrometry and in situ biosensors; *Analytical and Bioanalytical Chemistry* 2007, *387*, 455-467

[VII] X. Li, A. Fekete, **M. Englmann**, C. Götz, M. Rothballer, M. Frommberger, K. Buddrus, J. Fekete, C.Cai, P. Schröder, A. Hartmann, G. Chen, Ph. Schmitt-Kopplin: Development and application of a method for the analysis of N-acylhomoserine lactones by solid-phase extraction and ultra high pressure liquid chromatography; *Journal of Chromatography A* 2006, *1134*, 186-193

[VIII] M. Frommberger, N. Hertkorn**, M. Englmann**, S. Jakoby, A. Hartmann, A. Kettrup, Ph. Schmitt-Kopplin: Analysis of N-acylhomoserine lactones after alkaline hydrolysis and anion-exchange solid-phase extraction by capillary zone electrophoresis-mass spectrometry *Electrophoresis* 2005, *26*, 1523-1532

[IX] Ch. Götz, A. Fekete, I. Gebefugi, S.T. Forczek, K. Fuksová, X. Li, **M. Englmann**, M. Gryndler, A. Hartmann, M. Matucha, Ph. Schmitt-Kopplin, P. Schröder: Uptake, degradation and chiral discrimination of N-Acyl-D/L-homoserine lactones in barley (*Hordeum vulgare*) and Yam bean (*Pachyrhizus erosus*) plants; *Analytical and Bioanalytical Chemistry* 2007, *in press*

[X] X. Li, J. Fekete, A. Fekete, **M. Englmann**, F. Yang, G. Chen, Ph. Schmitt-Kopplin: Optimization of Gradient Elution in UPLC; a Core Study on the Separation of

Homoserine Lactones Produced by Bukholderia Ubonensis and Structure Confirmation with Ultra High Resolution Mass Spectrometry. *J Liq Chromatogr R T* 2007, *in press*

Book chapters

M. Englmann, M. Frommberger, Ph. Schmitt-Kopplin: Analysis of N-Acylhomoserine Lactones after Alkaline Hydrolysis by Anion Exchange Solid Phase Extraction followed by Capillary Zone Electrophoresis Coupled to Mass Spectrometry (CZE-ESI/MS)
In: Handbook of Methods Used in Rhizosphere Research; Editors: J. Luster, R. Finlay, Birmensdorf, Swiss Federal Research Institute WSL, 2006

M. Frommberger, **M. Englmann**, I. Gebefügi, T. Cataldi, G. Bianco, Ph. Schmitt-Kopplin: Analysis of N-Acylhomoserine Lactones by Gas Chromatography Coupled to Mass Spectrometry (GC-MS)
In: Handbook of Methods Used in Rhizosphere Research; Editors: J. Luster, R. Finlay, Birmensdorf, Swiss Federal Research Institute WSL, 2006

M. Frommberger, **M. Englmann**, Ph. Schmitt-Kopplin: Analysis of N-Acylhomoserine Lactones by Partial Filling Micellar Electrokinetic Chromatography coupled to Mass Spectrometry (PF-MEKC-ESI/MS)
In: Handbook of Methods Used in Rhizosphere Research; Editors: J. Luster, R. Finlay, Birmensdorf, Swiss Federal Research Institute WSL, 2006

M. Frommberger, **M. Englmann**, Ph. Schmitt-Kopplin: Analysis of N-Acylhomoserine Lactones by Nano-Liquid Chromatography Coupled to Mass Spectrometry (NanoLC-ESI/MS)
In: Handbook of Methods Used in Rhizosphere Research; Editors: J. Luster, R. Finlay, Birmensdorf, Swiss Federal Research Institute WSL, 2006

M. Frommberger, **M. Englmann**, Ph. Schmitt-Kopplin: Practical considerations for the analysis of ionic and neutral organic molecules with capillary electrophoresis/mass spectrometry
In: „CE from small ions to macromolecules“ Schmitt-Kopplin Ed., Series Methods in Molecular Biology, Molecular Medicine and Biotechnology (Series Editor: John M. Walker), Humana Press; *in press,* 2007

Ph. Schmitt-Kopplin, N. Hertkorn, M. Frommberger, M. Lucio, **M. Englmann**, A. Fekete and I. Gebefügi: Ion Cyclotron Resonance Fourier Transform Mass Spectrometry for Non-Targeted Metabolomics of Molecular Interactions in the Rhizosphere
In: Advanced Techniques in Soil microbiology, Soil Biology, Volume 11 (Series Editors: A. Varma, R. Oelmüller), Springer-Verlag Berlin Heidelberg, 2007

Posters

M. Englmann, M. Frommberger, Ph. Schmitt-Kopplin: Capillary Electrophoresis – Mass Spectrometry: Principles and Applications for the Analysis of Bacterial Signaling Molecules
Poster at 6th Igler MS Tage, Innsbruck, February 17th/18th, 2005

M. Englmann, A. Fekete, M. Rothballer, M. Frommberger, X. Li, J. Fekete, A. Hartmann, L. Eberl, Ph. Schmitt-Kopplin: Confirmation of the occurrence of N-acylhomoserine lactones (HSL) in different real samples by combined results of FTICR/MS measurements, UPLC^{TM} analysis, in silico predictions and by application of biosensor constructs
Poster at the 17th International Mass Spectrometry Conference, August 17th to September 1st in Prague

M. Frommberger, **M. Englmann**, M. Witt, Ph. Schmitt-Kopplin: Analysis of Quorum Sensing in Bacteria with Nano-LC/MS and FTICR-MS
Poster at 6th Igler MS Tage, Innsbruck, February 17th/18th, 2005

M. Lucio, M. Frommberger, N. Hertkorn, I. Gebefügi, X. Li, A. Fekete, **M. Englmann**, Ph. Schmitt-Kopplin, U.Schurr, B. Thiele, K. Wieland: An Interdisciplinary Platform for Plant and Rhizosphere Metabolomics
Poster at Plant Metabolomic Meeting, Reading, UK, April 8th to 11th 2006

M. Frommberger, N. Hertkorn, M. Lucio, **M. Englmann**, I. Gebefügi, A. Hartmann, Ph. Schmitt-Kopplin: Towards a better understanding of bacterial communication: Analysis of Quorum Sensing by capillary separation techniques coupled to mass spectrometry and by ultrahigh resolution FTICR mass spectrometry
Poster at the International Workshop “Development and control of functional biodiversity at micro- and macro-scales” Neuherberg, Germany, October 5th to 7th 2005

Abbreviations

ACN	Acetonitrile
AHL	N-acyl-homoserine lactone
APCI	Atmospheric pressure chemical ionisation
CE	Capillary electrophoresis
CZE	Capillary zone electrophoresis
DNA	Desoxyribonucleic acid
ESI	Electrospray ionisation
EOF	Electroosmotic flow
FT-ICR MS	Fourier-transformation ion-cyclotron-resonance mass spectrometry
FWHM	Full width at half maximum
GC-LIF	Gas chromatography-laser induced fluorescence
GC-MS	Gas chromatography-mass spectrometry
HETP	Height equivalent to a theoretical plate
HPLC	High performance liquid chromatography
HS	N-acyl-homoserine
HSL	N-acyl-homoserine lactone
LC	Liquid chromatography
LED	Light emitting diode
LLE	Liquid-liquid extraction
LOD	Limit of detection
LOQ	Limit of quantification
MALDI-MS	Matrix-assisted laser-desorption ionisation mass spectrometry
MEKC	Micellar electrokinetic capillary electrophoresis
mRNA	Messenger-ribonucleic acid
MS	Mass spectrometry
MS-MS	Tandem mass spectrometry
m/z	Mass to charge ratio
nanoLC-MS	Nanobore liquid chromatography-mass spectrometry
NB	Nutrient broth (medium)
PDA	Photodiodearray detector
PZT	Lead circanate titranate
RP-LC	Reversed-phase liquid chromatography
RSD	Relative standard deviation
SDS	Sodium dodecyl sulfate
SMT-PI	Surface mediated thermodesolvatation and photoionisation

S/N	Signal-to-noise ratio
SPE	Solid-phase extraction
TLC	Thin layer chromatography
TOF-MS	Time-of-flight mass spectrometry
UPLC	Ultra performance liquid chromatography™
UV	Ultraviolet light

Table of contents

Publications 4
Abbreviations 7
Abstract 12
1. Introduction 14
1.1. Molecular interactions in the rhizosphere 14
1.2. Quorum sensing and quorum quenching of N-acylhomoserine lactones 15
1.2.1. Quorum sensing 15
1.2.2. Quorum quenching 18
1.3. State of the art in homoserines lactone analytics 20
1.3.1. Bioassays 20
1.3.2. Liquid chromatography based methods 23
1.3.3. Gas chromatography-mass spectrometry (GC-MS) 23
1.3.4. Sample extraction methods 24
1.3.5. Capillary electrophoresis-mass spectrometry methods 24
1.3.5.1. Capillary electrophoresis- mass spectrometry in general 24
1.3.5.2. Homoserine lactone analysis by micellar electrokinetic capillary electrophoresis (MEKC-MS) 27
1.3.5.3. Capillary zone electrophoresis (CZE-MS) analytics after hydrolysation of the homoserine lactones 27
1.3.6. Homoserine analytics 28
1.4. Goals of the present work 29
2. Principles of ultra performance liquid chromatography (UPLC) 31
2.1. General principles 31
2.2. Injection modes 33
2.3. Column 36
2.4. Detection 37
2.5. Specific observations in ultra performance liquid chromatography 38
3. Results of the development of an analytical platform based on UPLC-PDA analytics 40
3.1. Introduction 40
3.2. Preliminary experiments 40
3.3. pH screening 43
3.4. Determination of the performance characteristics 47
3.5. Study of the kinetic of the hydrolysis 51
3.6. Real sample analysis 54

3.7. Conclusion 57
4. Integration of ultra performance liquid chromatography methods 58
5. Prinziples of piezo driven drop-on-demand dispensers and applications in analytical chemistry and life sciences 62
5.1. Introduction 62
5.2. Technology 63
5.3. Droplet production 65
5.4. Determination of the droplet size 67
5.5. Examples for applications 69
5.5.1. Applications in analytical chemistry 69
5.5.1.1. Mass spectrometry 69
5.5.1.2. Chemistry in a levitated droplet 70
5.5.1.3. Titrations 72
5.5.1.4. Sample application in capillary electrophoresis 72
5.5.1.5. Chromatographic quantifications 72
5.5.2. Applications in Biology 73
5.5.2.1. Dosage of single cells 73
5.5.2.2. Microarrays 73
5.6. Conclusion/outlook 73
6. Results for the application of a drop-on-demand dispenser system for chromatographic quantifications in real samples 75
6.1. Introduction 75
6.2. The dispenser 75
6.3. Determination of the average droplet volume 77
6.4. Reproducibility measurements 78
6.5. Determination of droplet speed and flight distance 80
6.6. Standard addition 84
6.7. Conclusion 88
7. Results in droplet mass spectrometry 89
7.1. Single droplet electrospray 89
7.2. Surface mediated thermodesolvatation and photoionisation (SMT-PI) 98
7.2.1. Introduction 98
7.2.2. Setups 99
7.2.3. Direct surface-mediated thermodesolvatation and photoionisation 103
7.2.4. Indirect surface-mediated thermodesolvatation and photoionisation 103
7.3. Summary 107
8. Conclusion and outlook 109

9. Appendix 111
9.1. Chemicals and consumables 111
9.2. Instruments 111
9.2.1. UPLC 111
9.2.2. Drop-on-demand dispenser 111
9.2.3. Ion trap MS 112
9.2.4. FT-ICR MS 112
9.2.5. Surface mediated thermodesolvatation and photoionisation (SMT-PI) 113
9.3. Software 113
9.4. Methods 113
9.4.1. Preparation of standards for UPLC analysis 113
9.4.2. UPLC analysis of HSLs beside HSs 114
9.4.3. Real sample analysis by UPLC 114
9.4.4. Real sample preparation for the standard addition experiment 115
9.4.5. Droplet volume determination via photography 115
9.4.6. Droplet volume determination by weighing the reservoir 116
9.4.7. Droplet volume verification by ultra performance liquid chromatography analysis 116
9.4.8. Sample preparation for the standard addition approach 116
9.4.9. UPLC analysis of the real samples for standard addition 117
9.4.10. Experimental determination of the dispensed droplet speed 117
9.4.11. Single droplet electrospray mass spectrometry 118
9.5. Analytes 118
References 121

Abstract

Interactions of organisms in complex ecosystems are ubiquitous and manifold. Microorganisms in the rhizosphere use chemical signalling compounds such as N-acyl-homoserine lactones (HSLs) to communicate among each other and to gain information about their population density and environment. Sensitive, selective and reliable methods for the quantitative analysis of these compounds are essential for the study of interactions among different organisms in the rhizosphere. Several methods were approached to analyse HSLs in real samples based on bioassays, as well as chromatography and capillary electrophoresis, both with mass spectrometric detection. In this work, new tools are presented which complement the existing methods with a focus on selectivity, speed and the ability to apply them for the analysis of small volumes of complex samples.

An ultra performance liquid chromatographic (UPLC) method with UV detection was developed and optimised for a wide range of unsubstituted HSLs besides their most important degradation products. The method was shown to be much faster than conventional approaches, highly reproducible and selective. The method was applied for the determination of HSLs in real samples as well as for the study of the first and most important degradation step for HSLs.

In order to address and handle small sample volumes, a piezo driven drop-on-demand dispenser which is capable of dosing smallest droplets, was tested for its suitability for quantitative dosage. Two methods for the determination of the dispensed volume, based on graphimetry and imaging, were compared and the results are found to be in very good agreement. The graphimetrical method was found to provide highest accuracy with relative standard deviations around 1 %. Also the reproducibility of the dispenser was found to be high. It was shown that the dosage of small volumes of a highly concentrated standard solution, added to the sample (standard addition) prior to UPLC analysis is suitable for the determination and quantification of a bacterial signalling compound metabolite in a real sample with minimal sample preparation.

Furthermore, the drop-on-demand dispenser was tested for its suitability for sample injection for mass spectrometry which provides highest selectivity and resolution. For the desolvatation and ionisation of the analytes which is necessary for the mass spectrometric analysis, the droplets produced were charged in a strong electrical field. This method was found to be applicable in principle but was highly irreproducible. To increase this, the desolvatation and the ionisation step were separately taken into account. The desolvatation was achieved by dispension of the sample onto a heated surface. The ionisation was performed by atmospheric pressure photoionisation using

a krypton discharge UV lamp. A modification of the experimental setup revealed the possibility to immobilise the sample directly o the heated surface and transfer it into the gas phase by the controlled application of solvents, provided by the drop-on-demand dispenser. Applying this method, HSLs could be identified in a real sample with high precision in combination with high resolution mass spectrometry.

1. Introduction

1.1. Molecular interactions in the rhizosphere

Interaction with its environment and responding to changes in its milieu is essential for every organism. Changes in the surrounding lead in many cases to activation and inactivation of specific genes which generate a specific response of the organism. Changes of the environment can be abiotic or they are induced by other organisms inhabiting the same ecosystem. The discovery and understanding of these interactions on a molecular level is elemental to understand the connections within ecosystems as well as to understand the activities of the organism itself.

The rhizosphere is a complex and diverse habitat which provides the scene for many interactions on different levels among organisms. One mechanism of interaction is the communication of bacteria by autoinducers like N-acyl-homoserine lactones. This mechanism is not restricted to the communication of bacteria within their own species; interventions of other organisms into this communication system are to be expected.

The exploration of these interactions is important not only to improve the understanding of these systems but also to develop new strategies for plant protection and pest control. Furthermore, these mechanisms are similar in all ecosystems, so findings in rhizosphere research may help improving strategies involved for example in the medical area.

An elemental premise to examine these mechanisms is the existence of reliable, sensitive and selective analytical methods which are capable of analysing samples of high complexity in relatively small amounts. A further improvement of existing analytical approaches as well as the development of new methods for different tasks is necessary advancing this field of research, in order to provide the possibility for improved analytics of known compounds in systems which are as close as possible to the natural situation, as well as to find new compounds which are involved in metabolic interactions.

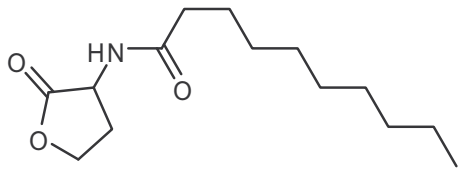
1.2. Quorum sensing and quorum quenching of N-acylhomoserine lactones

1.2.1. Quorum sensing

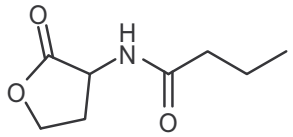
For many years, communication was thought to be restricted to so called “higher organisms” like animals and humans. The idea that bacterial cells communicate with each other to synchronise their behaviour depending on their density and their environment took some time to establish and changed the way these organisms were seen. One of the first observations of bacterial communication was made in the late 1960ies with *Vibrio fischeri*, a Gram negative marine bacterium which is able to generate luminescence [1]. In symbiosis with the Hawaiian bobtail squid (*Euprymna scolopes*), the luminescence of the bacteria, located at the ventral part of the animal’s mantle, prevents the squid from forming a shadow towards the brighter water surface and therefore it can not be detected as easily by predators [2, 3]. It was observed that luminescence takes only place when a certain density (“quorum”) of the bacteria is reached, planctonic individuals of the same species were not affected. Furthermore it was found that the information controlling luminescence is transported in the medium, affecting cells through a dialysis membrane. Kempner and Hanson [1] first discussed a specific inhibitor to prevent luminescence at lower densities but Nealson et al. [4] could show that the opposite is true: A self-produced autoinducer is responsible for this physiological reaction. Eberhard et al. [5] identified this factor to be N-3-oxo-hexanoyl-L-homoserine lactone some years later. Since that time, more and more of these bacterial signalling systems were identified. It is now assumed that nearly all bacteria may be involved in density-dependent communication [6]. Fuqua et al. [7] introduced the term “quorum sensing” for this kind of regulatory systems based on cell density dependent responses. While for Gram positive bacteria cyclical peptides serve as signalling compounds, Gram negative bacteria communicate preferably by derivatives of N-acyl-homoserine lactones, in most cases abbreviated as “AHL” or “HSL”.

N-acyl-homoserine lactones consist of a furen-2-on group with an acyl chain consisting of 4 to 14 (less frequently up to 18) carbons. Unsubstituted HSLs have a LogP between 0.03 for C4-HSL to 5.09 for C14-HSL. HSLs can be substituted at the β-carbon by a keto- or hydroxyl-function and the fatty acid side chain may be unsaturated. HSL biosynthesis derives from the fatty acid synthesis pathway. This is the reason why

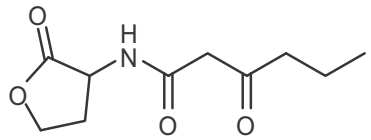
almost only HSL with an even numbered C-chain are found in nature[1]. The variety of HSLs may be due to prevent crosstalk which means that bacteria of different species use the same pathway for their communication [6, 11]. Some examples of HSLs found in nature for different bacteria are presented in figure 1.



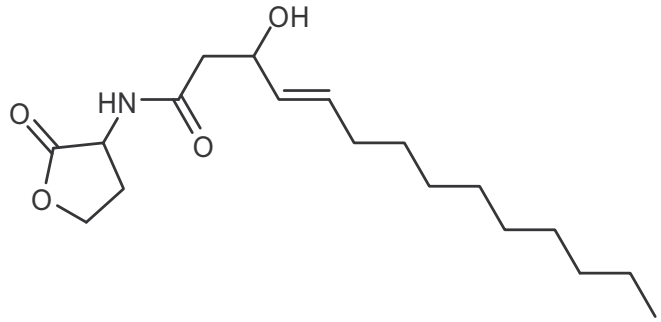
N-decanoyl-homoserine lactone (C10-HSL) *[II], [VIII]*



N-butanoyl-homoserine lactone (C4-HSL) [12]



3-oxo-N-hexanoyl-homoserine lactone (oxo-C6-HSL) [13]



3-hydroxy-N-tetradecenoyl-homoserine lactone (OH-C14:1-HSL) [14]

Figure 1: Examples of naturally occurring HSLs

The principle of quorum sensing is schematically presented in figure 2: The transcription of the protein LuxI leads to the synthesis of the autoinducer O-C6-HSL which diffuses through the cell membrane. Simultaneosly, the LuxR protein is

[1] Nevertheless C7-HSL was reported to be found in two samples by Lithgow et al. [8] and Horng et al. [9]. These exceptions are discussed to be due to a later modification of the molecule in the synthesis pathway [10].

produced. After reaching a certain concentration, the autoinducer binds to LuxR which leads to dimerisation of the protein. This complex binds to a special region of the DNA leading to transcription of the luciferase genes and simultaneously also an improved production of LuxI (autoinduction) [6].

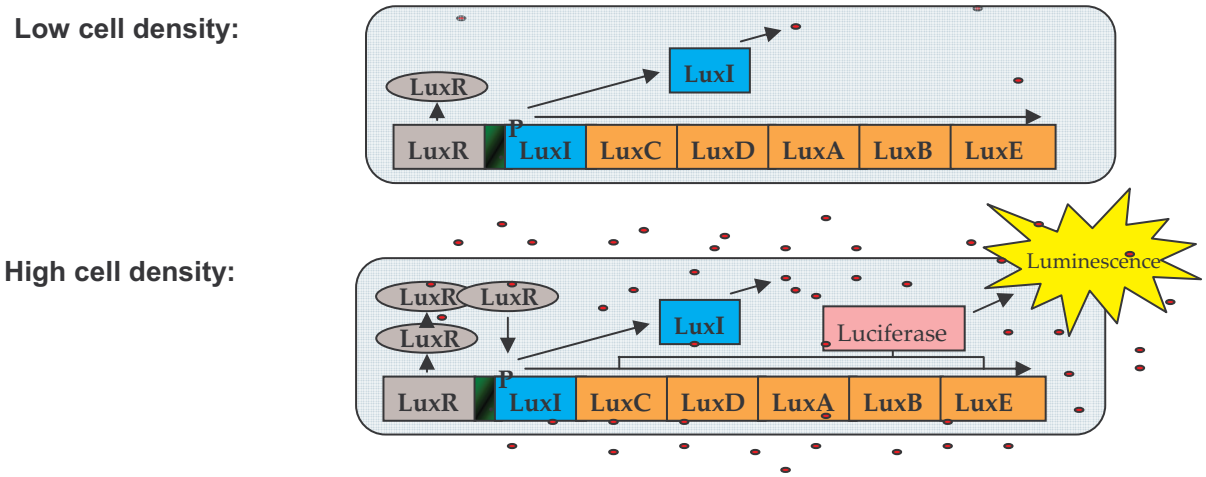


Figure 2: Schematical presentation of the quorum sensing system in *Vibrio fischeri*. Adapted from [15].

Quorum sensing is not restricted to luminescence, a wide variety of physiological reactions is controlled thereby: The most relevant ones are virulence factors of many kinds like exoproteases, siderophores, exotoxins and lipases or aggregation and biofilm development.

The continuous HSL production may be more economic than the permanent production of the quorum sensing target. Another reason for the existence of quorum sensing may be that a timely synchronisation of the bacteria is advantageous, for example when expressing virulence factors because the immune defence of the host organism may not react as long as the bacteria are harmless, so the pathogen is able to mount a “surprise attack” [11].

Having a closer look on how quorum sensing works in the natural environment for bacteria, different models were proposed. The original model of quorum sensing as sort of exchange of information among the bacteria about their own density was complemented and partially replaced by an alternative model by Redfield et al. 2002 [16] called “diffusion sensing”: According to this model, the bacteria gains information about its microenvironment by sensing the diffusion of the signalling molecule in its surrounding. This model accounts for the fact that many disturbances would influence the signalling according to the quorum sensing theory, like degradation, crosstalk, diffusion or mixing. According to the diffusion sensing model, the organism produces

signalling molecules to sense the diffusion of these compounds in its microenvironment. Recently, Hense et al. [17] proposed a third theory: It was shown that both approaches need to be combined. The cell can not distinguish between mass-transfer properties and spatial distribution; therefore it recognises a combination of both factors which provide on the other hand information about the efficiency for the expression of extracellular effectors. This model is therefore called “efficiency sensing”[2].

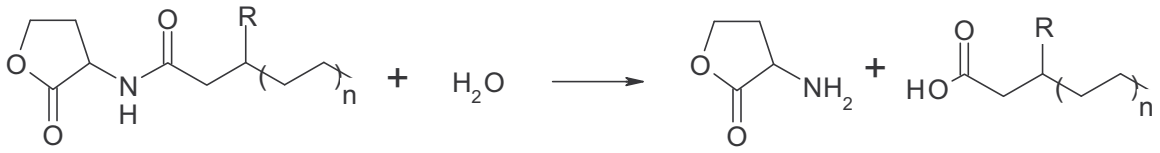
Because the structure of the microenvironment plays a central role for quorum sensing regarding these new models, it is obvious that bacterial cultures are not suitable to study these effects, because its homogeneity stands in clear opposite to the situation in nature as e.g. in the rhizosphere. This is a reason why future studies have to focus on in situ experiments.

1.2.2. Quorum quenching

In one of the first observations of quorum sensing by Kempner et al. [1] in 1968 already, a decline in the bacterial reaction in a culture depending on the pH was observed. This can be explained by an abiotic degradation of the bioactive compound. This abiotic degradation of HSLs in most cases is caused by hydrolysis of the lactone ring, resulting in the corresponding homoserine (see fig. 3b). This reaction takes place under alkaline conditions and is not reversible even when the pH is lowered afterwards again over a long time [18], *[VIII]*. The resulting serines are not bioactive and chemically relatively stable. This reaction was studied in detail and a mathematical model for the hydrolysis of selected HSLs is given in chapter 3.5.

[2] The term “quorum sensing” is well established and is still widely used even though it refers to a theory which is in progress of being intensively discussed. For clarity reasons, the term “quorum sensing” is also used in this work representatively for all models suggested.

a)



b)

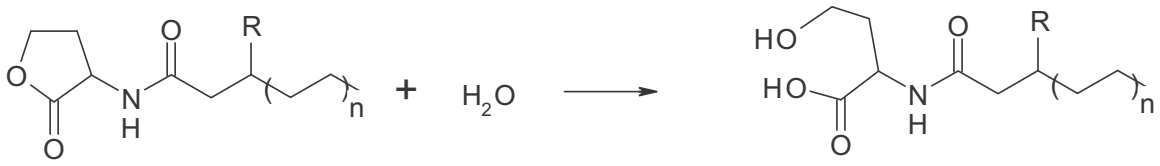


Figure 3: Degradation of HSLs: a) degradation by acylases, b) degradation pathway by lactonases as well as chemically under alkaline conditions

Degradation of HSLs does not only follow a chemical path, but can also be induced biologically. This effect is called “quorum quenching” and is in most cases accomplished by lactonases or acylases (see fig. 3) [19-21]. Lactonases work by breaking up the lactone ring of the HSL resulting in the homoserine. Acylases cleave the fatty acid from the HSL molecule by amide hydrolysis [20, 22, 23]. The degradation products are further degraded and consumed [20]. The main reason for a degradation of HSLs may not only be nutrition but an intervention in the quorum sensing system by another organism [21]. Besides an active degradation by quenching the signalling molecules, there are several other mechanisms found for a negative (or positive) regulation of quorum sensing. This is found to be accomplished by homologues of transcriptional regulators, an interference by small regulatory mRNAs or by structural mimics [24]. Even human hormones are found to interfere with bacterial quorum sensing [25].

Several observations indicate for a crosstalk of different organisms in the rhizosphere. It was shown by Wang et al. [20] that HSL degradation in diverse soils is up to a few hundred times higher than it would be expected for abiotic degradation. It was also shown that HSLs are under the conditions examined rapidly mineralized to CO_2. It is discussed that these effects lead to an aggregation of microbial colonies so that quorum quenching leads to further fine structurisation of the microhabitats. Several examples are shown which indicate an intense interaction of plants and bacteria by interferences with quorum sensing signals. This may be reactions of the plant in presence of HSLs, like the induction of defense genes [26] as well as direct interactions of plants in the quorum sensing system like inhibition of HSL production [27]. It was

recently shown that plants take up and translocate HSLs *[IX]*. Significant differences were observed within the two model plants examined: HSL uptake in yam bean (*Pachyrhizus erosus*) was much higher than in barley (*Hordeum vulgare*). It was shown that barley is capable of taking up two (C6- and C8-HSL) of the three HSLs examined (C6-, C8- and C10-HSL), while only C6-HSL was found in the shoots of yam bean[3]. Both plants discriminated the D-HSL as was revealed by a chiral GC-MS separation, but to a different extent. It is not yet known, whether the uptake and translocation is a passive process or if it is actively promoted by the plant. The effects of HSLs in the plant on the organism have to be examined in future studies.

The examination of interactions of plants and microbes by interference with the quorum sensing system is of high relevance, since these findings could lead for example to new methods for plant protection. It was already shown that transgenic plants equipped with genes coding for quorum quenching factors like lactonases showed high resistance against bacterial infections [19, 21].

1.3. State of the art in homoserines lactone analytics

1.3.1. Bioassays

A wide variety of analytical procedures for the analysis of N-acylhomoserine lactones was developed and is summarized in table 1. The most frequently applied method is based on thin layer chromatography with detection of the analytes by a reporter strain [28] (See fig. 4). This strain has a HSL-sensor construct using genes for autofluorescent proteins like green fluorescent protein (GFP) or red fluorescent protein / Dsred (RFP) fused to HSL-regulated promoters [29]. These biosensor strains have a deletion in their own HSL-biosynthesis. Therefore, the regulation of HSL-controlled promoters is entirely governed by extracellular HSLs. Depending on the different HSL-regulated promoters, either short or long chain HSLs can be monitored with very high efficiency. Other biosensors express different reporter genes or produce pigments when HSLs are provided exogenously *[VI]*.

[3] The analysis of the HSLs in this experiment was performed on ultra performance liquid chromatography (UPLC) applying a method, which is based on the one presented in chapter 3.

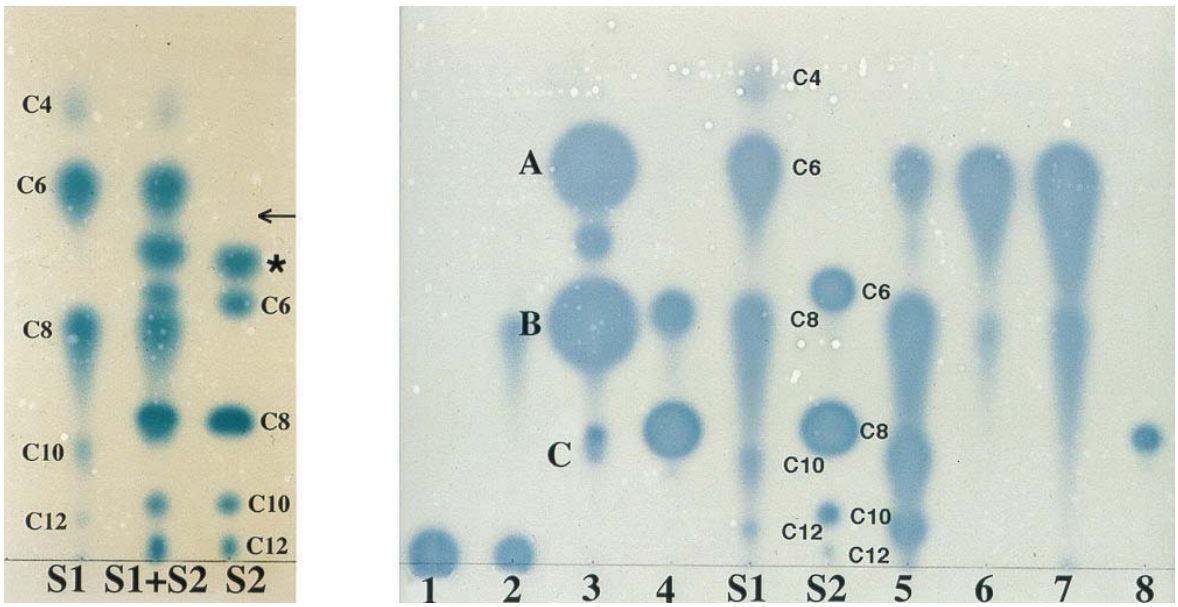


Figure 4: Examples for the identification of HSLs by TLC on a C18 plate and detection by a *Agrobacterium tumefaciens* reporter strain. From [28].

This method is relatively universal; almost every HSL is detectable. Other advantages are the fact that no expensive instrumentation is needed, the relatively high speed of the analysis and the high sensitivity. Detection limits go down to 0.5 fmol for oxo-C8-HSL but vary for the different HSLs in a wide band up to a few hundred pmol [28]. Nevertheless this method has important drawbacks already discussed in the original work: First, there is no detector strain which is sensitive to all HSLs, so the whole range of HSLs can never be covered by only one detector strain. Second, the sensitivities are different for different HSLs and different reporter strains and at high concentration cross reactions may occur [29]. The third drawback is that the mobilities of some HSLs are too similar because of similar polarities to be distinguished by the TLC [28]. Quantification of HSLs is performed by determination of the spot size. The accuracy and reproducibility of this method is limited. This is the reason, why over the last years several instrumental analysis methods were developed. They range from several HPLC-based methods over GC-MS to special CE-MS methods. These methods are applied after either liquid-liquid or solid phase sample extraction.

Table 1: Summary of methods developed for the determination of HSL-compounds.

Method	Origin of the sample	Targets	Sample pretreatment	Aim	Ref
RP-HPLC-MS	*E. Coli, P. stewartii, P. Aeruginosa*	oxo-C_6-. C_6-, C_{12}-HSL	SPE (Sep Pak Plus Silica)	Specification of HSL synthases, identification other HSL derivatives	[30]
Bioassay	cystic fibrosis patients	C_4-, C_6-,C_8-, C_{10}-, C_{12}-, oxo-C_6-, 3-oxo-C_8-, 3-oxo-C_{10}-HSL	LLE (dichlormethane) Fractionation with LC	Quantification of HSLs at different patients	[31, 32]
RP-HPLC-MS	*V. Anguillarum,* infected rainbow trout	OH-C_6-, C_6-, oxo-C_{10}-HSL	LLE (dichlormethane), fractionation with HPLC	Study of the synthesis of HSLs in *V. anguillarum*	[33, 34]
GC-MS, ESI-MS/MS	*Halomonas* species *Sinorhizobium meliloti*	C_4-, C_6-, C_8-, C_{12}-, oxo-C_6-HSL	LLE then factionation with HPLC	Identification of HSLs as signal molecules	[35, 36]
GC-LIF, GC-MS	Bacterial supernatants	C_6-HSL	LLE (ethyl acetatte) then fractionation with LC	Chiral separation of HSLs	[37]
RP-HPLC-PDA and MS	Bacterial supernatants	C_4-, C_6-HSL	LLE (dichlormethane), fractionation with HPLC	Study of in vitro biosynthesis of *P. aeruginosa*	[38]
Bioassay	*Agrobacterium tumefaciens*	C_6-, oxo-C_6-HSL	SPE	Comparison of different SPE methods	[39]
GC-MS	*Burkholderia cepacia*	C_4-, C_6-, C_7-, C_8-, C_{10}-, C_{12}-, C_{14}-HSL	LLE (chloroform)	Method development and identification	[40]
GC-MS	Marine isolate	C_4-, oxo-C_6-, C_8-, C_{12}-HSL		Identification of HSLs in marine bacteria	[41]
GC-MS	Flow cell cultures of *P. aeruginosa* (biofilm)	oxo-C_6-, oxo-C_8-, oxo-C_{10}-, oxo-C_{12}-, oxo-C_{14}-HSL	Derivatisation with pentafluoro-benzyloxime	Quantification of HSLs producing during the biofilm production	[42]
HPLC-MS	*Vibrio vulnificus* *P. aeruginosa*	C_4-, C_6-, C_8-, C_{10}-, C_{12}-, C_{14}-, oxo-C_6-, oxo-C_8-, oxo-C_{10}-, oxo-C_{12}-, oxo-C_{14}-	LLE (chloroform)	Method development	[43]
RP-HPLC-HRMS	Fillets of cod	hydroxy-C_8-, C_4-, C_6-, C_8-, oxo-C_8, oxo-C_{10}	LLE (ethyl acetate)	Study of bioluminescence in marine bacteria	[44]
RP-HPLC-HRMS pH control	Spoiled meat	oxo-C_6-, C_6-, oxo-C_8-, C_8-HSL	LLE (ethylacetate) than TLC	Identification of HSLs during spoilage with combination of microorganism identification	[45]
RP-HPLC-APCI-MS	Soil and bacterial supernatant	C_4-, C_6-, C_7-, C_8-, C_{10}-, C_{12}-, C_{14}-, oxo-C_6-, oxo-C_{12}-HSL		Study of degradation of HSLs by *Pseudomonas* sp.	[22]
RP-HPLC-ESI-MS	Bacterial biofilm	oxo-C10-,	LLE (ethyl acetate)	Study of HSL acylase, derivatisation with dansyl chloride	[46]
RP-HPLC-APCI-MS RP-HPLC-DAD	Standard solution	C_6-, oxo-C_6-, oxo-C_8-HSL		Study on degradation pathway of HSLs by oxidizing halogenated antimicrobials	[23]
nanoLC-ESI-MS	*Burkholderia cepacia*	C_4-, C_6-, C_7-, C_8-, C_{10}-, C_{12}-, C_{14}-HSL	LLE (chloroform)	Use of a self-packed capillary for nanoLC	[47]
HPLC-PDA	Different plant species	C_6-HSL		C_6-HSL stability during plant growth	[48]
CZE-ESI-MS	*Burkholderia cepacia*	C_4-, C_6-, C_7-, C_8-, C_{10}-, C_{12}-, C_{14}-HSL	LLE (chloroform) Hydrolysation, SPE	Determination of HSLs after their hydrolysis, method development	*[VIII]*
PF-MEKC-ESI-MS	*Burkholderia cepacia*	C_4-, C_6-, C_7-, C_8-, C_{10}-, C_{12}-, C_{14}-HSL	LLE (chloroform)	Partial filling MEKC, method development	[49]
GC-MS	Standard solution	HSLs with e.g. biphenyl group		Polymer-supported synthesis of HSLs	[50]
HPLC-HRMS	Spoiled bean sprouts	oxo-C_6-HSL	SPE (Strata X)	Identification of HSLs with bioassay, study of spoilage process	[51]

1.3.2. Liquid chromatography based methods

Over the last years the application of reversed phase liquid chromatography (RP-LC) for the separation of HSLs became more important. In most cases, the LC system is coupled online to a mass spectrometer by positive ion ESI [30, 43-47, 51] or APCI [22, 23]. In some cases, PDA detection was employed [23, 48]. LC was also applied for fractionation prior to different kinds of analysis like bioassays [31, 32] or GC analysis [35-37]. Mostly, HPLC systems are employed, but also a nano-LC method was developed by Frommberger et al. [47].

Most LC separation methods focus on a small number of detectable HSLs. Nevertheless some relatively universal methods were developed. Morin et al. [43] presented a LC-ESI-MS method for the analysis of HSL from C4 to C14 besides the 3-oxo-derivates from C6 to C14. In order to provide the separation of all analytes, a relatively large column (250 x 4.6 mm ID) was used applying a flow-rate of 0.4 mL/min of a water/methanol mobile phase. The flow-rate had to be splitted 1/12 after the column. The identification of the HSLs was performed based on MS-MS fragment ions, relative intensities and retention times. Quantification was performed focussing on the m/z 102 fragment with < 10 % RSD in real sample, which was a *Vibrio vulnificus* bacterial culture. The fragment was chosen due to its low signal to noise ratio.

Flodgaard et al. [44] described a LC-ESI-MS method for the analysis of C4-HSL, C6-HSL, C8-HSL, OH-C8-HSL, oxo-C8-HSL and oxo-C10-HSL. Quantification and a real sample analysis were not performed except for OH-C8-HSL; the intention for the application was to show the non-existence of these analytes in the bacterial cultures.

Frommberger et al. [47] developed a nano-LC-ESI-MS method for the analysis of C4- to C14-HSL including C7-HSL as internal standard. The self-packed column is capable of on-column sample preconcentration and therefore relatively high amounts of sample up to 5 µL can be injected. Identification of HSLs was made by MS-MS fractionation and identification of the characteristic fragment at m/z 102. Quantification was performed focussing on the same fragment by single reaction monitoring.

1.3.3. Gas chromatography-mass spectrometry (GC-MS)

Several GC-MS methods are reported for HSL analysis, although the vapour pressure of HSLs is relatively low. This limitation is overcome by application of derivatisation methods [42, 50] or by fractionation in combination with a concentration step prior to GC-MS

analysis [35-37]. Nevertheless, Cataldi et al. [40, 52] reported about methods for HSL analytics by GC-MS in real sample extracts without derivatisation. Wagner-Döbler et al. [41] made use of GC-MS for a non-targeted screening for HSLs in marine isolates. GC-LIF was successfully applied for chiral analysis of HSLs [37] as well as GC-MS was successfully applied to obtain chiral information on HSLs *[IX]*.

1.3.4. Sample extraction methods

For the analysis of complex real samples in most cases an extraction step is necessary due to reduce matrix effects and concentrate the sample in order to increase the concentration of the analytes. Also, enzymatic reactions in the natural sample may alter its composition during the time needed between sampling and analysis. This can also be stopped by extracting the analytes soon after sampling [47]. Another reason for an extraction step is the salt-sensitivity of electrospray interfaces [43]. Because most HSLs are relatively apolar (see chapter 9.5 in the appendix) and the sample is normally an aqueous solution, extraction is typically done by liquid-liquid extraction with a polar solvent like dichloromethane [31-34, 38], chloroform [40, 43, 47] or ethyl acetate [37, 44-46]. Morin et al. [43] tested different solvents (dichloromethane, chloroform, ethyl-acetate, ethyl-ether and hexane) and found dichloromethane and chloroform to be both optimum solvents providing highest yield.
For some cases, SPE extraction methods were alternatively developed [30, 51], *[VII]*, *[VIII]* which were shown to provide high yields and are much faster and easier to apply.

1.3.5. Capillary electrophoresis-mass spectrometry methods

1.3.5.1. Capillary electrophoresis- mass spectrometry in general

Some of the most advantageous methods for the analysis of unsubstituted HSLs are based on CE-MS [49], *[VIII]*. Therefore, this method is described in detail in the following section.
In principle, CE systems consist of a capillary and a high voltage supply with one electrode placed in a vial containing the separation buffer and the other electrode at the opposite end of the capillary. The capillary consists of fused silica with an outside coating of polyimide to increase the flexibility of the brittle material. The total outer diameter is

normally 360 µm, the inner diameter is typically between 50 and 150 µm. The capillary length in CE-MS is around 50 to 100 cm.

The different behaviour of the analytes in capillary zone electrophoresis (CZE) is due to a different time of active migration (based on the “mobility” of the analytes) within the overlying stream of liquid generated by the electroosmotic flow. The mobility is on the first hand side determined by the size of the component. The second factor is the charge of the analyte which is dependent of the pH. This is the reason why the migration and the migration time is mostly determined by the buffer pH. So, the buffer composition determines the speed of the separation (analogous to the flow resulting from the pressure applied in LC). Another way to separate the analytes is by micellar kinetic electrochromatography, where the analyte is enclosed in micelles, formed by a surfactant, which provide the charge for the separation.

CE can be coupled to different detection systems which are for example mass spectrometry (MS) [53], laser induced fluorescence (LIF) [54, 55] or UV spectrometry. Mass spectrometry provides the highest selectivity, combined with good selectivity. The coupling to the mass spectrometer is in most cases performed by electrospray ionisation (ESI). Electrospray ionisation is generally a very soft and universal ionisation technique which is capable of ionising relatively large molecules. An electrospray is formed, when a voltage of some thousand volts is applied on a liquid stream over a distance of some millimeters. This stream breaks up into droplets with a diameter of around 5 µm to 150 nm, depending on several parameters [56]. These droplets are highly charged on the surface. During the flight, these droplets undergo an asymmetrical breakup, resulting in smaller droplets which are highly charged and bigger drops with lower charge. The droplets are shrinking due to solvent evaporation until the charge is transferred to the analytes and they end up as ions. Both, positive and negative ions can be detected, depending of the spray voltage polarisation.

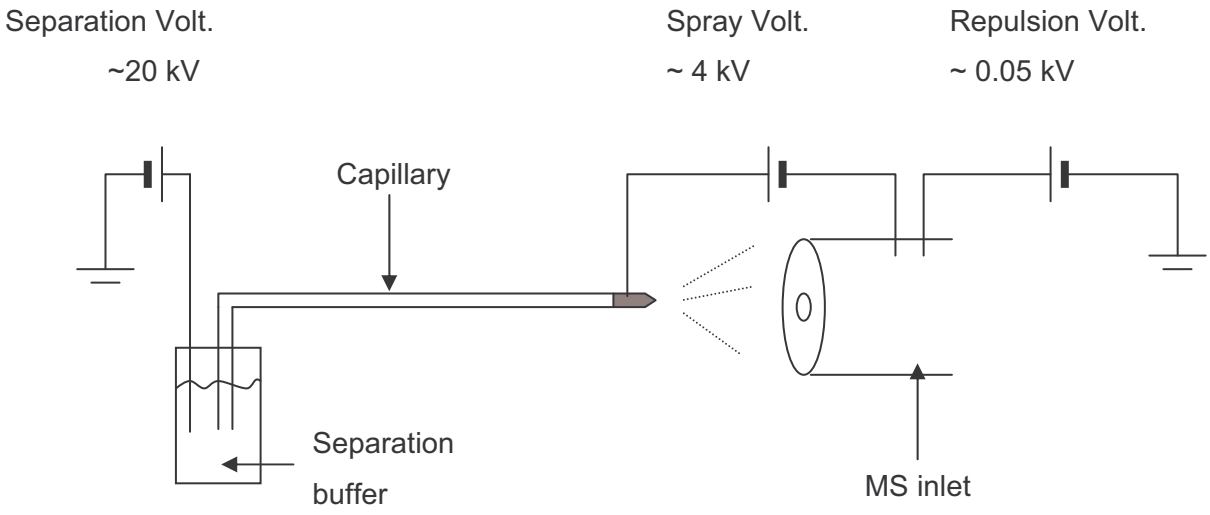


Figure 5: Schematic presentation of a typical CE-MS setup. The electrospray is in this case performed in positive ion mode: A voltage of around 20 kV is applied on the separation buffer; this induces the electroosmotic flow through the capillary. At the end of the capillary, a voltage of typically 4 kV is applied for the electrospray. A small voltage with the same polarity may be applied on the MS inlet for preventing the ions from attaching on the walls of the heated capillary.

Electrospray techniques can be divided into sheath liquid supported and sheathless techniques. Additionally in both cases, a gas flow applied coaxially, transversally or in opposite direction of the spray can be used to support the electrospray processes and stabilise the ion flow into the MS.

In sheath liquid supported sprays, the voltage application is mediated by the sheath liquid; the efflux of the capillary and the sheath liquid mix nearby or at the end of sprayer tip. These sprays have higher flowrates and form larger initial droplets [56]. The sheath liquid for a positive ion mode spray may typically be consisted of a higher percentage of organic solvent which helps in desolvatation and an acid which provides the proton excess for a protonisation of the molecules in positive ion mode. Additionally, the sheath liquid generally provides stable spray conditions, when the physical-chemical properties are varying, like for example the surface tension of the CE outflow. Generally, the coupling with CE does not afford special settings in the MS analysis compared to other separation methods. CE is coupled in most cases with a single- or triple quadrupole MS or in an increasing number of cases with ion traps. TOF-MS plays a minor role *[III]*. For HSL analytics, an ion trap was applied which provides the possibility of fragmentation, which is important for the determination of the HSLs. A schematic overview of a CE-MS setup is given in figure 5.

1.3.5.2. Homoserine lactone analysis by micellar electrokinetic capillary electrophoresis (MEKC-MS)

One possibility of HSL analytics on CE-MS is the application of micellar electrokinetic capillary electrophoresis-MS (MEKC-MS). Different surfactants were tested for the analysis of unsubstitutes HSLs from C4 to C14, as well as partial filling-MEKC to prevent contaminations of the surfactants in the MS interface and reverse migrating micelles, where the analyte migrated in the reverse direction and is handed over from micelle to micelle. In case of the surfactants, SDS was found to be optimal. The bile salts deoxycholic and cholic acid were tested as well but contamination was high and the solubility of the compounds limited the application to a pH range above 9. The method is fast and sensitive (LOD is around 1µM for S/N>3). An advantage of this method compared to the one described below is the applicability for detecting C4-HSL, the smallest and most polar analyte. Nevertheless, the method showed low reproducibility, which is due to not completely suppressed disturbances of the MS spectra by the surfactants. This makes the method not suitable for quantification. Another drawback in this specific case are the surfactant-like properties of the analytes which are assumed to form micelles by themselves and therefore reduce selectivity and sensitivity. Also the extensive method development is time consuming and probably needs to be performed for each variation of the instrumental setup (when, e. g., changing the instrument and using longer capillaries) [49].

1.3.5.3. Capillary zone electrophoresis (CZE-MS) analytics after hydrolysation of the homoserine lactones

As mentioned above, the analytes are not amenable to capillary zone electrophoresis (CZE) directly. This can be overcome by chemical alteration, in this case hydrolysation of the analytes as shown in figure 3b. This reaction takes place under alkaline conditions and can be considered to be irreversible. After a mixed-mode anion exchange solid phase extraction, the analytes are amenable to classical CZE. The hydrolysis products may occur also in natural samples. So the same extraction has to be performed with another aliquot of the sample without the hydrolysation step. The difference gives the amount of the unhydrolysed HSLs in the sample. This method is highly reproducible and stable. The speed is comparable to the one archieved by nanoLC-MS [47] and lies at around 20 minutes for the separation (see fig. 6). A drawback here is that C4-HS is lost during sample cleanup. The LOQs and LODs are 50 and 10 ng/mL and also in this case

comparable to the ones archieved with nanoLC-MS [47] and low enough for the analysis and quantification of the analytes in real samples *[VIII]*.

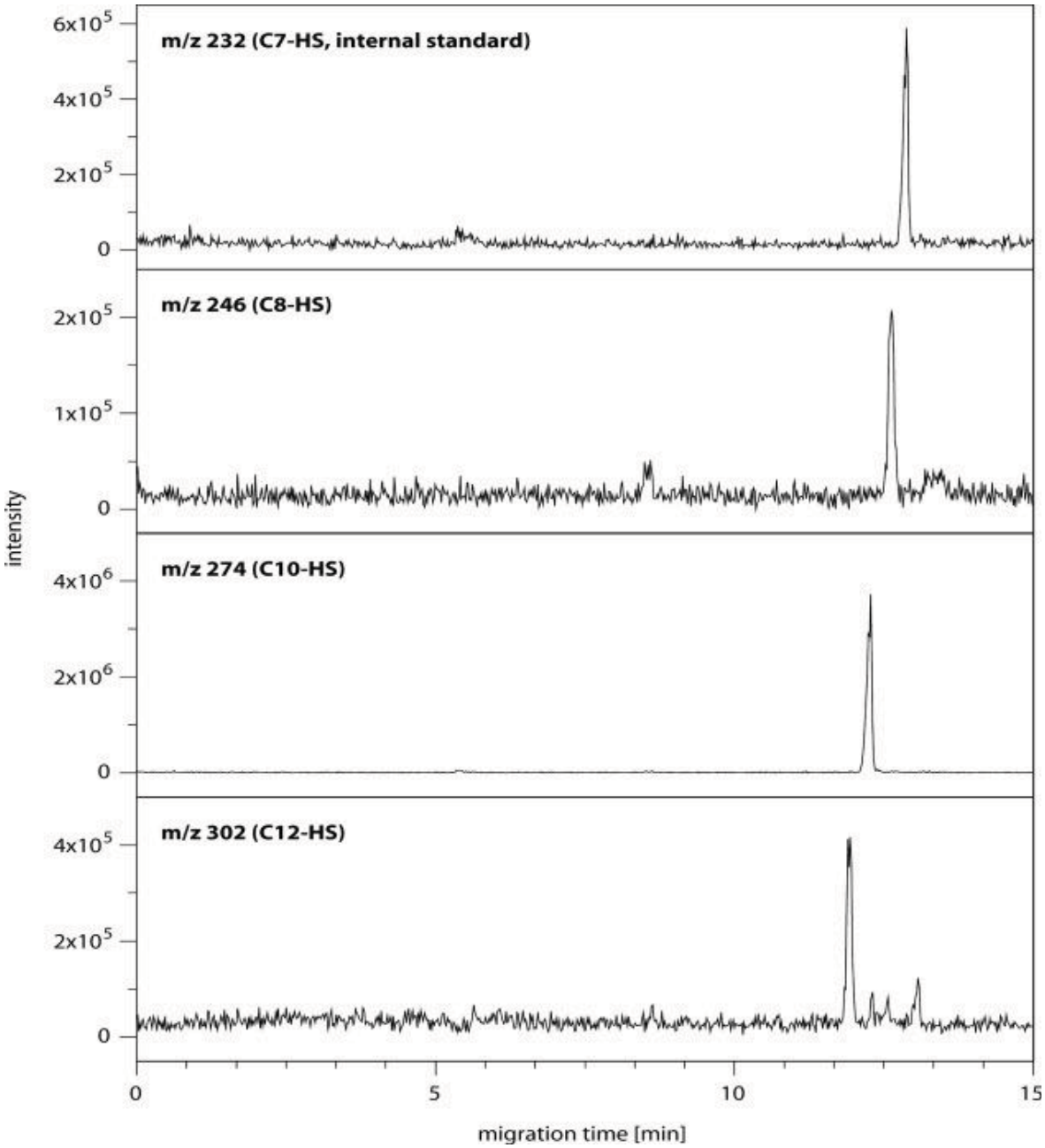


Figure 6: Example for a real sample analysis of four HS by CZE-MS. For details see *[VIII]*.

1.3.6. Homoserine analytics

HSLs are not very stable and the main products of chemical and biological degradation, the homoserines, should always be kept in focus, too (see chapter 1.2.2). Only three methods are found to describe the analysis of homoserines besides HSLs. Michels et al. [23] developed a HPLC-PDA method as well as a HPLC-MS method for the examination

of the degradation pathway of oxo-C6-HSL and C6-HSL. The measurement was performed under pH-control by addition of phosphoric acid to the eluent with detection at 200 nm. The confirmations were performed by HPLC-APCI-MS.
Huang et al. [22] developed a HPLC-APCI-MS method for the study of the degradation of several HSLs. The separation was performed applying methanol and water acidified by acetic acid.
The CE-MS method presented in [*VIII*] is based on the analysis of the hydrolysation products of HSLs, because HSLs are not amenable directly by CZE-MS. The quantification of the intact HSLs in the sample is only indirectly possible by subtraction of the amount determined in the unhydrolized sample from the one determined in the hydrolysed one (see chapter 1.3.5.3). The method was developed for the analysis of C6- to C14-HSL including C7-HSL.

1.4. Goals of the present work

Eventhough a vide variety of analytical methods for the determination of HSLs is already existing, there are still important drawbacks and gaps in each method. Focussing on the most universal alternatives to bioassays which are HPLC-MS and CE-MS, two aspects become obvious: first, the analysis time consumption is very high in both cases: typical chromatographic runtimes lie in the range of 20 to 40 minutes and beyond [30, 43]. One CZE-MS run takes around 20 minutes but every sample has to be measured twice to quantify the unhydrolysed analytes. Another drawback especially in CE-MS is the fact that the method is not automatizable. Current errors in the instrument are unavoidable from time to time which stop the analysis. Also the electrospray needs to be monitored. Both principles, LC-MS and CE-MS make use of mass spectrometers as detectors. Lactonization, the reverse reaction of the hydrolysation of HSLs is clearly observed in APCI [22] as well as in ESI [*VIII*] and limits quantification of lactones and serines. Even tough selectivity is high, MS instruments are rather expensive and elaborate. So, one goal of this work was to develop a fast and automatizable method which is capable of analysing a wide range of HLSs, preferably the most widespread unsubstituted, saturated ones, providing in addition a platform for the study of the hydrolysis reaction. A UPLC-PDA instrument was tested for its suitability for this task. The fact that HSLs are relatively unstable implements the need that all corresponding serines should generally be detectable by the same method.

All separation methods to be developed should generally be compatible with electrospray-mass spectrometry to preserve the possibility for combinational and confirmatory analyses on different instruments.

The time consumption of the separation runtime does not implement the effort needed for the sample extraction which is necessary in all methods reported so far. So, another goal of this work was to develop fast and efficient methods which are capable of detecting HSLs in small amounts of real sample quickly and quantitatively. The intention for this is the long-term goal to provide analytical tools for the analysis of HSLs in samples taken from the rhizosphere because in-depth understanding of quorum sensing must imply the possibility to analyze these reactions in the normal habitat of the organisms, since homogenous bacterial cultures differ widely from the fine structured and much more complex situation in nature [17, 20] (see also chapter 1.2.1). This should be realized by an UPLC method, which is capable of analysing samples with a minimum of sample preparation. Another approach is the controlled delivery of liquid samples for mass spectrometry by a drop-on-demand dispenser.

2. Principles of ultra performance liquid chromatography (UPLC)

2.1. General principles

In order to improve separation speed and selectivity in LC applications, several strategies were followed over the years [57]: One possibility is to increase the column temperature (up to above 100 °C). This opens the way to increase flow rates while keeping the backpressure low. The drawback of this approach is that not every column packing material is capable of these high temperatures. Also the analytes must be temperature stable which is often not the case. A technical challenge is to increase the temperature of the solvent quickly enough during the run.

Another approach is the application of monolithic column material. One advantage of this method is the applicability for conventional HPLC systems without technical modifications; only the column has to be replaced. Runtimes can be reduced up to one fifth as compared to conventional columns due to the improved permeability of the monolithic material. On the other hand, selectivity often can not be improved simultaneously [57]. Also, sometimes relatively low reproducibilities are still a drawback of this method compared to other approaches [58].

A third alternative is to improve separation efficiency by reducing the column particles diameters. The drawback here is that this modification goes along with a high column backpressure, so that these systems have to be operated at elevated pressure. Additionally, several modifications are necessary, like a reduction of the system dead volume. These are the reasons, why this method can not be applied reasonably in conventional systems and a redesign of the LC setup is necessary.

Ultra Performance Liquid Chromatography (UPLC™) is one representative of this new generation of LC instruments combining small particles and high pressure. A reduction in size of stationary phase particles results in a lower theoretical plate height and therefore in a higher separation efficiency [59]. This fact is made use of in these instruments: the particles size is reduced to around 1.7 µm diameter. The main result thereof is the much higher backpressure of these columns. The instruments are therefore equipped with pumps providing 15,000 psi, respectively 1,000 bar[4].

A reduction of the particle size diameter leads to a decrease in the theoretical plate height. This goes along with a shifting of the minimum plate height towards higher velocities, as can be seen in figure 7. The van Deemter plots also demonstrate that the minimum (which represents the optimum flow speed for the separation) of each curve for the different particle sizes is also very much broader in case of small compared to larger particles [60-

[4] The maximum pressure in conventional HPLC systems lies at around 400 bar.

63]. This leads to a significant reduction in analysis speed combined with an improvement in selectivity due to an increased solvent speed when operating in optimum conditions. The broader range of the optimum flow rate increases the flexibility when applying smaller particles.

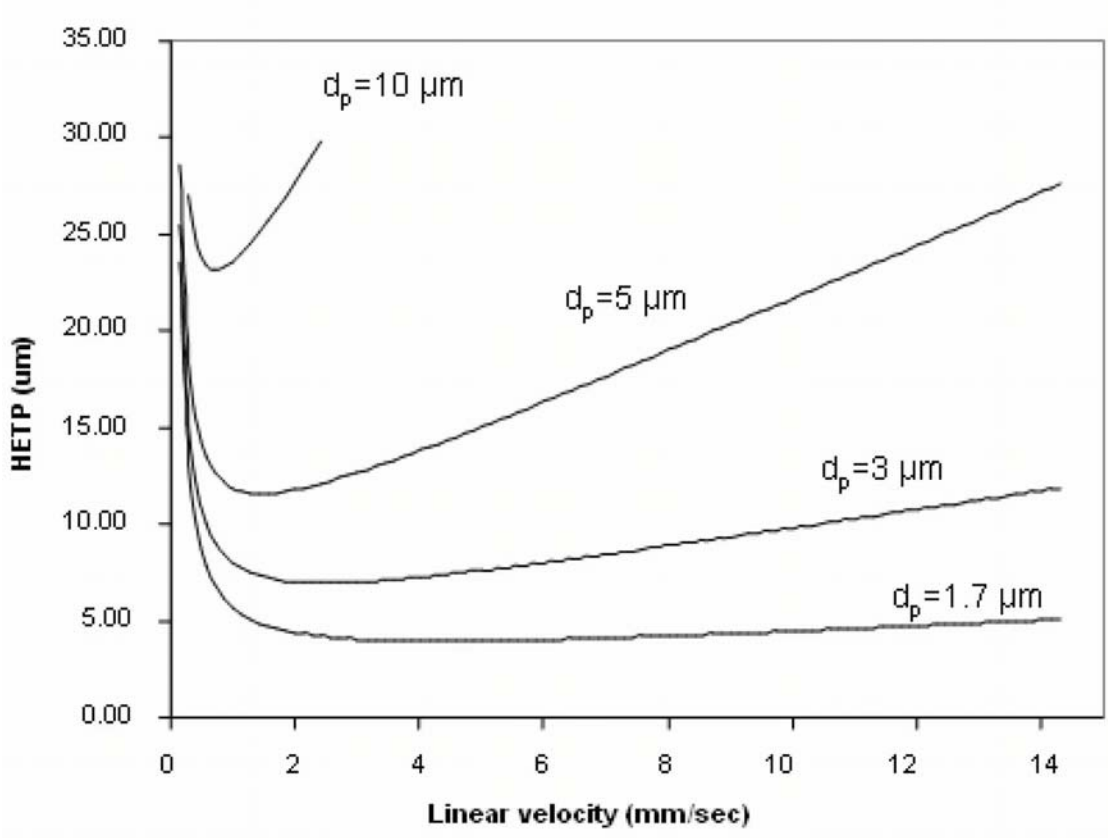


Figure 7: Comparison of van Deemter curves (linear velocity of the solvent and the resulting height equivalent to a theoretical plate, HETP) for different particle sizes (1.7 µm to 10 µm). From [60].

On the other side, applying these improvements to a conventional HPLC-system, the benefits would be partially destroyed or limited by peak broadening effects due to too broad sample plugs, dilution effects due to too high dead volumes and peak broadening as well as low resolution due to a too high detector cell volume and too low detector speed. This leads to the need for a reduced system dead volume of around 200 µL and advanced injection and detection methods. Implying these, the sensitivity generally can be increased due to sharper and higher peaks [64-71]. Due to shorter runtimes, also solvent consumption and eventually column expense per analysis could be reduced [66].
Yu et al. [72] reported a 10-fold increase in peak height in combination with a 2-fold decrease in peak width comparing HPLC and UPLC, each with optimized conditions, analyzing a drug mixture in rat plasma. LODs and LOQs could be two times reduced [58]

down to four times and lower [66, 72]. An improvement in sensitivity is not reported in every case. The sensitivity reached depends on the injection volume [73] and on the analyte [58] when comparing optimized HPLC to optimized UPLC conditions. A direct transfer or downscaling of HPLC methods for UPLC is not possible. After the transfer of the HPLC method a further optimisation is necessary which can be performed for example in view of highest sensitivity as well as highest speed or highest resolution leading to different results [74].
An overview of typical UPLC parameters compared to HPLC gives table 2.

Table 2: Comparison of some typical UPLC specifications to those of HPLC

	typical HPLC	typical UPLC
Particle size	3.5 µm	1.7 µm
typical column dimensions	5 x 100 mm	2 x 100 mm
max. pressure	400 bar	1000 bar
dwell volume	> 500 µl	~ 200 µl
runtime per injection	10 min.	1.5 min.

2.2. Injection modes

Three different injection modes are possible with UPLC:

1. Full loop injection
2. Partial loop injection and
3. Partial loop injection using needle overfill

Full loop injection is the classical way of injecting samples onto the column. The reproducibility is very high but an at least fourfold overfill is needed which results in high sample consumption. The sample plug is relatively large and the time consumption is relatively high compared to the other methods. Also, flexibility in the injected volume is not provided, only by sample loops of different sizes. The broadness of the sample plug is less relevant when a elution gradient is applied which leads to a sample preconcentration effect *[X]*. (See also fig. 8). With the UPLC system used, the highest amount of sample can be injected by full loop injection which is 20 µL. The maximum amount injectable by the other injection methods is 10 µL.

By application of partial loop injection, the sample is packed between two air bubbles which prevent peak broadening due to mixing of the sample with the solvent during transport through the system. The air is dissoluted, when the high pressure is applied. This method is fast and flexible, even though the resulting peaks are not as sharp as by application of the special overfill method (partial loop injection with needle overfill).

Partial loop injection with needle overfill is the most advanced method. The underlying principle is schematically presented in fig. 9: The sample is taken up between two bubbles like it is done by normal partial loop injection, but around 4 µL more, than the sample to be injected is taken up additionally. The sample is torn over the valve with the injection loop offline. After switching the valve and bringing the loop online, a part of the sample is injected into the loop. The valve switches again and the sample is applied on the column in the reverse direction. With this method, the two ends of the sample plug are “cut” which leads to an improved peak shape compared to normal partial loop injection, which is demonstrated in figure 8. This is only valid for isocratic runs. As can be seen in figure 8, the peak shape is similar in the gradient part of the chromatogram due to column preconcentration effect.

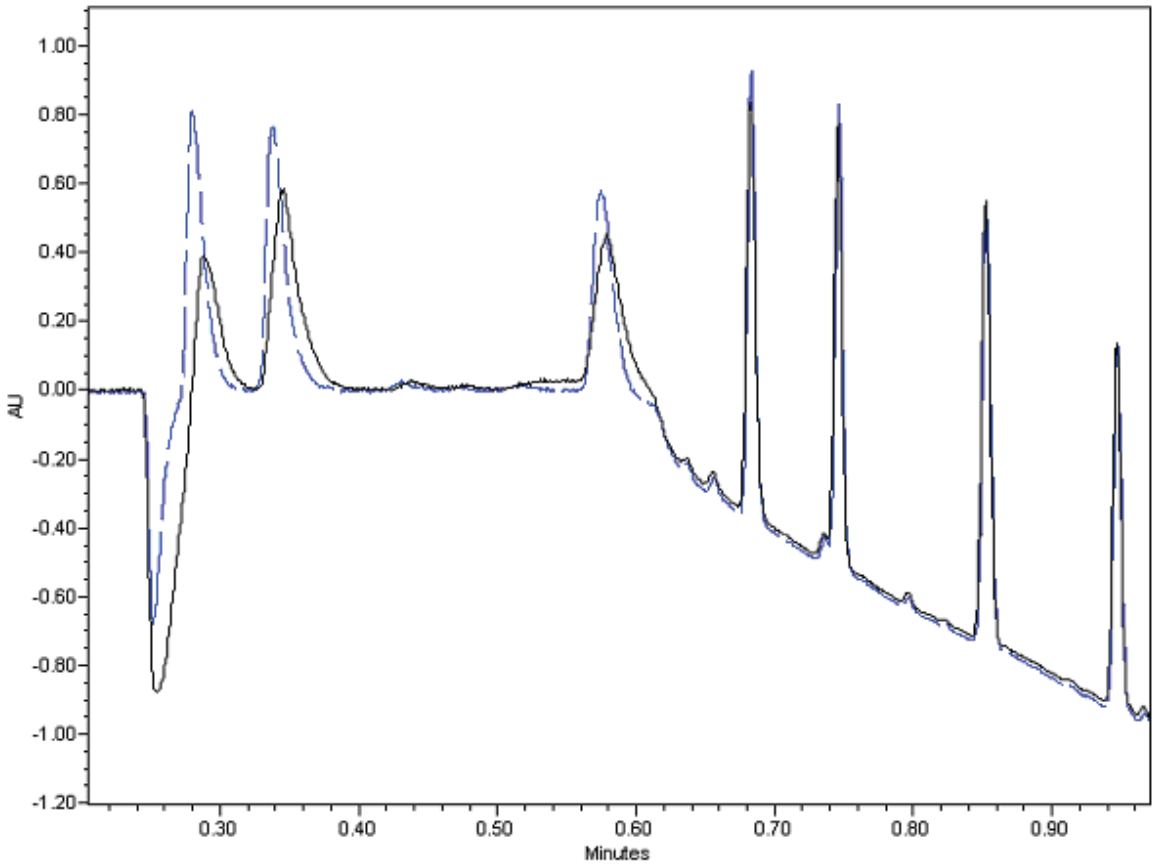


Figure 8: Comparison of both partial loop injection modes. 10 µL of a sample containing different HSLs is injected by partial loop injection with (broken line) and without overfill mode. The peaks in the isocratic part of the chromatogram are much narrower and higher in overfill mode than without. The retention times are not the same due to a different placement of the sample in the loop. In the gradient part of the chromatogram, the preconcentration effect leads to very similar peak shapes.

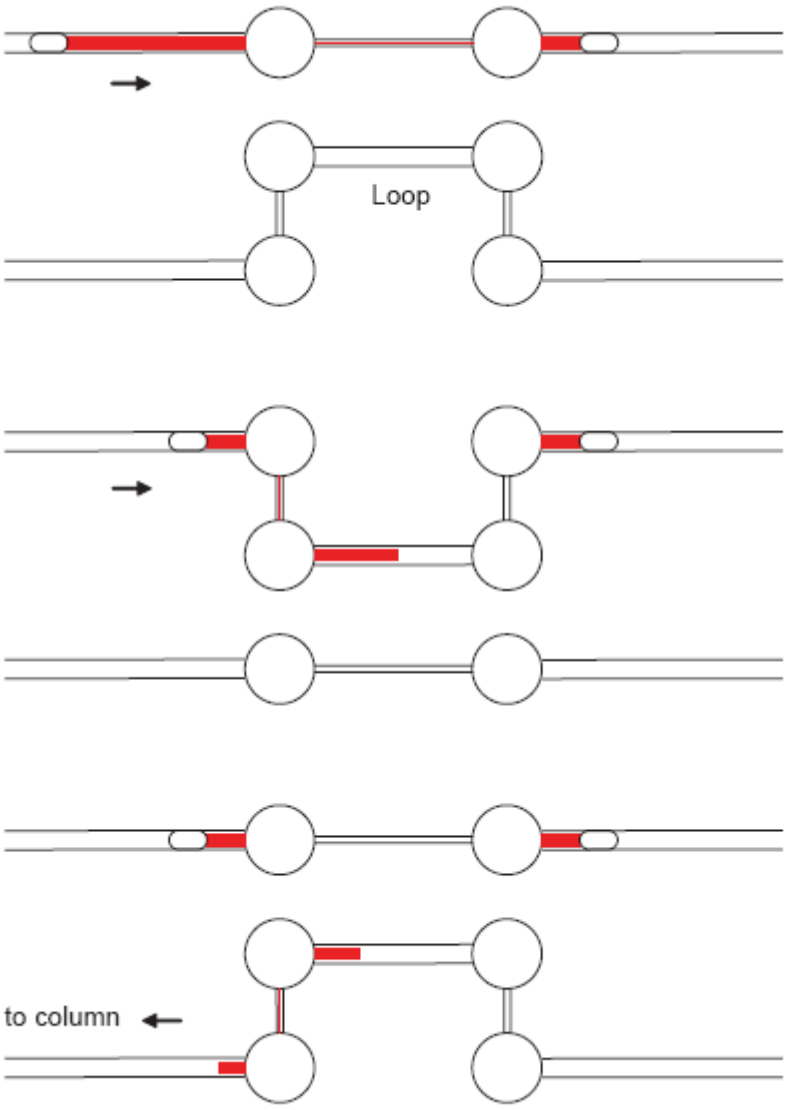


Figure 9: Schematic presentation of the partial loop injection mode using needle overfill: In the upper picture, the sample, injected by partial loop injection, is drawn by the valve with the loop offline. After switching and bringing the loop online, a part of the sample is drawn into the injection loop (middle). After switching again, the sample is brought onto the column by a flow in the opposite direction (lower part). The overfill left in the capillary is disposed.

2.3. Column

The column packing material is based on ethyl-bridged organic/inorganic materials which offers higher pressure resistance and can be applied over a wide pH range [75]. The stability of the material regarding pressure, pH and temperature results in a lifetime (number of injections) comparable to conventional HPLC column material [67]. The material shows compound dependent specific deviations from theoretical predictions,

compared to pure silica-based particles resulting in further sensitivity and selectivity improvements [68]. Typical column dimensions in UPLC are 1-2 x 50-100 mm, filled with packing material with 1.7 µm diameter. Generally, in gradient runs the highest peak capacity can be obtained either with a combination of short analysis time, short columns and high linear velocity or alternatively with a combination of longer columns and lower linear velocities which results in longer analysis time [65].

2.4. Detection

Peaks widths in UPLC are typically in a range of around one second. In order to obtain enough data points for a clear characterization of the peaks, a high data rate has to be ensured. Another challenge is to keep peak broadening as low as possible. Due to this, a UPLC separation can not easily be coupled with every type of detection system. The coupling with fast time-of-flight mass spectrometers was shown to be successful [76-79], whereas FT-ICR MS with around 1 Hz scanning frequency is too slow for online coupling to UPLC. Nevertheless, at-line coupling of UPLC to FT-ICR MS was shown to be possible to circumvent this problem *[V]* (see also chapter 4). The standard detection system is still photodiode array detection. At least 20 Hz scan rate can be realized with this detector which is fast enough for quantifications even with the narrow peaks observed. The peak broadening effect in the detector cell is addressed in a special way [80]: To provide a long pathway for the light and keeping the volume as low as possible, the light enters the detector cell in a defined angle to the flow direction (fig. 10). The inner surface of the cell is coated with Teflon AF^{TM} which reflects the light. This leads to an improvement in sensitivity by extending the light path length (10 mm) combined with a smaller volume (500 nL).

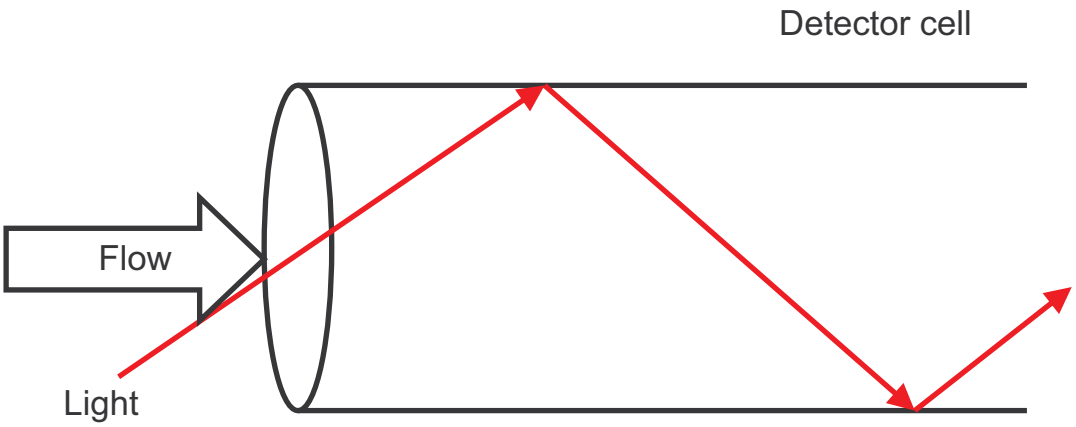


Figure 10: Schematic presentation of the UPLC PDA detector cell: The path of light has a certain angle to the flow direction. This leads to several reflections at the inner wall of the detector cell which results in an elongated path length combined with a low dead volume of the cell.

2.5. Specific observations in ultra performance liquid chromatography

The special properties of UPLC make some effects prominent which are not as important in HPLC. One of these is the dependency of the analysis time from the injection mode: while partial loop injection takes around 5 seconds, a full loop injection takes more than 30 seconds. Given a typical runtime of 1 minute, the overall time consumption is raised by 50 % depending on the injection mode.

Another observation is that the start of the gradient is in time with the injection of the sample. This results in an additional dwell time resulting from the volume between pump and injector: Figure 11 gives an example of a chromatographic run. The programmed run is an isocratic prerun of 0.2 minutes followed by a gradient of 0.5 minutes (see chapter 3.3 for more details). The breakpoint from isocratic to gradient run can be clearly determined by the start of the baseline drift at 0.6 minutes. So, the program start is at 0.4 minutes in the chromatogram. T_0 on the other hand side is determined by the system peak at around 0.2 minutes. This gives an additional chromatographic run time of around 0.2 minutes resulting from the time, the gradient start takes until reaching the injector. In the given example, the first peak at 0.35 minutes could not be analysed in gradient mode.

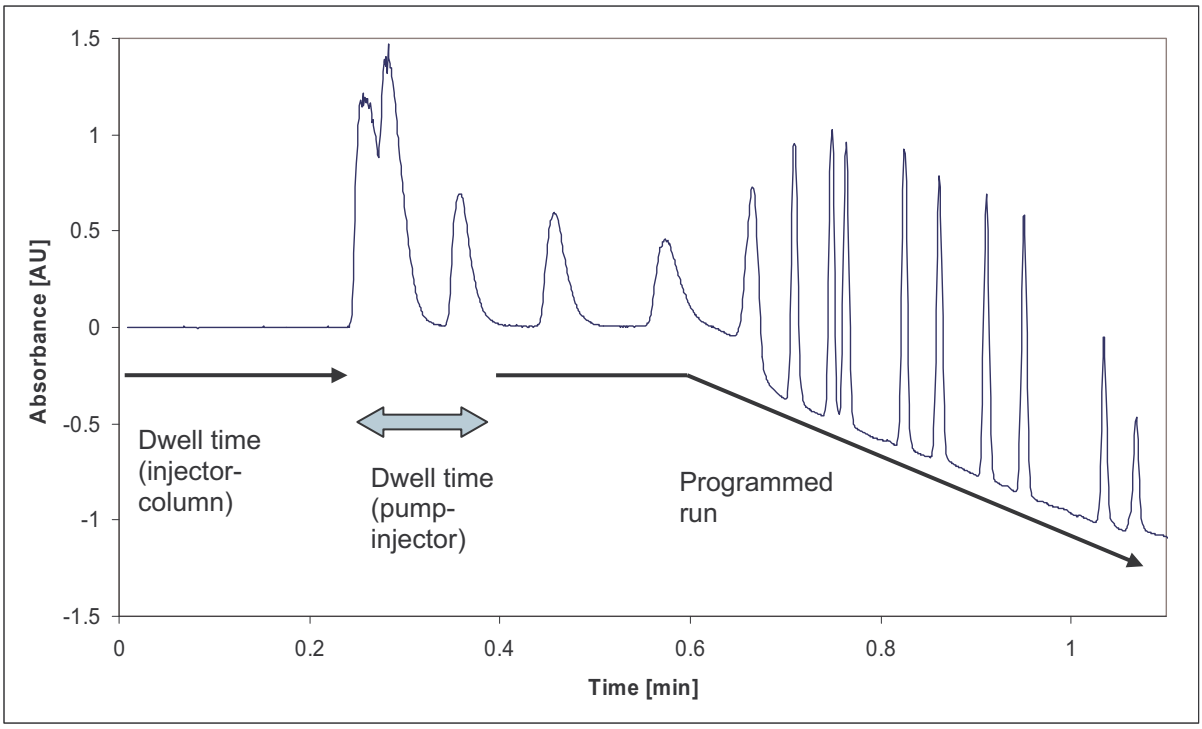


Figure 11: Example of a chromatogram run with 0.2 minutes isocratic prerun before a gradient of 0.5 minutes. The total dwell time results of two dwell volumes: between injector and colum (start of the measurement until the system peak reaches the detector) and between pump and injector (system peak until start of the programmed run).

The high pressure provided by the pump system requires highly pure solvents. Especially acetonitrile turned out to be critical. HPLC grade acetonitrile caused pressure drops during the run due to malfunctions of the pump check valves. The application of acetonitrile of special high grade, provided by some manufacturers, reduced these problems.

3. Results of the development of an analytical platform based on UPLC-PDA analytics[5]

3.1. Introduction

The applicability of UPLC-PDA was tested for the simultaneous and fast analysis of unsubstituted, saturated HSLs and HSs even though these components have almost no chromophores *[VI]*. The separation was optimized in sense of optimal resolution and analysis speed by following various parameters such as gradient settings, solvent pH, and flow rate. The method had to be suitable as well for C7-HS and C7-HSL which is frequently used as an internal standard [43, 47], *[VIII]*. With the optimized method, quantitative performance characteristics were determined and different application examples are given: First the pH-dependent hydrolysis of HSLs over time could be analyzed and modelled. Additionally it was made use of the characteristic of the HSLs to hydrolyze for a further indirect confirmation of their identification in real samples.

3.2. Preliminary experiments

For the separation of the targets, reversed-phase liquid chromatography with C18 as solid phase and a mobile phase consisting of ammonium formate buffer due to the acidic property of HS and acetonitrile (ACN) due to its low UV-cut-off was chosen since HSLs lack chromophore groups and their absorbtion maxima lie in the deep UV part of the light spectrum. A linear solvent strength gradient had to be applied because of the high range of the solubility of the analytes; the difference in the logP values of the analytes was more than 5 (fig. 12). The initial condition for the separation of the mixture of analytes was a gradient setting from 30% ACN in buffer to 100% ACN at a flow rate of 0.9 l/min at 60 °C which resulted in a backpressure of 900 bar (13,000 psi). As injection mode, full loop injection (20 µl) was found to be most suitable, because it guaranteed best reproducibility and sensitivity compared to the different partial loop injection modes possible with UPLC. Although overloading was assumed, it was not observed because of the peak compression effect in gradient runs. With the initial parameters, the asymmetry factors of the analytes were between 0.8-1.2 and the apparent theoretical number was higher than 1000 for the less strongly retained compounds which reflects the suitability of the full-loop injection and the C18 modified silica as a solid phase.

[5] These results presented in this chapter were partially published in *[II].*

At the concentrations used, HSL with longer acyl chains were not soluble in water. The most hydrophobic compound (C14-HSL) was soluble in water with organic solvent of at least one third at 27° C at the highest concentration used. Acetonitrile was chosen as the organic solvent because with methanol, methanolysis of some HSL was observed and confirmed by exact mass measurements using ultrahigh resolution mass spectrometry (FT-ICR MS, data not shown).

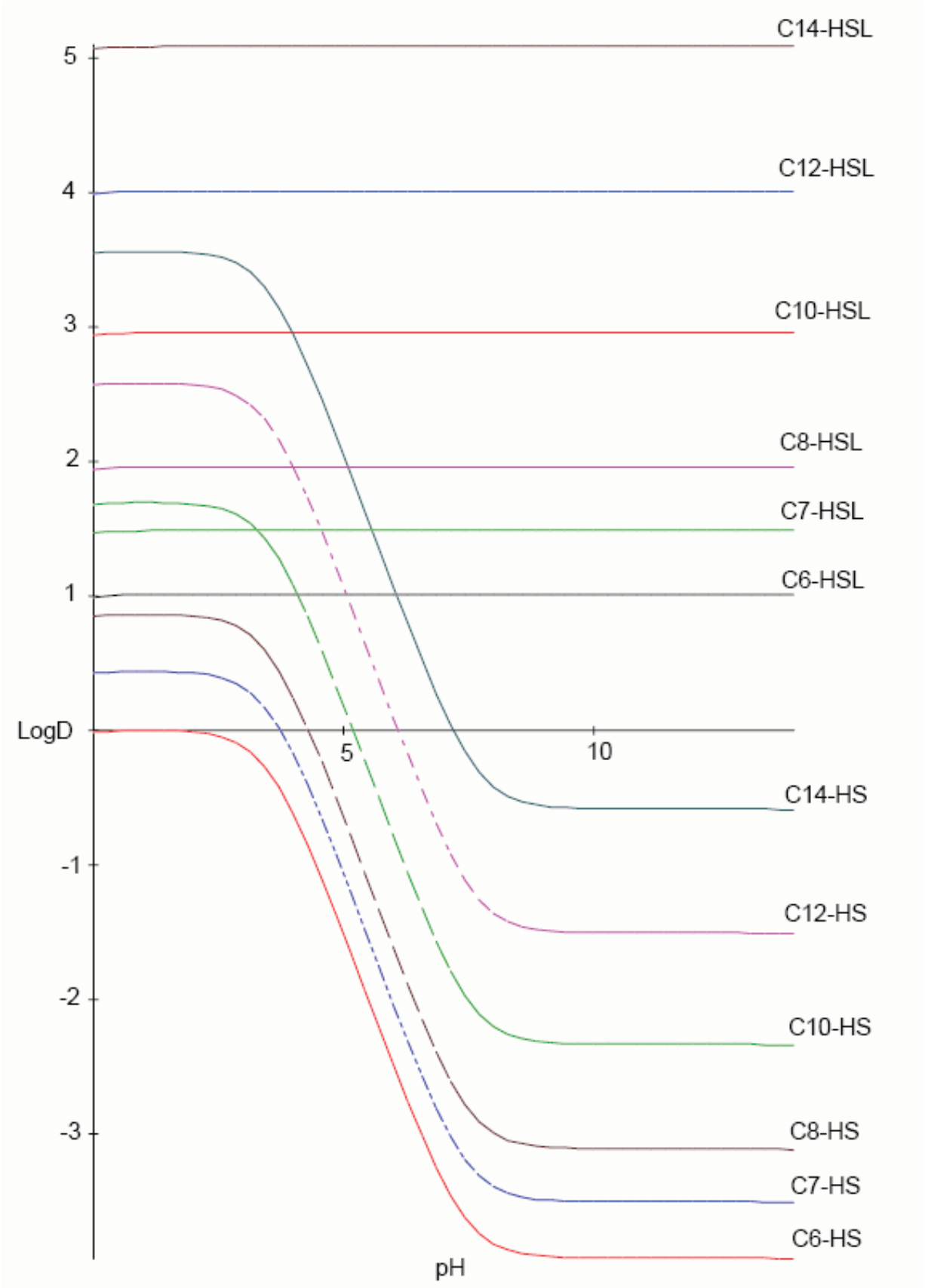


Figure 12: LogD versus pH for the examined *N*-acylhomoserines.

3.3. pH screening

Before the final tuning of the separation conditions aiming the baseline separation of the HSLs and its hydrolysation by-products, the logD values (logarithm of the octanole-water distribution coefficient) were calculated as shown in figure 12. The pK_as of the HSs are similar in the range of 3.2, thus robust separation of the targets could be achieved if the pH of the mobile phase is less than 1.5 but this is too acidic for the chromatographic hardware. On the other side the logP values of the HSLs and HSs are too close together for having baseline separation at highly acidic conditions. Therefore, to achieve the best separation efficiency, the pH was set to different pH values in the range of $pK_a \pm 2$. In that range, the retention times of the HSLs and HSs were linearly dependent on the carbon number of the alkanoyl chain as given in table 3.

Table 3: Formula of the linear correlation curves for the retention times versus the LogD values for the HSL and HS, each group from C4 to C14 at different pH. The gradient settings were a gradient of 1.0 min without an isocratic part.

	pH		R^2
HSL	3.00	y= 6.22 x + 2.20	0.9972
	3.25	y= 6.26 x + 2.25	0.9972
	3.50	y= 6.28 x + 2.24	0.9967
	3.75	y= 6.23 x + 2.16	0.9976
	4.00	y= 6.25 x + 2.20	0.9972
	4.25	y= 6.59 x + 2.62	0.9979
	4.50	y= 6.30 x + 2.27	0.9977
HS	3.00	y= 5.48 x + 2.61	0.9994
	3.25	y= 5.49 x + 2.61	0.9991
	3.50	y= 5.72 x + 2.64	0.9995
	3.75	y= 5.77 x + 2.60	0.9995
	4.00	y= 5.91 x + 2.63	0.9994
	4.25	y= 5.97 x + 2.68	0.9937
	4.50	y= 6.32 x + 2.63	0.9998

The linear correlation coefficients were around 0.997. The slopes of the correlation curves were independent on the pH for the HSLs but light dependency was observed for the HSs. This phenomenon might be caused by the occurrence of another interaction as apolar-apolar (e.g. H-bonding) of the free silanol groups with the carboxylic group as a function of the pH. The linear correlation of the logP and retention time gives the possibility to predict the retention time of derivatives of HSLs (differing in the length of the side chain and/or the number of double bonds) which are not commercially available *[VI]*.

For the final tuning of the separation with the goal to achieve baseline separation of all targets, the pH of the buffer, the gradient time and the influence of an isocratic pre-run

before the solvent gradient was systematically studied (fig. 13). Also the flow rate was later taken into account. The key parameter was the resolution of the critical pairs which were C6-HSL/C7-HS, C8-HS/C6-HSL, C10-HS/C7-HSL, C10-HS/C8-HSL, C10-HSL/C12-HS and C12-HSL/C14-HS as was suspected from the logD plot (Fig. 12).

For the screening, the gradient duration was varied from 0.25 to 1.50 min, the influence of an isocratic pre-run at the initial solvent composition was studied as well. Additionally, the pH was varied from 3.0 to 4.5. At a pH equal to the pK_a of the HSs the separation of the 12 analytes was incomplete (fig. 13). Increasing the gradient time at pH 3.5, coelutions could not be avoided. At lower pHs, the number of the critical pairs decreased but co-elution of C6-HSL and C7-HS could still be observed. For this reason, a mobile phase with a pH higher than 3.5 had to be taken into consideration. Figure 13 also reflects the high complexity of this optimisation and the large influence of all parameters on the separation. As was expected from the logD plot, the number of the critical pairs decreased tendentially with rising pH. The number of critical pairs was generally lowest when the pH of the buffer was 4.25 therefore this setting was examined in detail (fig. 14a).

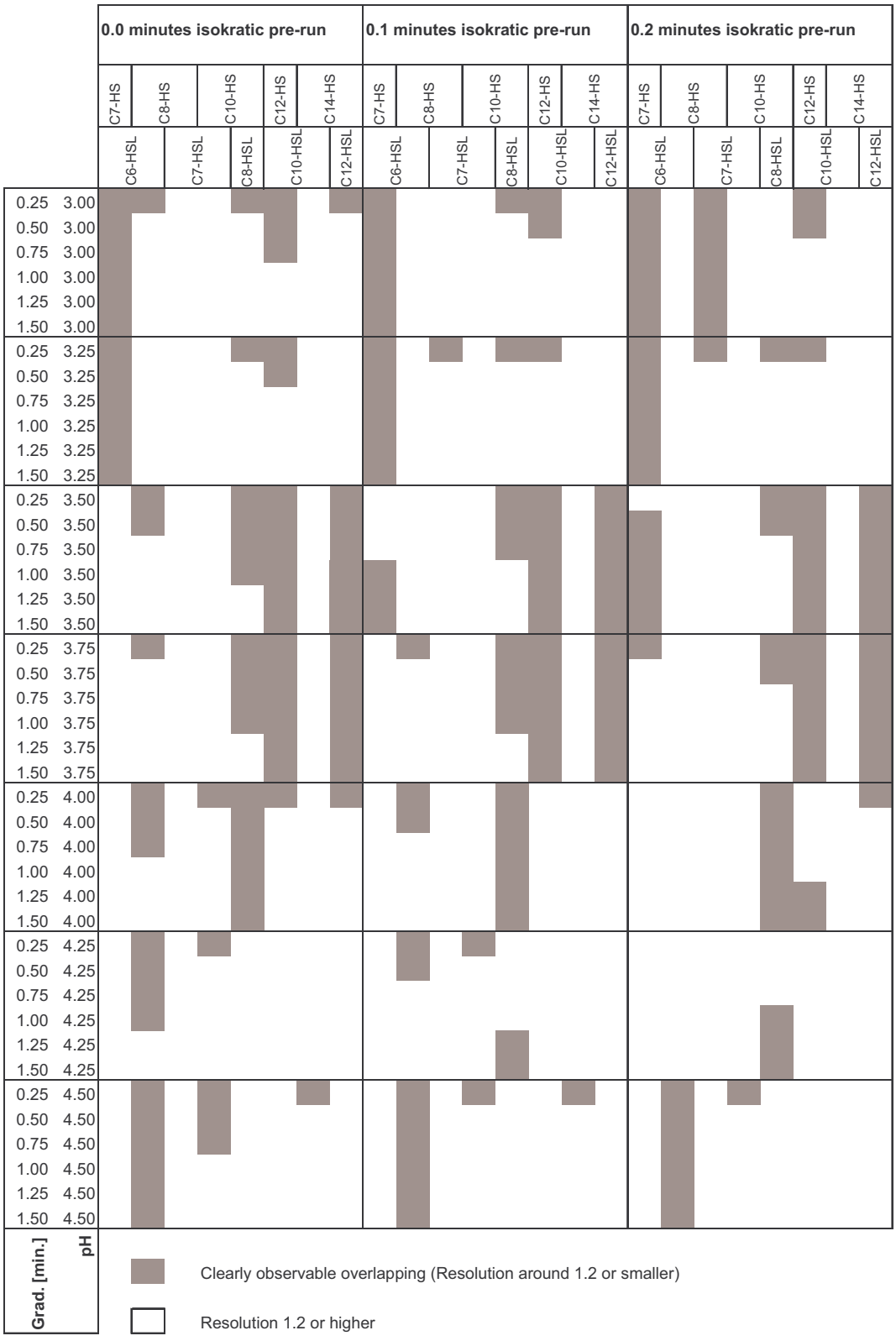


Figure 13: Results of the screening in the UPLC method development showing peak overlappings of HSL- and HS peaks in dependency of the pH, the isocratic pre-run and the gradient duration. The horizontal blocks mean different pHs. Each line gives the gradient duration at this pH. The vertical blocks mean the different pre-run settings. Gray fields mean a clearly observable overlapping (resolution around 1.2 or smaller) of the two analytes given above.

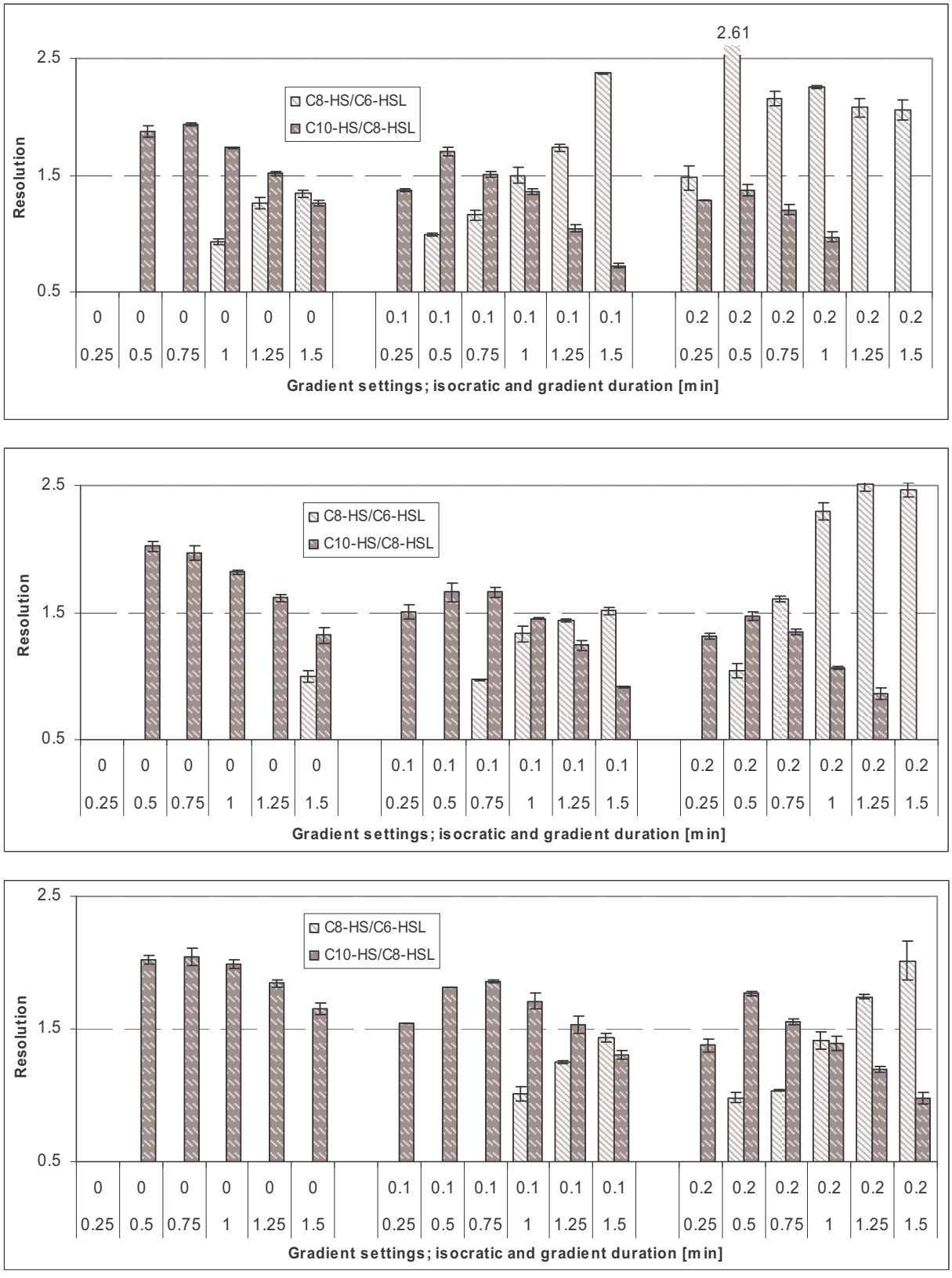


Figure 14: Resolution of the peak pair C8-HS and C6-HSL and of the peak pair C10-HS and C8-HSL at the given gradient settings at pH 4.25. The first line on the x-axis means the duration of the isocratic pre-run and the second line gives the following gradient duration. a) at a flow rate of 0.9 mL/min b) at a flow rate of 0.8 mL/min and c) at a flow rate of 0.7 mL/min.

As shown in Fig 13, the isocratic pre-run had also influence on the retention behaviour at all investigated pH settings. Generally, the number of the critical pairs in the early eluting part of the chromatogram decreased compared to that one without the isocratic pre-run but this parameter also had a high impact on the analytes eluting later.
Having a closer look at the results with pH 4.25 and the critical pairs at this setting (C8-HS-C6-HSL and C10-HS-C8-HSL), it can be observed that at two settings, 0.1 min isocratic run before 1.0 min gradient time and 0.2 min isocratic run before 0.5 min gradient time (0.2/0.5 min), each peak pair was nearly separated; the resolution of all critical pairs were higher than 1.5 except for C10-HS/C8-HSL (1.4 in both cases) as illustrated in figure 14a. Because at 0.2/0.5 min, the first peak pair is clearly separated (an effect of the isocratic-gradient breakpoint), compared to a resolution of only slightly above 1.5 in the other case, and due to the shorter analysis time, the setting 0.2/0.5 min was chosen as the optimum method for the separation of the analytes at a pH of 4.25 and a flow rate of 0.9 mL/min. Figures 14b and 14c show the resolutions at lower flow rates (0.8 and 0.7 mL/min). Also here, no setting is found where the resolutions could be improved compared to the measurements at 0.9 mL/min.

3.4. Determination of the performance characteristics

The chromatogram achieved with the final separation condition is shown in figure 15. The breakpoint from the isocratic to the gradient part lies at 0.6 min, which is between the peaks of C6-HSL and C8-HS. The negative slope of the gradient part of the chromatogram is due to the higher absorbance of the buffer compared to acetonitrile. The breakpoint of the baseline is therefore an indication of the switching from isocratic to gradient run. The breakpoint of the isocratic and gradient part lies at 0.4 min, after program start. This delay may be due to a dead time of 0.25 min between the injection and the detector (dwell time in the narrower sense), and 0.15 min due to an unalignment of the gradient start and the injection respectively the time shift for the gradient start reaching the injector (see chapter 2.5).

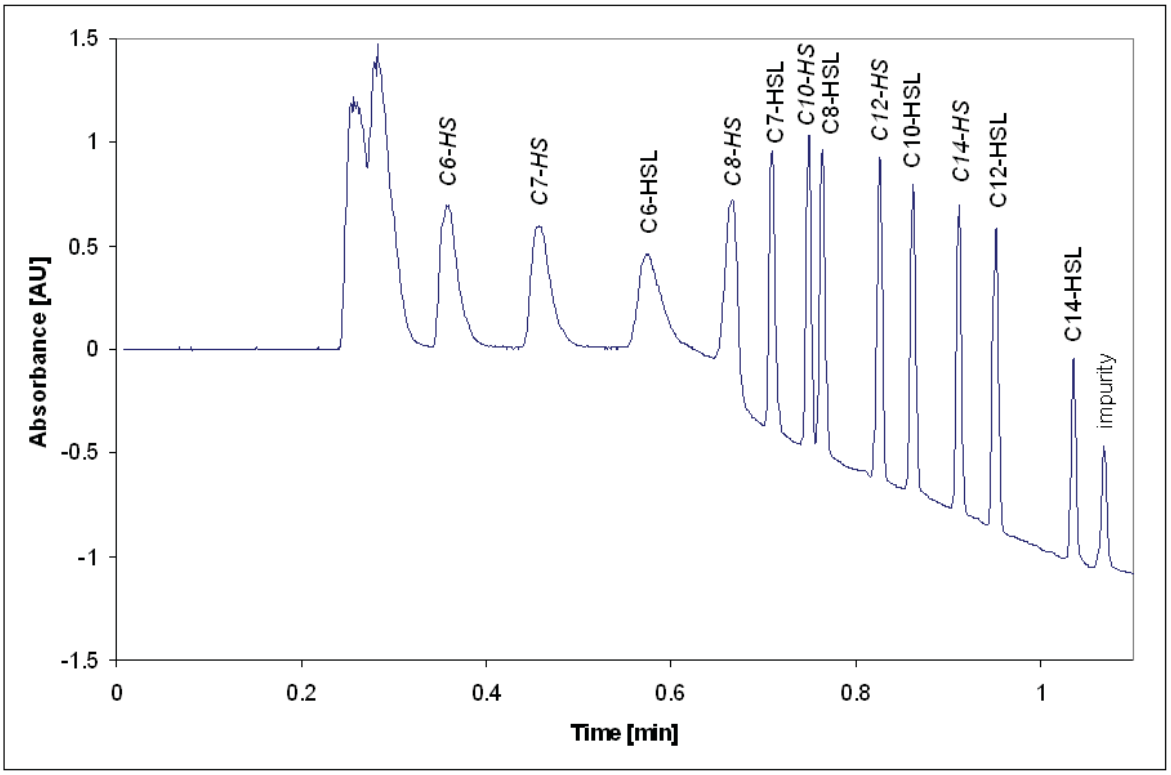


Figure 15: Chromatogram of the twelve examined compounds at pH 4.25 applying a gradient from 30 % to 100 % acetonitrile at a flow rate of 0.9 mL/min in 0.5 min following an isocratic flow of 0.2 min with the initial composition. The last peak is an impurity probably due to the filtration process.

The repeatabilities of the retention times were high since the relative standard deviations (RSDs) were below 0.1 % (0.005 min).

As it was expected, the first three peaks, lying on the isocratic part were relatively wide (0.037 to 0.050 min), while the peaks eluting later are much sharper (0.023 min for C8-HS and 0.010 to 0.012 min for C7-HSL to C14-HSL) caused by the peak-compression effect in solvent gradient (Fig 15). The symmetry factor of the peaks in the isocratic pre-run was higher for C6-HS, C7-HS and C6-HSL. The peak of C8-HS showed a slight fronting, resulting from the isocratic gradient-breakpoint (tab. 4). The symmetry factor for the compounds eluting in the gradient part was determined to be between 0.85 and 1.14.

For C10-HS and C12-HS, the selectivity factor was determined over the whole pH range examined (3.0 to 4.5) at the gradient setting 0.2/0.5 min. The values were always in a range between 1.18 and 1.20 which is a narrow band and shows the high quality of the column packing material [75] since selectivity is only due to the apolarity of the compounds.

Table 4: Separation characteristics of the *N*-acylhomoserine lactones and N-acylhomoserines at the optimum settings.

Analyte	Retention time [min]	Symmetry factor	Resolution to previous peak
C6-HS	0.358	1.79	-
C7-HS	0.458	1.66	2.78
C6-HSL	0.573	1.97	2.72
C8-HS	0.665	0.85	2.61
C7-HSL	0.709	1.14	2.50
C10-HS	0.748	1.06	3.34
C8-HSL	0.763	1.07	1.37
C12-HS	0.825	1.00	5.53
C10-HSL	0.862	1.03	3.16
C14-HS	0.911	1.02	4.44
C12-HSL	0.951	1.03	3.77
C14-HSL	1.035	1.02	8.19

For the determination of the quantitative performance characteristics, calibration curves were measured at three different days with freshly prepared standard solutions. Each calibration curve consisted of six concentrations from 0.75 mg/L to 23.8 mg/L (maximum concentration possible with the used standard preparation method). Therefore, the absolute amount of standards on the column ranges from 15 ng in case of 0.75 mg/L to 0.476 µg in case of 23.8 mg/L. Each standard solution was prepared 3 times for every concentration out of the days stock solution and every dilution was injected 3 times. The average R^2 of the three days were above 0.991 and in the most cases above 0.995 (see tab. 5). They were lower for C10-HS and C8-HSL which may result from the non complete separation, as well as it is lower for C8-HS which may be due to the breakpoint from isocratic to gradient near to the peak (see also fig. 15).

The mathematical limits of detection (S/N>3) were above 1.0 mg/L for the peaks during isocratic elution and better than 0.5 mg/L for the other analytes; however these concentrations could be easily detected in practice. The relatively high theoretical detection limits were due the fact that the examined compounds have no chromophore groups and therefore the absorbance is relatively low.

The robustness of the method for the different analytes is illustrated in figure 16: The repeatability of the peak area increased strongly with the retention time. This was clearly due to the increasing sharpness of the peaks in the gradient part of the chromatogram

and a therefore better peak integration (see also fig. 14). As expected, the repeatability also increased with the concentration. Repeatability is extremely low for C6-HS and C6-HSL as a result of a very problematic peak integration of the very broad peaks at the beginning and the end of the isocratic part. For C6-HSL it decreases at 1.5 mg/L (6.7 %) to increase again strongly at 3 mg/L (10.6 %). This is again the result of the shape of the baseline. At a concentration of 1.5 mg/L, the peak can be clearly distinguished from the baseline-breakpoint, whereby it could not be distinguished from the breakpoint at concentrations of 3 mg/L or higher because of the larger and wider peaks. Setting the limit to 5 % RSD, the method was suitable from this point of view for C6-HSL to a concentration down to around 6 mg/L (where the RSD is 4.8), for C6-HS and C7-HS the limit may lie between 3 and 6 mg/L which was roughly in agreement with the values determined as the theoretical limits of quantification (see tab. 5).

Table 5: R^2 of the average linear regression curves of the *N*-acylhomoserine lactones and *N*-acylhomoserines and the LOD (S/N>3) and the LOQ (S/N>10), given in mg/L and in absolute amounts when 20 µl are injected.

Analyte	R^2	LOD [mg/L]	LOD [ng]	LOQ [mg/L]	LOQ [ng]
C6-HS	0.9997	1.64	32.8	4.49	98.8
C7-HS	0.9984	1.63	32.6	4.90	98.0
C6-HSL	0.9984	1.04	20.8	5.21	104.2
C8-HS	0.9934	0.41	8.2	1.45	29.0
C7-HSL	0.9959	0.32	6.4	1.50	30.0
C10-HS	0.9919	0.11	2.2	1.03	20.6
C8-HSL	0.9949	0.18	3.6	1.17	23.4
C12-HS	0.9973	0.34	6.8	1.37	27.4
C10-HSL	0.9974	0.30	6.0	1.33	26.6
C14-HS	0.9986	0.38	7.6	1.53	30.6
C12-HSL	0.9989	0.36	7.2	1.54	30.8
C14-HSL	0.9998	0.51	10.2	1.77	35.4

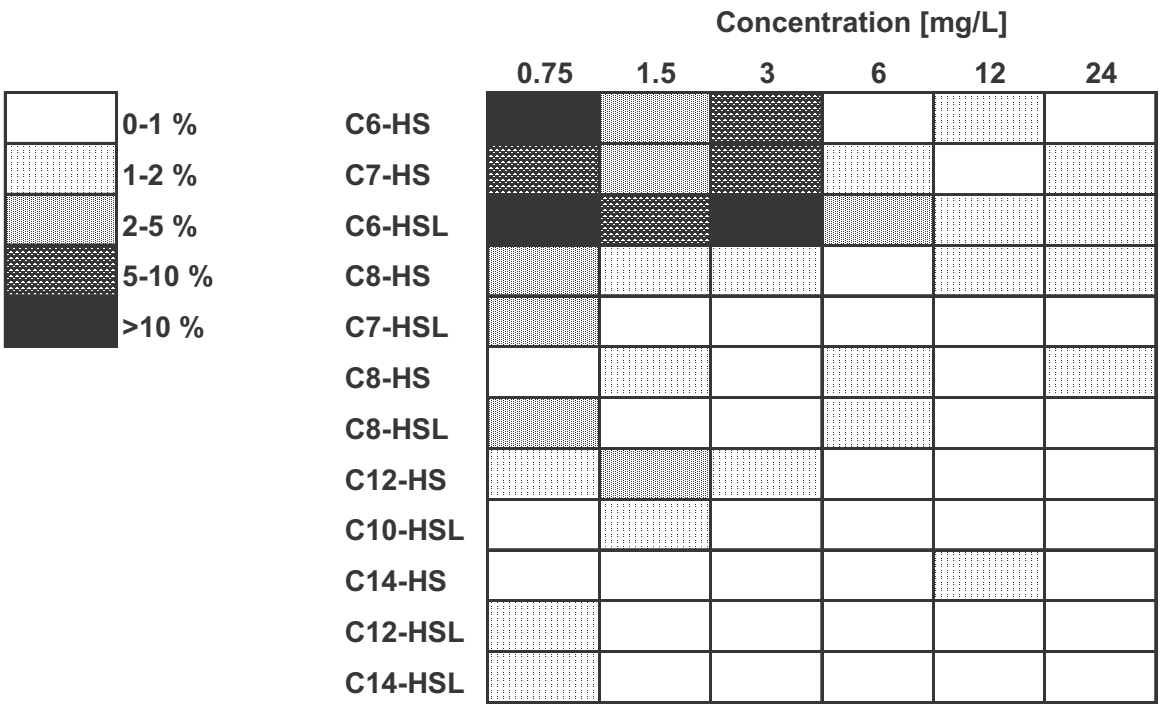


Figure 16: Average RSDs of the peak areas obtained for the different analytes from vial to vial (each standard-solution was injected three times). The analytes are sorted in the order of their retention times.

3.5. Study of the kinetic of the hydrolysis[6]

Since parallel determination of the HSLs and their alkaline hydrolysis products is possible, the effect of the reaction on the pH was investigated over time. It has been reported [18] that the half time inversely proportional depends on the pH of the medium, but no dependence of the side chain was found. Since microorganisms produce very different HSLs, the hydrolysis of the most common quorum sensing molecules, namely C8-HSL and C10-HSL were investigated.

The targets were spiked to a final concentration of 20 mg/L in 10 mmol/L phosphate buffer at pH of 7, 7.5, 8, 8.5 and 9, and the solution was measured repeatedly through 13 hours.

The basic formula for an exponential decay of a HSL reads

$$(1) \qquad HSL(t) = HSL_0 \cdot e^{-\lambda_{PH} t}$$

[6] Mathematical models were developed in cooperation with the Institute for Biomathematics and Biometry at the GSF National Research Center for Environment and Health, Neuherberg. Thanks to Christina Kuttler.

where HSL(t) denotes the actual HSL concentration at time t, HSL_0 the initial HSL concentration and λ_{PH} the degradation rate of HSL (may depend on the pH and also may differ slightly for different HSLs).
The model could be fitted very well to the experimental data. Furthermore, the fitting could also be done for the N-acyl-homoserines (HSs) (see Fig. 17):

$$(2) \qquad HS(t) = HSL_0 - (HSL_0 - HS_0) \cdot e^{-\lambda_{PH} t}$$

HS(t) denotes the actual HS concentration and HS_0 the initial value. In case of the initial concentration of HS being zero ($HS_0 = 0$) and assuming that the product of *HSL(t)* and *HS(t)* remains constant ($HSL(t) + HS(t) = HSL_0$), equation (2) can be simplified as follows:

$$(3) \qquad HS(t) = HSL_0 \cdot (1 - e^{-\lambda_{PH} t})$$

The resulting values for λ_{PH}, using the data for HSL and HS, respectively, are in the same range for the HSLs in case of higher pH; for lower pH (around 7) the hydrolysis is so slow that only for a few points in time the HSs are on a level above the detection limit and cannot be used very well for such a fitting procedure. So, there seems to appear further reactions which were not considered here.
Taking together the resulting λ_{PH} values for each type of HSL (see also Fig. 18) yields the following formulae for the half time $T_{1/2}$, dependent on pH:

$$(4) \quad \text{C8-HSL:} \qquad T_{1/2}(pH) = 168 \cdot e^{-2.1(pH-7)} h$$

$$(5) \quad \text{C10-HSL:} \qquad T_{1/2}(pH) = 162 \cdot e^{-2.1(pH-7)} h$$

Generally, both types of HSL considered here are more stable than the formula in Schaefer et al. [18] states, even though a different HSL compound was used there (oxo-C6-HSL).

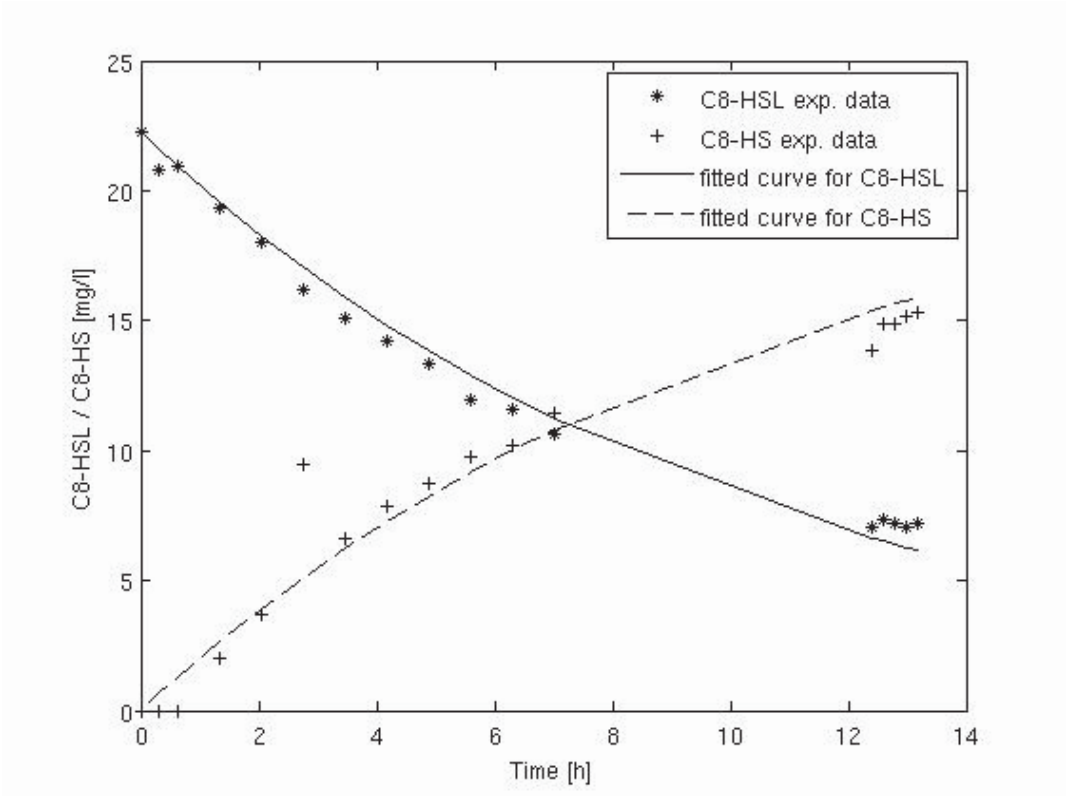


Figure 17: Comparison of experimental data and fitted curve: a time course (in minutes) of C8-HSL and C8-HS at pH 8.5.

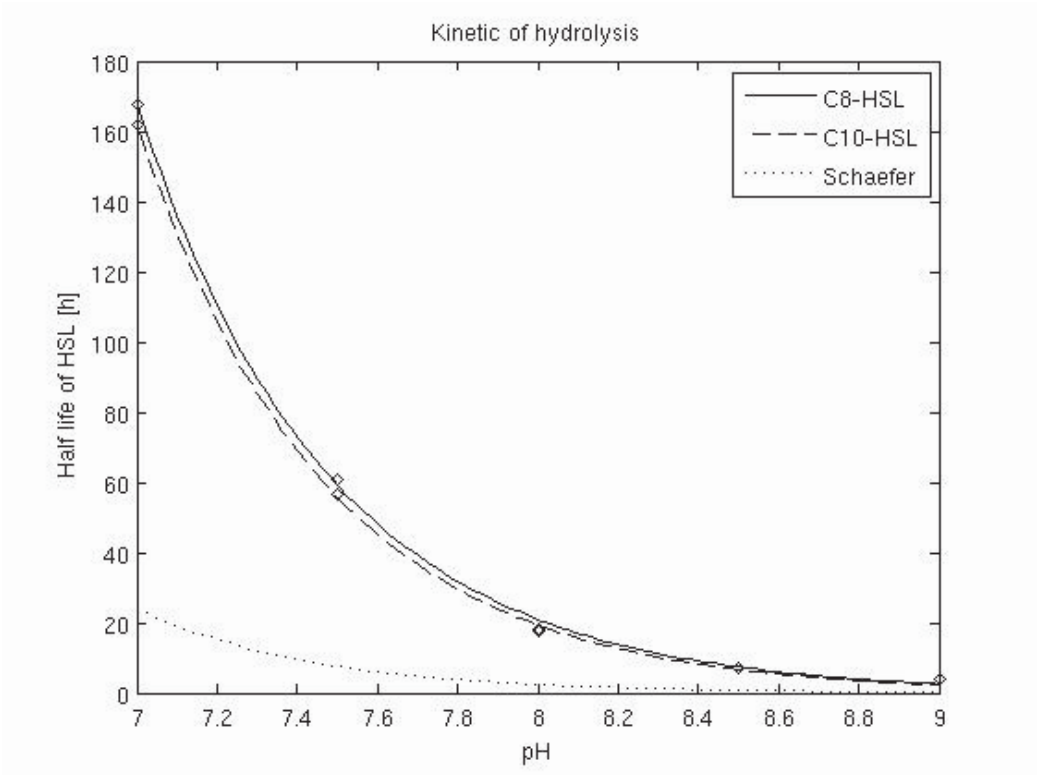


Figure 18: Dependence of the half life of HSLs (in minutes) on the pH value and comparison of the results with the formula of Schaefer et al. [18] which seems to underestimate the half life.

3.6. Real sample analysis

To enable real sample analysis, the sample has to be extracted. One method applied here was developed for the solid phase extraction of bacterial culture supernatants for UPLC analysis *[VII]*. In this work, several reversed phase SPE cartridges were tested. The wide range of the polarity of the compounds was the critical factor, so the goal for the determination of the optimum elution solvent composition was to increase the recovery of the polar analytes while simultaneously maintaining the one of the unpolar ones. Generally, elution with iso-propanol showed the highest recoveries which were however still poor for C4 and C14-HSL. Hexane, toluene and tetrahydrofuran were tested in different rates and hexane was found to be best. The optimum was found to be 25 % hexane and 75 % iso-propanol (v/v) which increased the recovery of C12 to above 95 %. The recovery of C14-HSL was still at around 75 %. For the washing of the loaded solid phase, a mixture of water with 15 % Methanol was found to be suitable to remove also polar compounds without lowering the recoveries. Matrix effects could be reduced by addition of 25 % acetonitrile to the sample before applying it on the column.

The optimized method resulted in recoveries higher than 90 % for C6-, C7-, C8-, C10- and C12-HSL, while C4- and C14-HSl can be determined only semiquantitatively. The RSDs were determined to be between 1 % and 4 %. The method was successfully applied for different culture media.

The chromatogram resulting from the analysis of the supernatant of a *Burkholderia* culture is shown in figure 19 a. The concentrations determined in the non-hydrolyzed sample were 1.61 mg/L (0.90 % RSD, n=3) for C10-HSL, 0.82 mg/L (2.20 % RSD, N=3) for C10-HS and 0.23 mg/L (0.97 % RSD, n=3) for C8-HSL. The last 2 values were below the limit of quantification (see tab. 5). This shows that the method is suitable for the determination and quantification at least of the compounds that are highly expressed by the bacteria. For lower concentrations, a more sensitive detection (i. e., mass spectrometry) would be necessary. A simultaneous quantification of C10-HSL and C10-HS is possible and the “critical pair” (see 3.3) C10-HS and C8-HSL is relatively well separated. Matrix effects were lower when applying a pH controlled method compared to a water/acetonitrile gradient applied by Li et al. *[VII]*, where the same sample was used. In this work, the same lactones were found with another UPLC method.

When hydrolyzing the sample, the lactone peaks disappear completely (fig. 19b). The concentration, determined for C10-HS was in this case 2.43 mg/L (0.45 % RSD, n=3). This shows that the lactones were hydrolyzed completely:

6.33 µM C10-HSL were determined in the unhydrolysed sample besides 3.00 µM C10-HS. In the hydrolyzed sample, 8.91 µM C10-HS were determined. The stochiometric

deviation was therefore lower than 5 %. Applying this method, it is therefore possible to determine HSLs by their hydrolysis behavior.

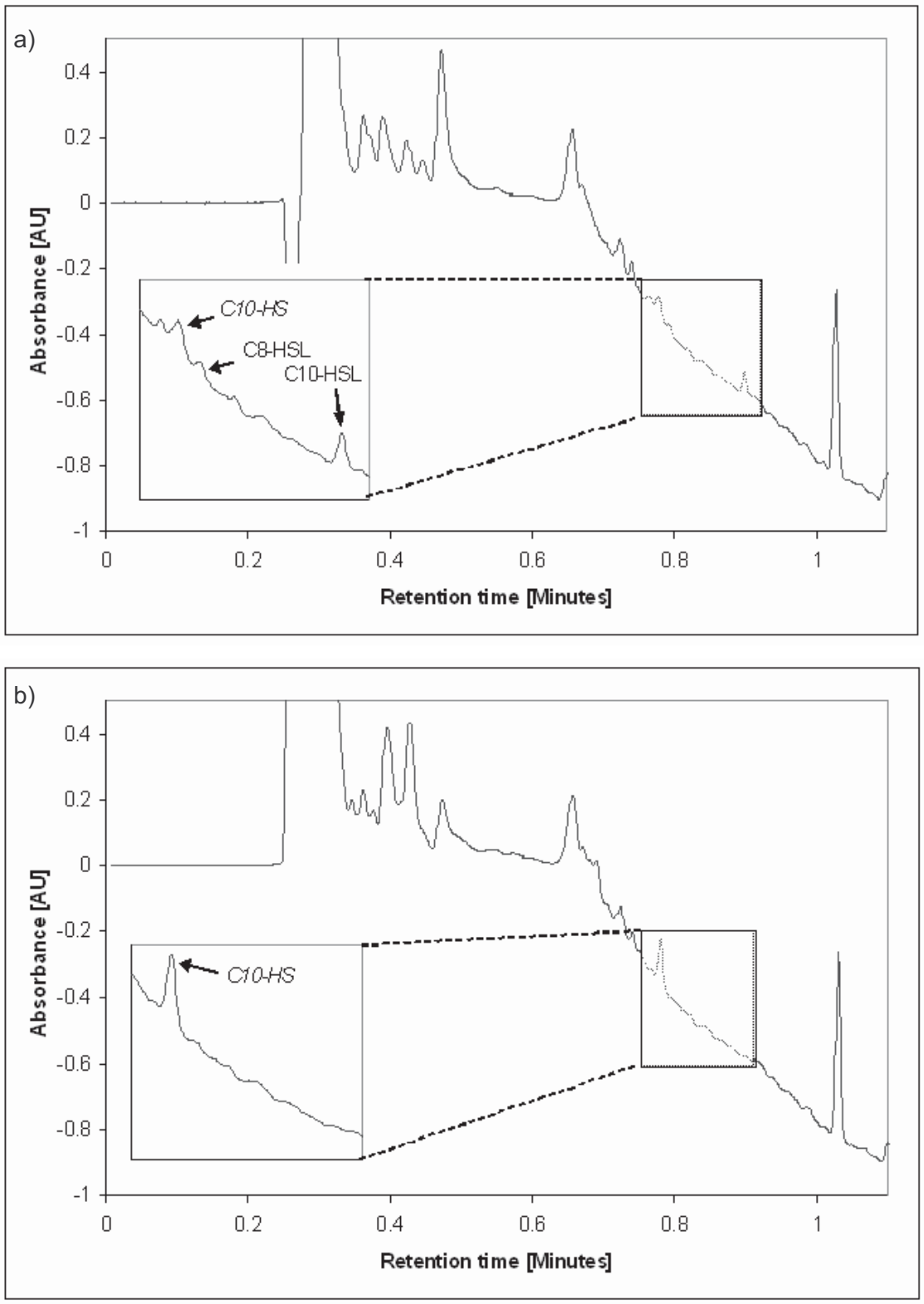


Figure 19: Chromatograms of a real sample (supernatant of *Burkholderia cepacia*, strain LA-3, which was grown in LB medium and after SPE extraction redissolved in acetonitrile/water, 30/70, v/v which results in a 10fold concentration) examined with the developed method. Fig 8a shows the unhydrolysed sample, fig. 8b, the sample after hydrolysation under alkaline conditions. C10-HS, C8-HSL and C10-HSL are determined in the unhydrolysed sample, in the hydrolysed sample, only C10-HS could be determined.

3.7. Conclusion

Running the system at pH 4.25 from 30 % to 100 % acetonitrile at a flow rate of 0.9 mL/min in a gradient of 0.5 min following an isocratic flow of 0.2 min with the initial composition was proved to be the optimum setting for the separation of *N*-acylhomoserine lactones with a chain length of 6, 7, 8 ,10, 12 and 14 carbons together with the corresponding *N*-acylhomoserines. Although resolution may not be complete and peak shapes were not optimal for all compounds, the presented method was shown to be the best compromise for this challenging separation task. The separation was performed within around one minute, which is extremely fast compared to conventional normal speed HPLC methods (up to more than 40 min [43]), especially when considering the fact that the method was optimized in view of optimum resolution and not in view of shortest analysis time. The method was optimized for standard solutions at concentrations at least down to 6 mg/L for C6-HS, C7-HS and C6-HSL and at least down to 1.8 mg/L for the other analytes. This is shown to be sufficient for the determination and quantification in real samples when solid phase extraction is used as cleanup and for preconcentration. Much higher sensitivities are expected to be reached when UPLC^{TM} is coupled to fast mass spectrometry which is directly possible with the developed method as only volatile buffer salts were used. Already the sensitivity with PDA opens possibilities for further experiments using standard equipment. The hydrolysis kinetics of two HSLs was studied and a half-life depending on the pH was determined and found to be in good agreement with mathematical models. By hydrolysis of the samples, the lactones can easily be transformed to the serines which can be used as an additional confirmation method, decreasing the risk of miss-identification.

4. Integration of ultra performance liquid chromatography methods

All single methods for the determination and quantification of HSLs have clear limitations: UPLC is fast, automated, selective and highly quantitative but limited in sense of sensitivity and provides poor information about the analytes. FT-ICR MS on the other hand side provides plenty of structural information of the analytes but quantification is difficult and sensitivity is limited due to the matrix compounds. The best information on the biological activity of HSLs provides the bioassay approach which is on the other hand side not very selective and encloses the danger of false positive results [28]. So, to achieve sufficient information for the identification of HSLs in unknown samples, several approaches have to be combined with each other.

Online coupling of UPLC to FT-ICR MS is not possible due to the low scan rates of the mass spectrometer and the high speed of the UPLC measurement. One way to circumvent this is at-line coupling, respectively fractionation. A method for the at-line coupling of UPLC to chip-electrospray FT-ICR MS for the analysis of HSLs was developed by Li et al. *[V]*. The fractions were manually collected after PDA detection in realtime. The efflux of the UPLC separation was collected droplet-wise. In order to keep the sample collection in time witch the data aquisition, a delay lop was inserted in the UPLC efflux. Typically two or three droplets represent one fraction, respectively one peak of the separation. The method was adjusted to gradient runs, where changes in droplet speed and volume due to a changing composition of the solvent were corrected. In a gradient run of 1 minute, recoveries were over 90 % for early eluting peaks and more than 60 % for later eluting compounds (see fig. 20).

The fractions were collected in micro-titer well plates which are amenable for chip-based electrospray ionization. A further automatisation towards a robotics driven fraction collection into the well plates is generally possible.

This method is perfectly suited to combine fast separation and reliable quantification with identification and confirmation applying the high resolving power of FT-ICR MS.

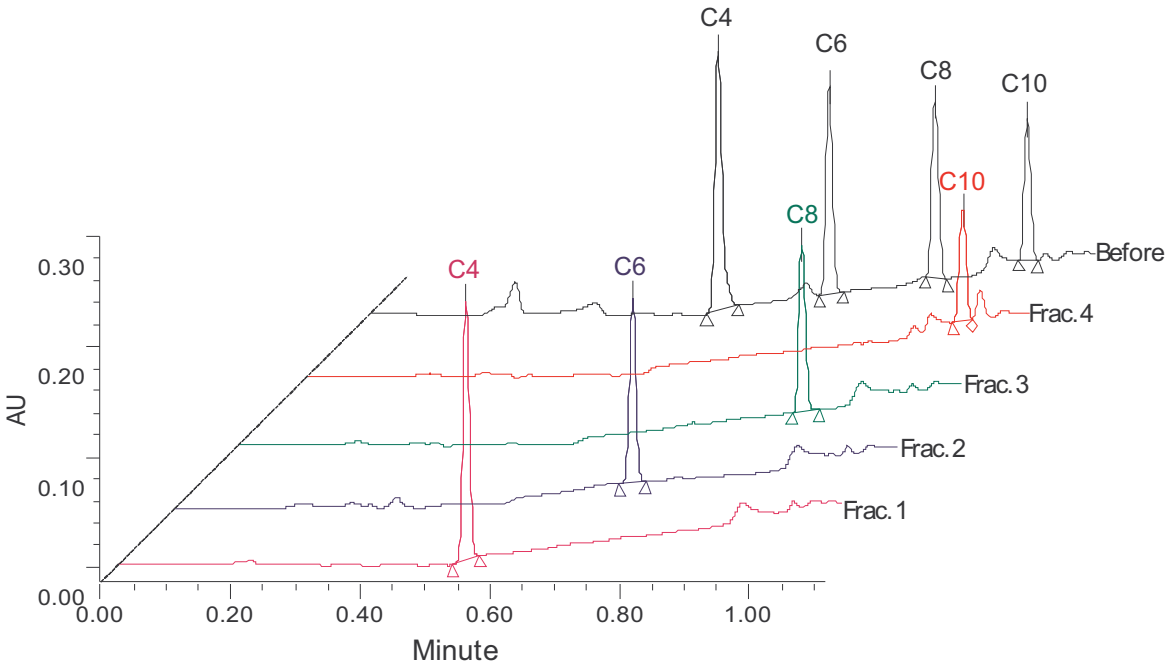


Figure 20: UPLC chromatogram of a sample containing C4-, C6-, C8- and C10-HSL before the fractionation and chromatograms of each fraction reinjected.

Another approach for the combination of four different methods for the determination of HSLs in real samples by Fekete et al. *[VI]* is schematically displayed in figure 21: In this approach, different bacterial culture supernatants were screened for the presence of HSLs, whereby not only unsubstituted HSLs were taken into account but all theoretically possible substituted and unsaturated HSLs could be determined. Analytical standards are only available for some HSLs, mostly unsubstituted ones. The analyte was determined by the intersection of results obtained by different methods: A UPLC analysis of the extracted bacterial culture supernatants similar to the one described in chapter 3 but without pH control (the method was only applied for the detection of unhydrolysed HSLs) and steeper gradient was applied. This resulted in around 50 peaks. These results could be further filtered by comparison of the peaks with the retention times expected for all possible HSLs. These retention times could be obtained applying an in-silico prediction which is based on the linear dependency of the retention times of the logP values of analytes within a homologous series[7]. The peak spectra gave additional weak hints for the focusing on around 5 candidates. The complementary approach was based on FT-ICR MS analysis of the same sample. The analysis results in around 15,000 peaks exceeding a signal to noise ratio of 4. These results were further reduced by comparison with a database containing the exact masses of all possible HSLs presuming either protonisation or Na^+ cationisation. These are 84 possible ions overall.

[7] This method is based on the Martin rule [81]

The intersection of these results was closer examined by confirmation of these results by TLC with detection by reporter strains.

Table 6 gives the results obtained for the bacterial culture supernatant of *Acidovorax sp.* N35, where OH-C10-HSL could be detected.

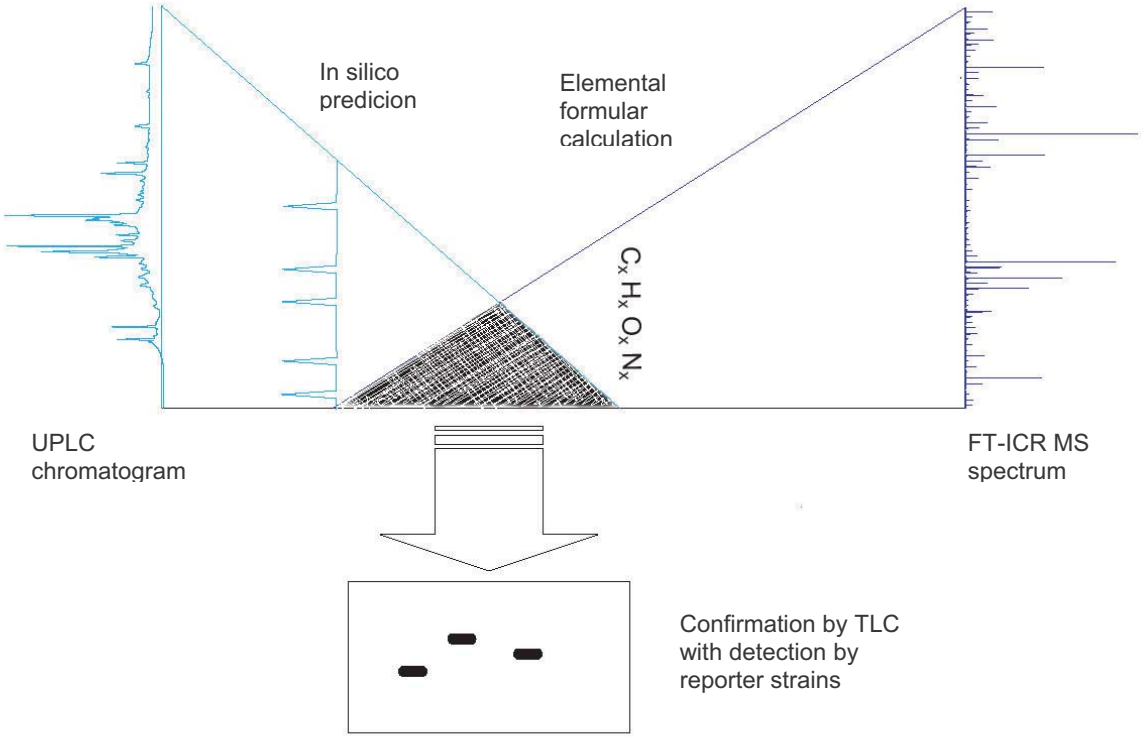


Figure 21: Schematical presentation of one example for the integration of several methods for the determination of HSLs in real samples. The peaks obtained by UPLC analysis were reduced by filtration of the data by in silico predictions of possible HSLs. The data obtained by FT-ICR MS were stripped down to the peaks corresponding to the elemental compositions possible for HSLs. The intersection of the candidates was confirmed by TLC with application of detector strains.

HSL	UPLC + prediction	FT-ICR MS + database
OH-C4-HSL		
oxo-C4-HSL		
OH-C6:1-HSL		
oxo-C6:1-HSL		
OH-C6-HSL		
C4-HSL		
oxo-C6-HSL		
C4:1-HSL		
OH-C8:1-HSL		
oxo-C8:1-HSL		
OH-C8-HSL		
oxo-C8-HSL		
C6-HSL	x	
C6:1-HSL		
oxo-C10:1-HSL		
OH-C10:1-HSL		
oxo-C10-HSL		x
OH-C10-HSL	x	x
oxo-C12:1-HSL		
C8-HSL	x	
OH-C12:1-HSL		
C8:1-HSL		x
oxo-C12-HSL		
oxo-C14:1-HSL		x
OH-C12-HSL	x	x
OH-C14:1-HSL		x
C10:1-HSL		
C10-HSL		x
oxo-C14-HSL		x
oxo-C16:1-HSL		
OH-C14-HSL	x	
OH-C16-HSL:1		
C12-HSL:1		
C12-HSL		
oxo-C16-HSL		
oxo-C18-HSL:1		x
OH-C16-HSL		
OH-C18-HSL:1		
C14-HSL:1		x
C14-HSL	x	x
oxo-C18-HSL		x

Table 6: Results obtained by different analytical methods for a supernatant of a *Acidovorax sp.* N35 culture. The candidates marked with x in the left column are the ones obtained with the combination of UPLC and prediction. The ones marked with x in the right column are the candidates obtained by FT-ICR MS analysis and comparison of the elemental formula. OH-C10 was confirmed by the bioassay. Nomenclature: “oxo-“, or “OH-“ for the substitution at the β-carbon. “:1” indicates a double bond in the alkyl-chain.

5. Prinziples of piezo driven drop-on-demand dispensers and applications in analytical chemistry and life sciences

5.1. Introduction

Dispensers for the exact dosage of small volumes were initially developed for inkjet applications in the 1950ies first for industrial applications. Modern drop-on-demand dispensers were developed in the 1970ies and became popular with the market success of the first inkjet printers about ten years later. In inkjet technology, among some others, two methods are the most widespread: “continuous” and “drop-on-demand”. Continuous inkjets are mostly applied in industrial applications i.e. for the printing of the expiration date on food packages. A continuous flow of ink is acoustically disrupted into single droplets. These droplets are charged and can be deflected in an electrical field. By application of zero or a basic electric field, the droplets are captured in a funnel and recycled into the ink reservoir. Applying a certain electric field will result in a deflection of the drops which are directed onto a surface o be printed on [82]. This method is fast and reliable but the frequency normally can not be changed and the amount of dispensed fluid has to be quite high because the system must be kept running continuously. In contrast to this method, the term “drop-on-demand” was created which means that distinctive droplets are created at a freely choosable point in time. In most cases, the pulse is applied by a piezo element[8]. After application of the pulse, the system relaxes. This does not mean that this kind of dispensers can not be run in continuous mode but in this case the frequency will not be as high as in a continuous system. Around 400 Hz is the highest frequency for stable and reproducible droplet production in conventional dispensers. The period between two pulses is in this case still about 50 times higher than the pulse duration.

The main properties of the instruments can be derived from the inkjet application they are developed for: To produce a clear and high resoluted print layout, the droplets of ink (and accordingly the pixels) have to be first as small as possible and second be exactly positioned on the surface to be printed on. In most cases, the distance to travel before the impact is relatively short. Reliability and stability are also important factors for everyday usage. For the printing of ink, the reservoir of the ink is typically huge compared to the volume of the droplets. This is a fact which may be critical in some applications outside

[8] A prominent alternative would be the thermal inkjet, where a thermally induced expansion of an air bubble provides the overpressure needed or the mechanical application of a pulse [82]

inkjet technology because especially in life sciences, the solutions to be dispensed may not be available in larger amounts.
An inkjet is optimized for one specific fluid (the ink). It is not designated for changing to a different fluid. An application in chemistry or life sciences may require this feature but this limitation can be overcome by changing the pulse parameters. Many liquids with a wide range of physical properties are successfully dispensed after optimisation of the pulse parameters.

5.2. Technology

A drop-on-demand dispenser system consists of three major parts: the capillary, the piezo element and a control unit. To visualize the droplets, a setup to provide this should be included.
The capillary is in most cases made of glass and with a tapered, cylindrical hole in the nozzle. A tapered end is advantageous compared to a cylindrical end, because of the lower fluid impedance and the therefore lower pulse impedance needed for ejection as well as a faster refill and therefore higher speed [82]. In some cases, the wetting of the nozzle surface by the fluid to be dispensed is an important factor to provide stable conditions [83]. The capillary is cylindrical surrounded by the piezo element. Nowadays, in contrast to the cylindrical capillaries, microchip based systems are more frequently applied. Here, the volume, as well as in some cases the orifice is rectangular and the piezo element is flat and is positioned below the chip. The advantages of these chip-based printheads are the low volume, the small size and advantages in the manufacturing. These systems are relatively easy to integrate in larger setups [84]. On the other hand side, still conventional dispensers are often more reliable and stable. Figure 22 shows two commercially available dispenser heads, one conventional dispenser and a chip based one.

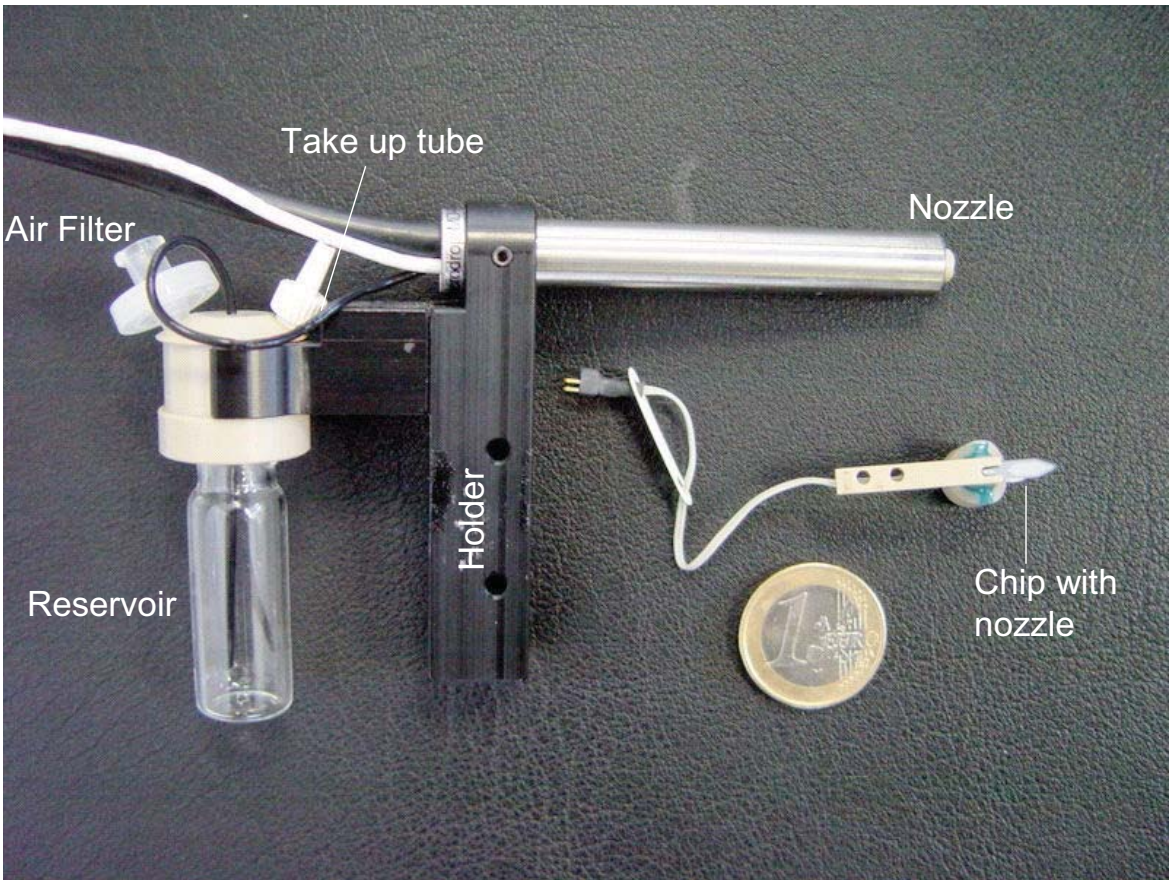


Figure 22: Two examples of dispenser heads: The larger dispenser is a MD-K-130 HV system from Microdrop Technologies, Norderstedt, Germany, the small dispenser is a chip based PICPIP dosage system by GeSiM, Großerkmannsdorf, Germany.

Most piezo elemets are based on lead circanate titranate (PZT) ceramics. It provides the pulse by contraction when voltage is applied onto it. Hereby, the length of the contraction is approximately the same as the pulse duration and the pulse voltage is approximately proportional to the deflection of the piezo element. It some cases it may be advantageous to define the steepness of the edges of the pulse [85]. A third parameter which may play a role in the droplet production is the frequency of the dispensing: While at low frequencies, the time distance between two pulses is large enough, at high frequencies the system may not relax completely so that the fluid is still oscillating, when the next pulse is applied which leads to a different droplet production.

The visualisation of the produced droplets is performed by a light source which is coupled to the frequency generator during continuous dosage and produces flashes of light at the same frequency. In most cases, this is a LED diode. By changing the delay time of the flash relative to the pulse, different stages of the droplet production can be observed as a standing picture (see also fig. 37 in chapter 7.1). A magnification device is needed to visualize the drops which are a few µm in size.

A rough check, if the dispenser runs well can be performed by the experienced operator by observation of the droplet stream illuminated in front of a dark background or by observation of the droplets impacting on a mirror. The droplet ejection, the direction and the appearance of misdirected satellite droplets can be controlled this way without the need for a visualisation apparatus [86].
The accuracy of the dispensers is very high: typically relative standard deviations in the range of 1% are reported [87-89], *[I]* whereby in most cases the determination of the accuracy may be limited by the method applied, so that the real accuracy of the dispensers is even higher.

5.3. Droplet production

Apart from the fixed parameters like the inner diameter of the nozzle which has a high influence on the droplet size [90], a proper droplet production depends on several parameters influencing each other: On the fluid side it is viscosity and surface tension, on the instrument side this is pulse length, pulse amplitude and in some cases the dispensing frequency. The droplet production is therefore a very complex process and the optimum settings of the instrument have to be found for every fluid individually and experimentally [82]. Generally, the pulse parameters stand in relation to each other: It is not always possible to change only one parameter without also changing the other parameter implying that still stable droplet production is guaranteed. Wu et al. [91] showed that with increasing viscosity and surface tension, the droplet becomes tendentially slower but more stable. Stable temperature conditions are important, since temperature influences viscosity strongly which again has a high impact on droplet formation.
After application of the pulse onto the capillary, a sinus-like pressure wave elongates in the fluid and causes an aliquot of the liquid to be ejected from the nozzle [91]. This is ejected in form of a column during time of overpressure which breaks near the nozzle, when liquid pressure in the capillary goes down. Due to oscillations within this longish volume, one or more constrictions occur which break the droplet in normally two parts[9]: The bigger main droplet at the front end and a smaller satellite drop which has a higher speed and unites with the main droplet within the first µm of flight [91]. After that, still oscillations within the droplet are observable which relax after some time. It should be noted that during flight, the droplet is not completely spherical due to aerodynamic forces [92]. Nevertheless this deviation is small for sub 100 µm droplets and therefore in most cases negligible [82].

[9] In some cases, two constrictions lead to the formation of three separate drops, which unite one after another [90], [91]

Frequently observed malfunctions in the droplet production are schematically presented in figure 23. In most cases deviations from normal function are caused by particles on the nozzle surface or by air bubbles in the capillary which absorb the pulse completely or partially and can have large influence on the physics underlying droplet production in several ways [93, 94]. A cleaning of the nozzle followed by an emptying and slow refill (eventually several times) of the capillary normally solves theses problems.

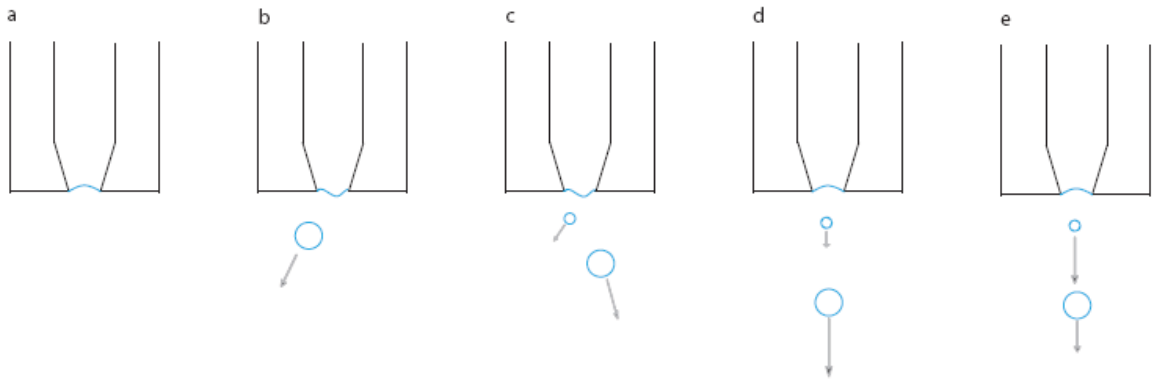


Figure 23: Schematical presentation of frequently occurring droplet production malfunctions and effects: a: no droplet is ejected. The reason therefore may lie in electronical failures or an air bubble is enclosed in the capillary which may absorb the pulse. b: A misdirected droplet may be caused by particles on the nozzle surface or small air bubbles in the capillary. c: Asymmetrical waveforms caused by particles or small air bubbles may also be the reason for the production of several droplets flying in different directions. Wrong puls parameter settings may cause the same effect. d: A satellite droplet which has the same trajectory than the same droplet but a lower speed will not unify with the main droplet and is also an indication for bad pulse settings. e: A satellite droplet with higher speed than the main droplet is often unavoidable and can not be seen as a malfunction because it unites with the main droplet.

For some applications, it may be necessary or advantageous to produce charged droplets. This is performed by applying an electrical field between the dispenser and the target. One example of a method for the production of charged droplets is given in figure 24: The droplets produced by the dispenser (which is grounded) fly through the holes in two parallel isolated plates. The plate at the dispenser side is also grounded, while a voltage of 500 V is applied on the other plate. The droplets (charged due to the electric field between dispenser and second plate) fly through the holes in the plates. When the kinetic energy becomes lower, the trajectory of the droplets changes and they discharge on the edges of the first, grounded plate, as can be clearly observed on the picture. The

droplets are in this case oppositely charged to the voltage applied on the second plate. A charging of droplets may be advantageous for example to increase the flight distance, the speed or to deflect them in an electric field.

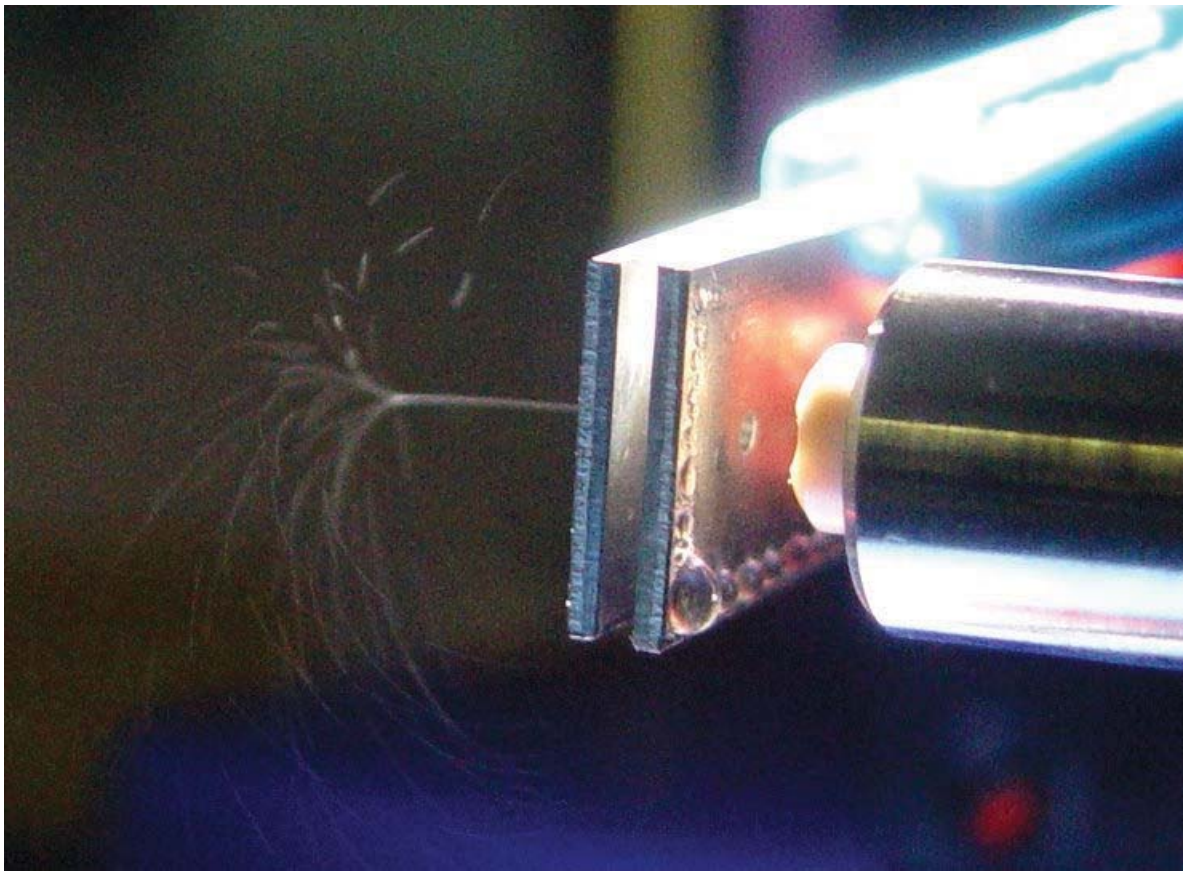


Figure 24: Production of charged droplets. The dispenser (at the right side of the picture) and the right plate are grounded, while a voltage is applied on the left plate. The droplets fly through holes through both plates, before they change their trajectory and discharge on the edges of the first, grounded plate.

5.4. Determination of the droplet size

The determination of the size of the droplets produced is important, especially, when quantitative or semi-quantitative dosage has to be performed. Generally two main approaches can be made by use of standard laboratory equipment: The determination of the droplet size via imaging of the droplet and graphymetrical approaches. A third way could be the verification of the results by chemical quantifications of a dispensed analyte (see chapter 6.4). More elaborate and complex optical methods are only mentioned for

completeness[10]: The phase Doppler technique is based on the detection of the phase shift of scattered light detected by two detectors which are positioned in a defined angle to each other. In the interference method, fringes are analysed which result from interferences of light scattered by the droplet. In the white light method, the droplet size is derived from the intensity of scattered white light. Glare points are optical effects resulting from interferences which allow droplet size determination in the glare point method. In the rainbow method, the droplet size is derived from the rainbow effect resulting from the light scattered.

In most cases, the droplet size is determined by photographing one or several droplets at the same stage of their production and measuring the area or the diameter on the photo. However, this method has important drawbacks: first, during the exposure time, the droplet travels. This means that even, when a bright light source is employed, a certain blur in the direction of the droplet movement is unavoidable. The fact that the droplet is not spherical should be kept in mind and can be corrected. Another, much more important drawback in practice is that the diameter respectively the radius which is measured enters the formula for the calculation of the droplet volume to the three. This means that small uncernities in the determination of the radius or the diameter results in huge deviations in the calculated volume. Therefore, a high quality of the photo and of the image editing software is crucial.

The drawback of graphymetrical approaches is the evaporation of the solvent. The determination of the mass of a certain number of droplets is therefore not possible because evaporation will severely falsify the result. Another possibility is the weighting of the dispenser before and after the dosage of a certain number of droplets. If this is not possible, the weighting of the reservoir may be an alternative *[l]* (see chapter 6). It was shown that with this method a comparable result to an imaging-based approach can be made with much lower uncertainty. Under normal laboratory conditions, with this method, only the average droplet volume can be determined because a certain number of droplets is needed for achieving good results with a conventional microbalance.

The dosage of a certain amount of analytical standard and the analysis of the dispensed solution is a third way for an indirect determination of the droplet volume. This can be by classical chemical analysis of standard dissolutions prepared *[l]* or scintillation of radioactive standards [95]. These methods are the most elaborate possibilities (see chapter 6).

[10] See [90] for details

5.5. Examples for applications

5.5.1. Applications in analytical chemistry

5.5.1.1. Mass spectrometry

One possibility to engage drop-on-demand dispensers in mass spectrometry is the improvement of electrospray ionisation (ESI): ESI is an efficient and soft method for the desolvatation of a liquid sample combined with an ionisation of the analytes. The breakup of the liquid stream into small, charged droplets in which the solvent evaporates and transfers the charge on the analyte molecules is a highly complex process which is not completely controllable [96]. The high voltage needed and the asymmetrical break-up of the droplets which fly relatively undirected are the main causes for problems and insufficiencies. These problems are addressed in two ways by engagement of dispensers.
Berggren et al. [85] report about a selfmade dispenser which is capable of producing distinctive, charged droplets. The charge is provided by an electrode in the solution which creates a potential difference around 4,000 V to the MS inlet. The system was capable to produce droplets down to 10 pL in volume. The ionisation efficiency was comparable to a continuous electrospray. The authors produced a spectrum of insuline from a single droplet which was 80 pL in size (which corresponds to 80 amol) which is displayed in figure 25. The alignment of the dispensing frequency to the scan rate of the MS may be an interesting perspective[11].
Aderogba et al. [97] follow a similar strategy: They used an ultrasonic ejector array with several nozzles operating simultaneously [98]. The operation parameter are 1-5 MHz and nozzle inner diameters between 3 and 10 µm, producing droplets in the range of around 3 µm diameter. With this setup, it is possible to create ions by application of a charge as low as 100 V which allows a very soft ionisation. The application of a Venturi-tube to guide the droplets to the MS inlet increases the sensitivity [99].

[11] A similar approach was followed in chapter 7.1

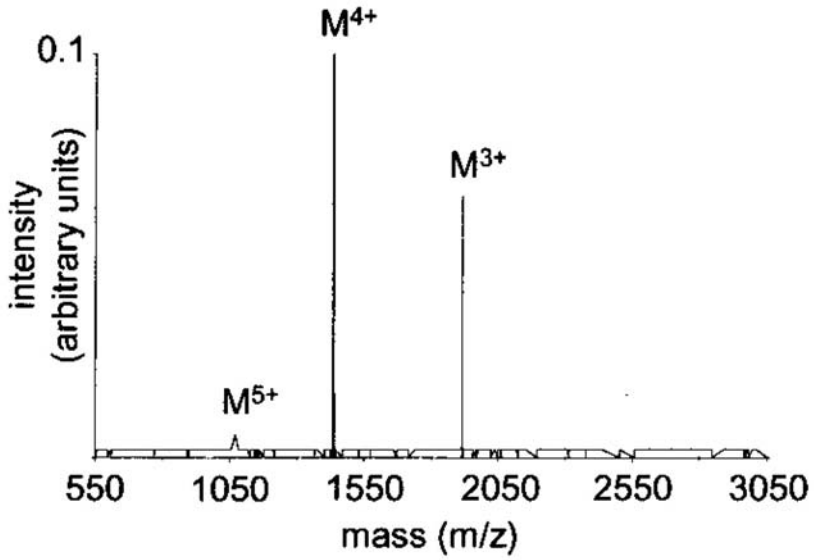


Figure 25: Mass spectrum derived from a single 80-amol pulse of an insulin solution. The volume was 80 pL, the sample solution was held at 4,700 V. From [85].

One application, where the small volumes to be produced and the high local precision of dispensers are advantageous is the spotting on MALDI plates [100, 101]. Another improvement here is the contactless application of the sample. Also, sensitivity and reproducibility were significantly improved by analysis of DNA, because the sample spot on the target was small enough to be covered completely by the laser irradiation profile [101]. This method could be further improved by implementation of flow-through dispensers [102]. These instruments are capable of shooting small aliquots out of a continuous liquid stream. This opens the possibility to couple liquid chromatography to MALDI-MS analytics [84, 103]. The changing of the physical properties of the fluid in gradient runs were overcome by changing the pulse parameters during the run. An easy way of sample enrichment could be applied by depositing several droplets on one spot which increases sensitivity [84]. The setup could be highly automated and was capable of analyzing 100 protein samples in 3.5 hours [103]. Further improvements increased sensitivity up to 50 times compared to conventional setups [104].

5.5.1.2. Chemistry in a levitated droplet

An ideal combination is the drop-on-demand dispenser with a device which is able to levitate single droplets. There are several ways to levitate small amounts of liquids: Optical, diamagnetic, electrostatic, aerodynamic and acoustic levitation [105]. The method

most applied is acoustic levitation, where the droplet is located in the nodes of a standing ultrasonic wave [106]. One challenge is to position the droplet in the system because whenever surfaces are involved, the attraction to the surface is much stronger than the forces, holding the droplet in position. This is the point, where the dispenser is involved, because it is possible to shoot defined droplets over a certain distance and build up a levitated drop in the levitron (Fig. 26). The advantage of these setups is that volumes can be handled surfaceless [88].

Many applications of chemical processes in a levitated droplet are described which are for example sample enrichment prior to capillary electrophoresis [107], liquid/liquid extraction in a levitated drop [108], as well as wall-less titrations [106]. The evaporation in droplets held in an electrodynamic balance before being spotted on a surface is for example made use of in sample preparation for MALDI-MS [109, 110].

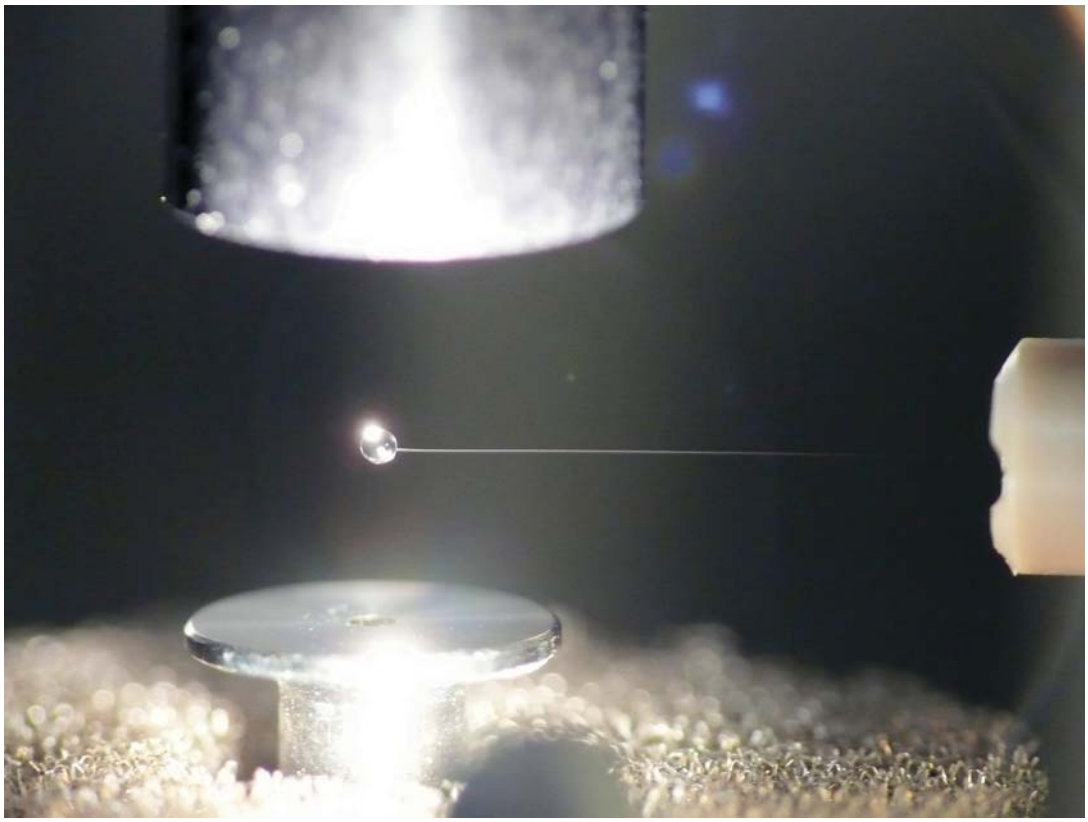


Figure 26: Droplet levitated in an ultrasonic levitator between transducer (lower part) and reflector (upper part). The droplet is fed by a stream of smaller droplets produced by a drop-on-demand dispenser on the right side of the picture.

5.5.1.3. Titrations

Litborn et al. [111] constructed a setup for a fully automatised and fast titration in 9-nL sample volumes in a small scale application by engagement of drop-on-demand-dispensers in combination with laser-induced waveguide fluorescence detection. Titration rates of down to 5 s can be achieved with this setup on smallest size.
Tuckermann et al. [106] described the additional application of a levitation device (see chapter 5.5.12) for the wall-less titration in a levitated droplet under absorption spectrometric control using an indicator.

5.5.1.4. Sample application in capillary electrophoresis

Sziele et al. [112] described the application of a drop-on-demand system for the sampling in capillary electrophoresis. The sample was shot directly into the end of the capillary by the dispenser which allowed the application of small volumes of around 110 pL. This could be performed contactless. The detection of 250 fmol of methionine was possible with UV detection at a signal-to-noise ratio of 10:1.
Petersson et al. [107] described a similar approach by implying a levitation device which allowed additional sample preconcentration due to solvent evaporation before the application for capillary electrophoresis for separation after this preconcentration step.

5.5.1.5. Chromatographic quantifications

The high accuracy and reproducibility of the dispensing of small amounts makes drop-on-demand dispensers a suitable tool for dosage in quantification approaches when a reliable method for the droplet volume determination is applied. This can be made use of for example for the preparation of calibration curves for LC analytics. Especially the application for standard addition approaches is interesting since in this case the dosage of small volumes of a high concentrated standard solution to the sample allows fast and precise quantifications of analytes even in complex real samples *[I]*. A detailed description of the method is given in chapter 6.

5.5.2. Applications in Biology

5.5.2.1. Dosage of single cells

Schober et al. [95] showed that bacterial cells can be dosed by drop-on-demand-dispensers without significant damage due to the sonication of the dispenser and without clogging the nozzle. Bruns et al. [87] developed a method based on the production of small volumes containing only one or few cells for the inoculation of bacterial samples based on dispenser technology. Their method was shown to be more accurate and faster than conventional ways (most probable number approach) for the isolation of single bacteria out of natural liquid samples. Also here, the automatisation, the small volumes to be dosed and the speed of the dispenser had significant advantages compared to an conventional approach which is based on dilution series.

5.5.2.2. Microarrays

The engagement of drop-on-demand dispensers in the applications for microarrays is well developed. Commercially available instruments based on this technology are already available [89]. The local precision and the high speed combined with automatisation abilities is also in this case the driving force to engage dispensers to produce arrays with higher densities which can therefore be also smaller in size providing higher efficiency [113].

5.6. Conclusion/outlook

The given examples show that drop-on-demand dispensers are applicable in many different areas in analytical chemistry and life sciences. The main advantages compared to alternative methods for the dosage of liquids lie in the small volumes to be dosed, the high reproducibility to be reached, the high local and timed precision and the possibility to dose contactless over a certain distance. It is also shown that automatisation is an important perspective. Even though, a number of successful applications are described, it may wonder, why this method has not gained more attention over the years, keeping in mind that dosage in general is a main application in almost every lab. It may be expected that these instruments will have their breakthrough to mainstream applications in case the

trends towards a further downscaling and automatisation of processes may continue. Also the development towards lower dispensing volumes may open up many new possibilities in many fields. The threshold to the femtoliter area for droplet production is already taken [114] and the improvements towads smaller instrument sizes and lower production costs may open up new possibilities as well. The development of new dispenser heads with smaller dead volumes which will reduce the distance between applied and dosed volume, will make these systems applicable for exact dosage, when only smallest sample volumes are available. Even for the dosage of larger volumes, the application of small-volume-dosage-systems may be interesting: The continuous dosage of defined single volumes guarantees an almost constant accuracy over a wide volume range which is advantageous compared to volume-based dosage systems which are still mostly applied.

6. Results for the application of a drop-on-demand dispenser system for chromatographic quantifications in real samples[12]

6.1. Introduction

The applicability of a drop-on-demand dispenser was examined for the dosage of small amounts of liquid to apply these for standard additions on bacterial culture supernatants for the analysis of HSLs. The control of physical properties (size, volume) of the droplets produced and the accessibility of these parameters are of key importance. Berggren et al. [85] found agreement within 20% by comparing a visualizing method and an approach based on a way to determine the average mass of single droplets by weighing the dispensed volume. Eberhardt and Neidhart [88] claim for their setup an accuracy of better than 1% and a precision of less than 1% relative standard deviation (RSD) for the determination of the droplet mass. Bruns et al. [87] found deviations “usually less than 1%” whereas Jacob et al. [115] reported deviations below 5% with their instrument. Niles and Coassin [89] found root mean square deviations of less than 0.64%.

No application has been shown to use these devices to generate precisely diluted standards for classical analytical purposes (highly reproducible and accurate dilution series, standard addition procedures in quantitative analysis). In this study, a simple, commercially available dosage system was tested for the quantification of homoserines in real samples without extraction of the sample as a fast screening and quantification method for the presence of homoserines lactones in bacterial cultures. Since HSLs tend to be hydrolyzed, it is more reasonable to determine a sum parameter of the active and the formerly active HSLs in a culture.

6.2. The dispenser

The dispenser applied consists of a capillary with a 30-µm nozzle, a surrounding piezo actuator and a reservoir. The void volume in the dispenser was determined to be 91 µL (including the take-up tube). The reservoir can hold around 4 mL of fluid. The liquid is transported into the capillary only by capillary forces.

The time between two pulses, the duration of the pulse and the pulse voltage can be set. The system can be run in continuous mode as well as externally and manually block-triggered. The maximal block length is 999 pulses; the minimum is one pulse. A trigger

[12] The results presented in this chapter were partially published in *[I]*.

pulse is shown in figure 27 which was captured while the dispenser was running. Oscillations along the pulse are due to resonances of the vibrating piezo crystal. The dispensed droplets can be visualized by a stroboscope diode, the delay of which can be set between 0 and around 600 µs.

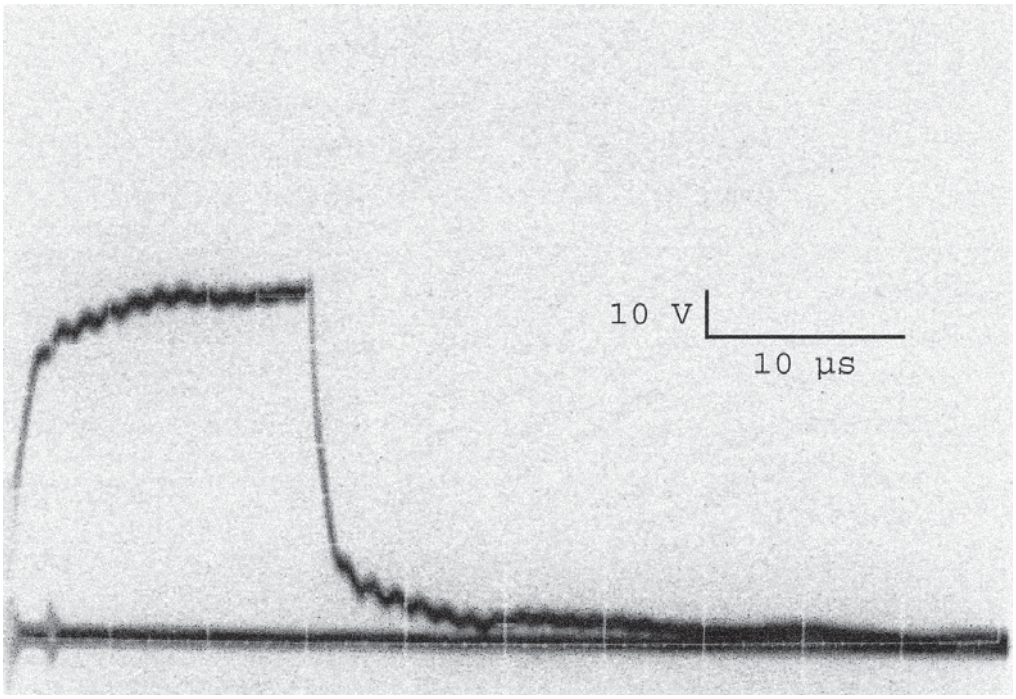


Figure 27: Trigger pulse with a width of 15 µs and an amplitude of 70 V.

The period, and the displaying of it, underlies constant oscillations in the sub-10-µs range, so the value has to be rounded to 10 µs. By comparison of the results obtained in continuous mode with those of the dispensing of a fixed number of shots, an additional average error of the displayed value of 1.7% was found and in all experiments, which were performed in continuous mode, was rectified.

A medium frequency of around 200 Hz was chosen for the experiments (around 100 Hz, respectively 9000 µS period between two pulses for the single droplet direct ESI experiment). All the experiments were performed under normal laboratory conditions which means that the laboratory environment was subject to normal shifts in temperature and humidity.

6.3. Determination of the average droplet volume

First the water droplet volume produced by the dispenser was determined within three different settings by an imaging and by a gravimetric approach in order to compare these two methods. The imaging approach was based on photography of the standing droplet and the determination of its volume by measuring the droplet diameter on the photo. The graphimetrical approach is based on the weighting of the reservoir of the dispenser before and after the dosage of a defined amount of droplets (at least 500,000 drops) to calculate the single droplet volume. Water was used as test the medium because most biological solvents are water-based.

Figure 28 shows the results of the calculation of the droplet volumes obtained by photographic and gravimetric methods with three different settings. Both results are in very good agreement for all experiments and are suitable for the determination of the droplet volume (no systematic underestimations or overestimations). The RSDs for the photographic method are relatively high and decrease with decreasing droplet size: 8.7% for the biggest droplet, 7.5% for the medium-sized droplet and 5.4% for the smallest droplet. The RSDs obtained by applying the weighing method are much smaller: 0.73% for the largest droplet, 0.67% for the medium-sized droplet and 1.07% for the smallest droplet. This reflects the high accuracy of this simple method, based on gravimetry.

Droplet size strongly depends on the pulse parameters: the shorter the pulse duration, the smaller is the resulting droplet. With water, a highly reproducible droplet volume of down to around at least 30 pL is shown to be easily achievable.

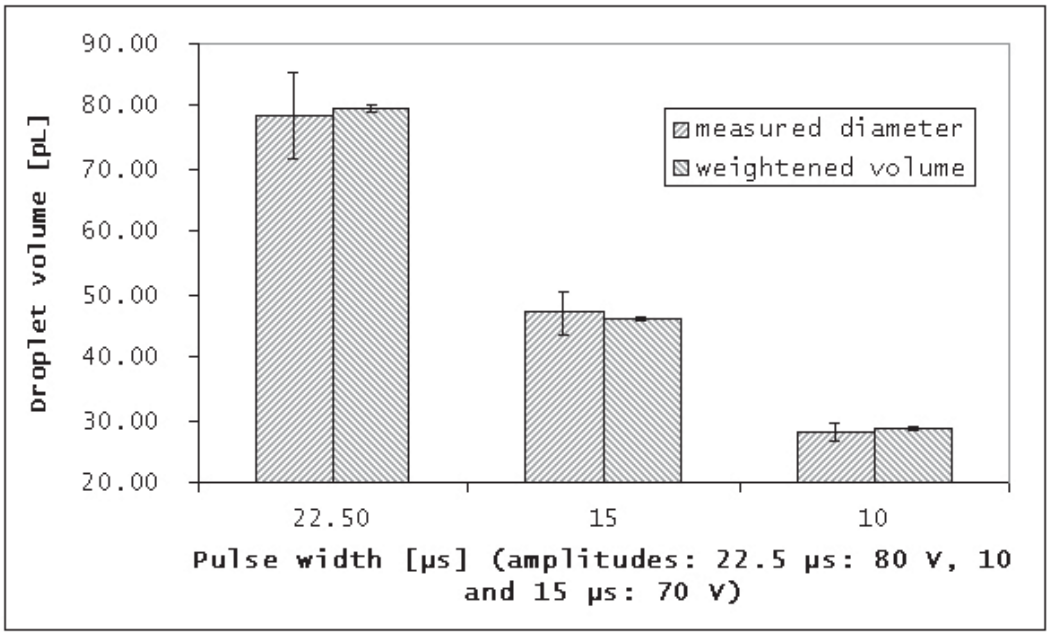


Figure 28: Comparison of the results for the determination of the volumes of one droplet obtained by measuring diameters on a photograph and by weighing the dispensed volume with standard deviations with the usage of three different pulse parameters.

6.4. Reproducibility measurements

In order to obtain information about the reproducibility of the dosage, the RSDs were determined for a caffeine solution prepared in 1 mL-scale by engagement of the dispenser and in the classical way in 200 mL-scale by dosage with pippetes.

The accuracy of a dispenser-based dilution of an analytical standard, prepared on a 1-mL scale, was compared with that of a classic approach using Eppendorf™ pipettes and conventional glassware. The latter was performed on 200-mL scale. The validation was made using UPLC analysis following the dosage of a defined volume of a caffeine stock solution. Caffeine was chosen because of its high solubility in water and its convenient use in UPLC analysis.

Two setups for preparing 1 mg/L solutions from a 1,000 mg/L stock solution were compared.

- One preparation, a typical method of laboratory-scale sample preparation, was done on a 200-mL scale, using 200-mL graduated glass flasks and dosing 200 µL of the stock solution with a 200-µL pipette.
- In the alternative setup, 1 µL of the stock solution was dispensed directly into the UPLC vials (12mmx32 mm, screw-neck glass vials, Waters), and 999 µL of water was added using a 1,000-µL Eppendorf pipette.

The weighing method described above was used to determine the droplet volume for pulse parameters of 22.5-µs pulse length, an amplitude of 80 V and a repetition rate of 5,050 µs. The droplet volume determined (79.41 pL) for the caffeine solution resulted in 12,590 droplets being dispensed in 20 blocks of each 630 pulses.

The results of the UPLC measurements of the 1 mg/L caffeine solutions obtained in the two different ways (pipette and dispenser) are displayed in Fig. 29. The average RSD for the measurement-to-measurement reproducibility in the classically diluted samples is 0.26% and in the dispensed samples 0.54%. The day-to-day reproducibility is 0.48% RSD for the classic dilution and 1.59% RSD for the dispenser-based dilution. It has to be kept in mind that the pipettes were calibrated every day, and the dispenser only once. The total mean deviation between the two setups is 1.46%. The accuracy of the UPLC method was independently determined to be 0.11% RSD from measurement to measurement (N=5).
On all days, an underestimation of the caffeine concentration seemed to occur for the dispensed samples. Only the measurements on the first day are an exception. This may be caused by the uncertainty in the determination of the droplet volume. These variations are in a very narrow band and by taking into account the errors of the different steps of preparation, it is more reasonable not to over-interpret these variations. An accuracy of around 1.5% RSD was also observed in preliminary experiments and this seems to be just the limit of the accuracy of the dispenser for day-to-day observations.
Over-all, it can be found that within 1 day, RSDs of below 1% are to be expected, while for day-to-day observations deviations should be around 1.5%.

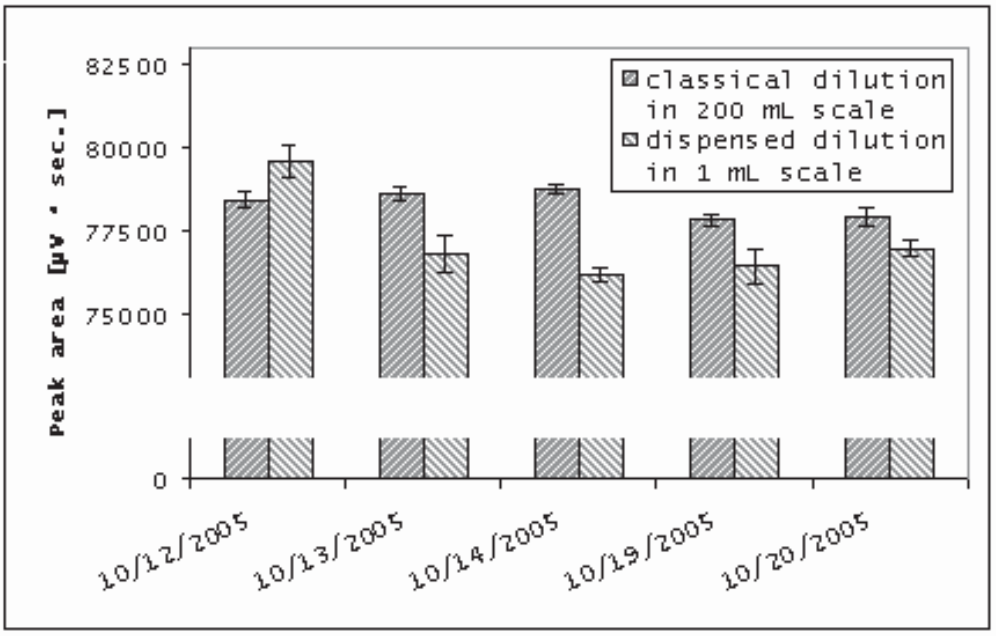


Figure 29: Reproducibility measurements and comparison of the results obtained by classic pipette preparation in 200-mL volume (Eppendorf™ pipette) and by dosing with the dispenser directly into the 1-mL analysis vials.

6.5. Determination of droplet speed and flight distance

For the applicability of the dispenser, knowledge about the droplet speed and derived from that the decline of the speed during the flight is important to determine the flight distance. A comparison was made of the behaviour of the speed of the droplets theoretically and experimentally applying three different pulse parameters.

The formula for the speed drop of a droplet can be derived as follows:
Generally two forces are acting:

a) Vis Inertiae:

$$(6)\quad F_t = ma$$

whereby F_t is the vis inertiae, m the mass and a the acceleration. Since acceleration is the second derivative of the distance x with respect to time the vis inetriae can be expressed as

(7) $F_t = m\ddot{x}$

b) Frictional force which can be described by the Stokes law:

(8) $F_r = 6\pi\eta r v$

whereby F_r is the frictional force, π is the Ludolph's number, η the viscosity of the air, r the radius of the droplet and v the speed.

Since speed is the first derivative of the distance with respect to time:

(9) $F_r = 6\pi\eta r \dot{x}$

Assuming that no other forces are involved, the sum of the two forces equals zero

(10) $F_t + F_r = 0$

so, applying formulars (8) and (9)

(11) $m\ddot{x} + 6\pi\eta r \dot{x} = 0$ respectively $\ddot{x} = -\frac{6\pi\eta r}{m} \dot{x}$

after one integration, formula (11) can be expressed as

(12) $v = \dot{x} = -\frac{6\pi\eta r}{m} x + v_0$

where v_0 ist the initial speed. Since the formula of the mass is as follows

(13) $m = \varsigma V = \varsigma \frac{4}{3}\pi r^3$

whereby ς is the density of the droplet forming liquid and V is the droplet volume, the formula for the speed of the droplet at a given distance from the nozzle can be expressed as

$$(14)\ v = -\frac{9\eta}{2\varsigma r^2}x + v_0$$

It has to be kept in mind that some assumptions were made to simplify the model: first, the Strokes law is only valid for laminar flows. Since the critical Reynolds number, where laminar flows turn into turbulent ones, is a system constant which is unknown for the system examined, no information can be given about that. The second assumption is that the droplet is completely spherical which is only an approximation for droplets moving through air [82]. A third assumption made is that the droplet radius and volume is constant which is only the case, if no evaporation occurs during the flight.

Figure 30 shows the results for the determination of the decline in speed of the droplets produced applying three different pulse parameters which where found to provide stable droplet production of water. The volumes were determined by the graphimetrical method to be 79.5 pL (22.5 ms/80 V), 46.1 pL (15 µs/70 V) and 28,7 pL (10 µs/70 V). From the two settings which differ only in the pulse duration, it can be derived that smaller droplets are produced at shorter pulse length and these have a lower initial speed and therefore a shorter flight distance. The decline of the droplet speed is approximately linear which is an indication that evaporation is small and therefore negligible in this short time, since formula (10) gives the equation for a straight line (if radius, viscosity of the air and density of the liquid remain the same). Assuming 1.86 * 10^{-5} Ns/m^2 for the viscosity of air at around 21 °C, and taking into account the radius determined experimentally as well as the experimentally determined initial speed, the slope of the theoretically determined line for the droplet speed is less steep than the experimentally determined one as can be seen in table 7. It can also be observed that the difference seems to be dependent from the droplet size or initial speed since this difference is only 8 % for the smallest and slowest droplet and 40 % for the largest and fastest droplet. The reasons for this deviation could be explained by a stronger deformation of a faster or bigger droplet by the air flow. This is implausible since the droplets are all small enough to be expected to be strongly deformed [82]. Another and more reasonable explanation would be that formula (10) can not be applied here because the Stokes law is based on laminar flow. Turbulences are also expected to be bigger in faster and bigger droplets. Table 7 gives the experimentally determined Reynolds numbers which correlate with speed and/or size of the droplet. So it can be estimated that the critical Reynolds number for this system (droplet flying through the laboratory air) is somewhere below but near to the Reynolds number determined for the smallest droplet which is 4.4.

The distance, the droplet travels is also a quite theoretical value. A droplet near to zero speed is much stronger affected by occasionally occurring air flows and gravity than by its own kinetic energy. A sort of fume is formed at a certain distance from the nozzles, where slow droplets accumulate and are carried away by the air. Nevertheless, the flight distance derived from the experimental results is much shorter for the smallest respectively slowest droplet with around 7 mm than for the biggest respectively fastest droplet which is flying around 23 mm.

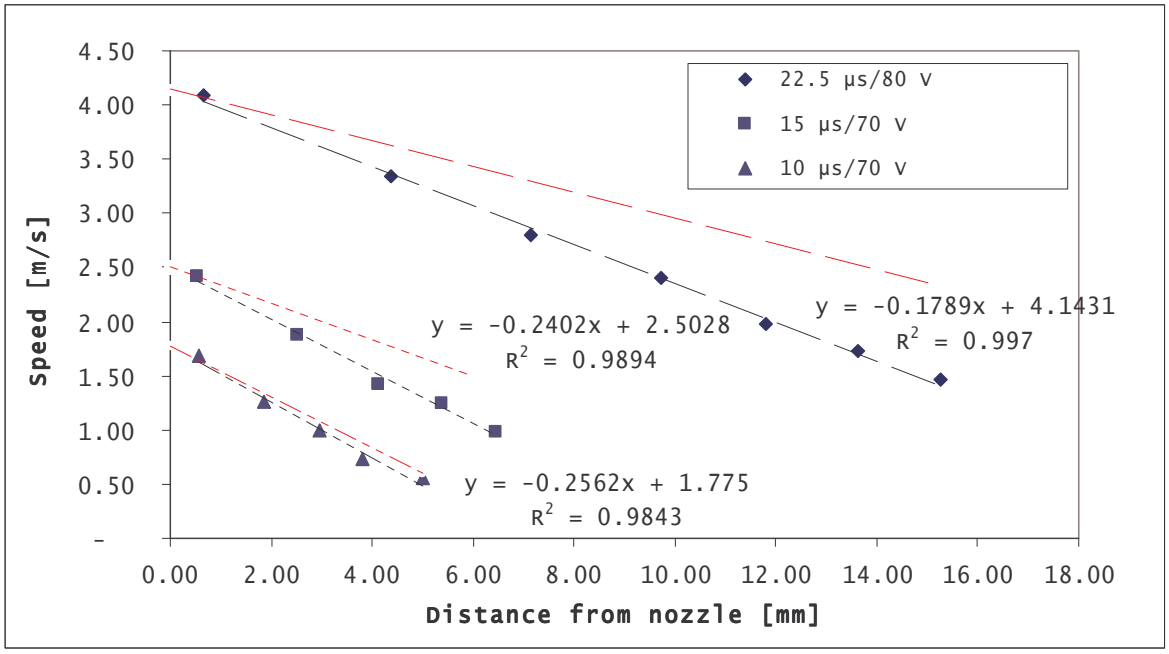


Figure 30: Comparison of the theoretical and the experimentally determined speed chart for droplets resulting from three different pulse parameter settings. The corresponding volumes were determined to be 79.5 pL (22.5 µs/80 V), 46.1 pL (15 µs/70 V) and 28,7 pL (10 µs/70 V). Equations are given for the experimental results. The slopes in the experimental approaches always turned out to be steeper.

Table 7: Overview over the results obtained for the droplets applying different pulse parameters experimentally and theoretically by application of formula (14). The determined droplet radius and initial speed was determined experimentally and had the same values for both approaches. The viscosity of air was estimated to be 1.86 * 10^{-5} Ns/m^2

Pulse parameters	22.5 µs/80 V	15 µs/70 V	10 µs/70 V
Droplet radius (µm)	26.58	22.39	18.86
Initial speed (m/s)	4.13	2.50	1.78
Flight distance exp. (mm)	23.16	10.42	6.93
Flight distance theor. (mm)	34.87	14.95	7.52
Experimental slope	-0.18	-0.24	-0.26
Calculated slope	-0.12	-0.17	-0.24
Deviation of experimental from the calculated slopes	40%	36%	8%
Reynolds number	14.44	7.35	4.39

6.6. Standard addition

For the development of the standard addition method, spiked nutrient broth medium was used. The freshly made medium was spiked with the N-decanoyl-homoserine standard to get a final concentration of 10 mg/L.

The concentration in the sample was raised by a certain amount of standard dosed by the dispenser and the resulting difference in the peak areas was extrapolated to determine the concentration in the original sample.

The calibration of the dispenser was performed with the same parameters as used for the verification of the droplet volume. The standard solution was dispensed directly into the vials. The dispensed volume was dried under nitrogen, before 200 µL of spiked medium, or real sample, was added to it. For the development of the method, 0, 100, 500, 1,000, 5,000 and 10,000 droplets were dispensed in three parallel experiments. For the analysis of the real sample, 0, 500, 1,000 and 5,000 droplets were dispensed. Every sample was injected three times.

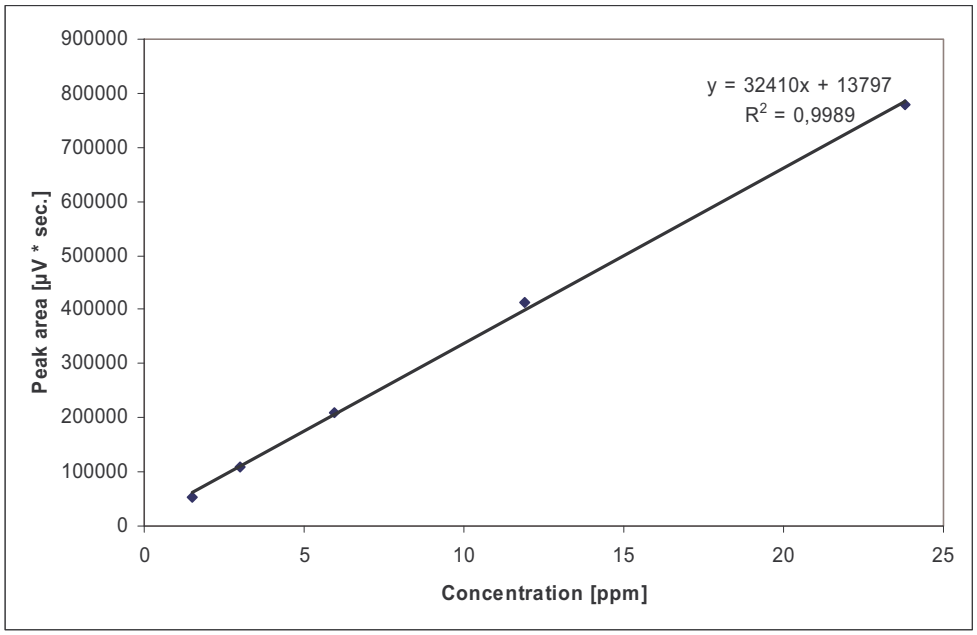
The intention was to establish a fast and easy-to-use screening method for the detection of this homoserine lactone in bacterial cultures of *Burkholderia cepacia.* The ratio of lactone and corresponding serine changes with time [10], *[VIII]*. If the lactone is hydrolyzed to serine, the amount of serines determined represents a sum parameter of

both molecules. Because of considerable matrix effects in microbial extracts, identification and quantification via external calibration curves is frequently inferior and unreliable in comparison with precise addition of standards. Because of limited sample amounts, the quantification has to be performed with small sample volumes.

The external calibration and the calibration curve resulting from the additions to the spiked medium are compared in figure 31. The slopes of the two curves differ by 4% which may be partly due to a slight extension beyond the linear range at 24 mg/L in the external calibration curve. The calibration curve of the additions shows excellent linearity which demonstrates again the highly reproducible and correct dosage. The complexity of the matrix does not influence this accuracy.

The results of the real sample measurements are shown in table 8 and figure 32. Three settings are to be compared with the results obtained by external calibration. The deviation within the 500 droplet standard addition set is relatively high. This may be due to a too small number of droplets, so small deviations in the droplet volume result in a relatively large deviation when the amount of standard added is too small in relation to the amount in the sample. With addition of 1000 droplets, the deviation is much smaller and the agreement with the approach involving the addition of 5,000 droplets is very high. This shows that this method is applicable for real samples, producing reliable results.

(a)



(b)

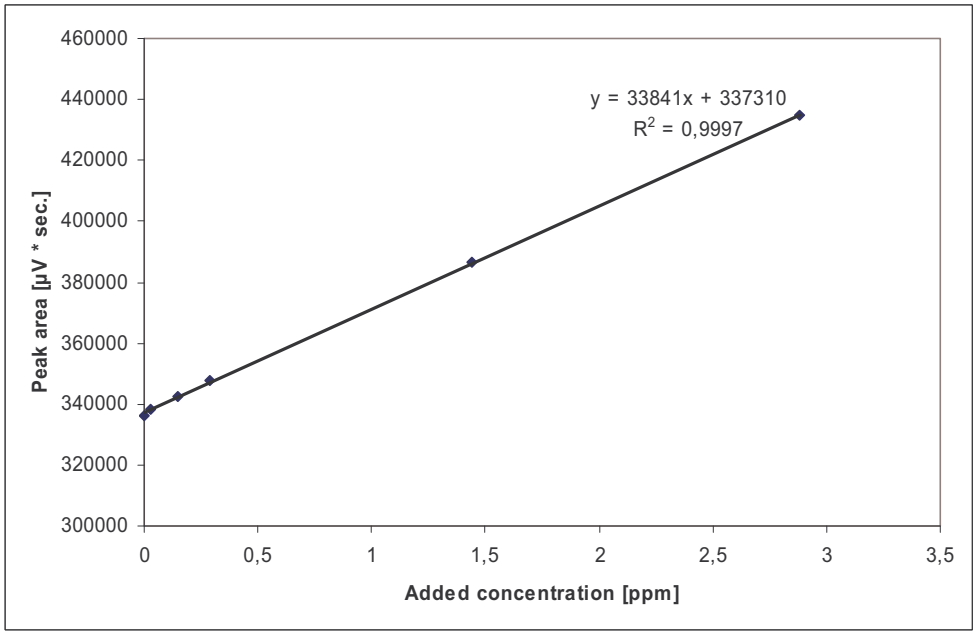


Figure 31: Calibration curves for (a) the external calibration and (b) the concentration resulting from the standard addition to the spiked samples.

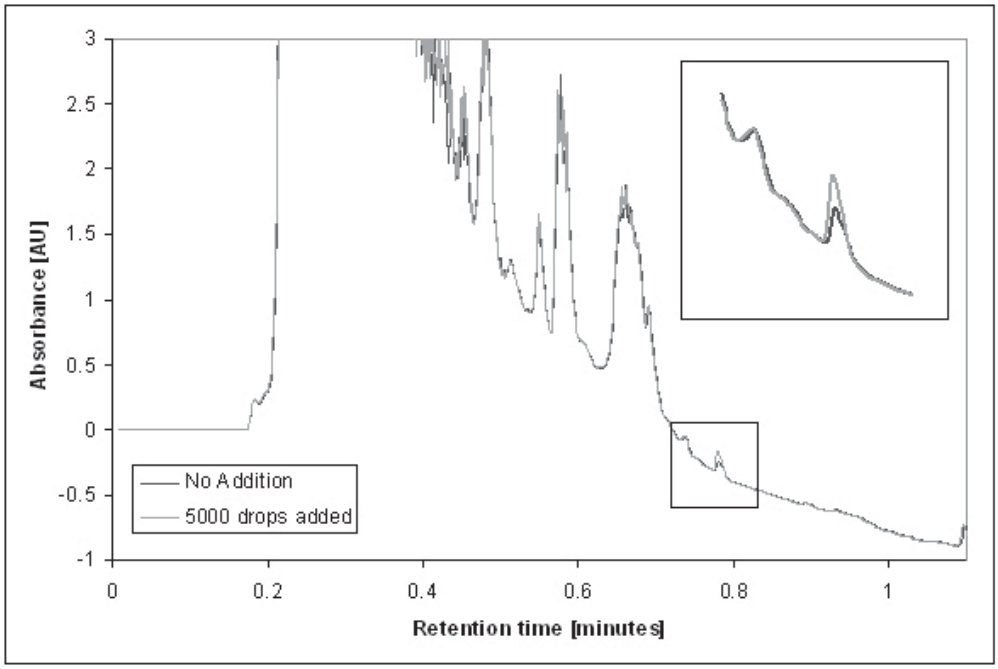


Figure 32: Chromatogram of the original *Burkholderia cepacia* culture supernatant and the same sample with standard addition. The N-decanoyl homoserine peak is enlarged.

Table 8: Results of the real sample measurements. The raised concentration means the concentration difference due to the standard addition. The concentration determined in the original sample compensates for the four-fold preconcentration of the sample.

	Raised conc. due to addition [mg/L]	Measured conc.[mg/L]	Determined conc. in original sample [mg/L]	Deviation from external calibration results
External calibration		2.23	0.56	
500 Droplets addition	0.16	2.48	0.62	11%
1000 Droplets addition	0.32	2.17	0.54	3%
5000 Droplets addition	1.59	2.24	0.56	0.4%

One huge advantage, not directly obvious from the results presented herein is the convenience and the speed of this method: The calibration of the dispenser may be time-consuming but once it has been calibrated, different volumes can be dosed just by pushing a button. The approach is also automatizable for preparation of many highly reproducible standards in large-scale experiments. This may increase the operator-to-operator reproducibility and prevents errors resulting from misusage of alternative dosage

systems. The smallness of the volumes allows application directly in the vial used for the subsequent analysis without dilution of the sample in the case of the standard addition method.

6.7. Conclusion

With low RSDs, namely, 1.5% from day to day and below 1% from measurement to measurement, the dispenser presented herein is a reliable and easy-to-handle device for dosing volumes even in the microliter range and below with high precision to prepare small liquid samples of an exact analyte concentration (ideal for calibration solutions in routine analysis in large-scale analytical laboratories) prior to quantitative chromatography. The accuracy and the reproducibility are comparable to those for the classic method of sample preparation.

The strength of the dosing approach using single droplets lies in the constant accuracy over a wide volume range (over a wide number of created droplets), because the droplet volume is constant over time. The reproducibility of the system was shown to be very high and the key approach, the determination of the average volume of one single droplet, can be made with the same high accuracy in a very simple way (only a micro-balance is needed). Additionally this leads to much lower consumptions of sample and solvents compared with conventional methods (in this work, a 1-mL scale dilution showed results comparable to that of a conventional 200-mL-scale dilution).

It was shown that the system is applicable for quantifications of HSs in real samples without extraction via standard addition as an example. It also shows the potential for a wide range of different applications, wherever volumes in the low volume range have to be handled in a highly accurate and reproducible way, a key demand for further downscaling processes.

7. Results in droplet mass spectrometry

7.1. Single droplet electrospray

The high precision and the small volumes which can be dosed by application of a drop-on-demand-dispenser led to an approach which is capable of combining the small volumes and the high selectivity of mass spectrometry. Especially, the application of Fourier-transformation ion-cyclotron mass spectrometry (FT-ICR MS) is interesting since the ultrahigh resolution of FT-ICR MS in excess of 200,000 FWHM (full width at half maximum) in broad band measurements (or up to 1,000,000 FWHM in high resolution mode) and a mass accuracy of routinely less than 0.5 ppm, allows especially in high field (12 Tesla) an advanced chemical characterization of metabolites of known plus hitherto unknown structure in complex and heterogeneous samples of biological origin. This can be performed by a deviation of the elemental composition of the analyte due to the high resolution as well as by comparison with simulated isotope patterns [116-120], *[VI]*.

The first setup of the single droplet based direct electrospray was based on the one applied by Berggren et al. [85]: The dispenser was positioned 0.5 to 1 cm in front of and in line with the heated capillary. A charged droplet is produced by the dispenser due to an electric field between the heated capillary of the MS and the electrode in the dispenser solution. The solvent of the droplet evaporates and the charge on the droplet surface is transferred on the analyte during flight, like in conventional electrospray processes [96]. As a test solution for the optimisation of the setup, 10 mg/L caffeine in methanol/water (1:1, v/v) plus 0.1% formic acid was chosen due to the high ionisation efficiency of caffeine.

The result for the optimisation regarding the intensities at different voltages is given in figure. 33. This result is produced, applying the ion trap MS. The intensity at voltages around 3 kV is very low with less than 10 % of the maximum intensity at 4.2 kV. At higher voltages, the intensity drops very fast down to 20 % of the maximum intensity. The RSDs are relatively high at all settings. The RSD at the maximum was determined to be 18 %.

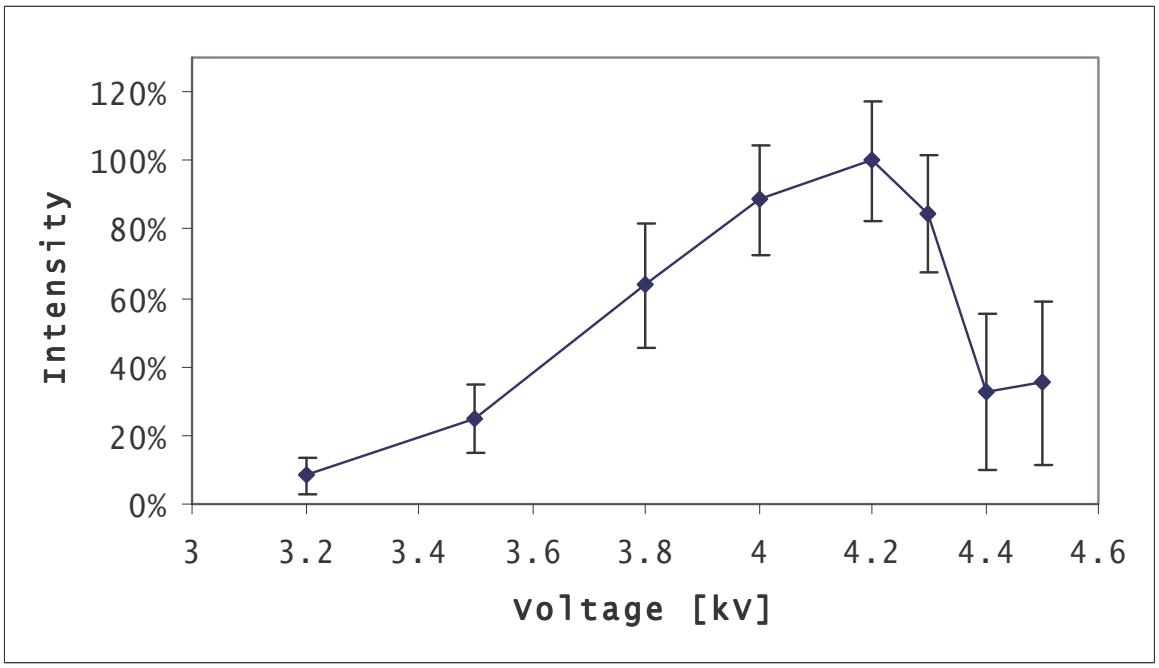


Figure 33: Relative intensity of the signal achieved by application of different voltages at a distance of 0.5 cm to the heated capillary. Measurements were performed on the ion trap MS.

The dependency of the signal intensity of the distance between dispenser nozzle and heated capillary is given in figure 34. A slight maximum at around 0.6 to 0.7 cm was determined applying a voltage of 4 kV. Also here, the RSDs are relatively high. At the maximum at 0.7 cm, the RSD was 24 %.

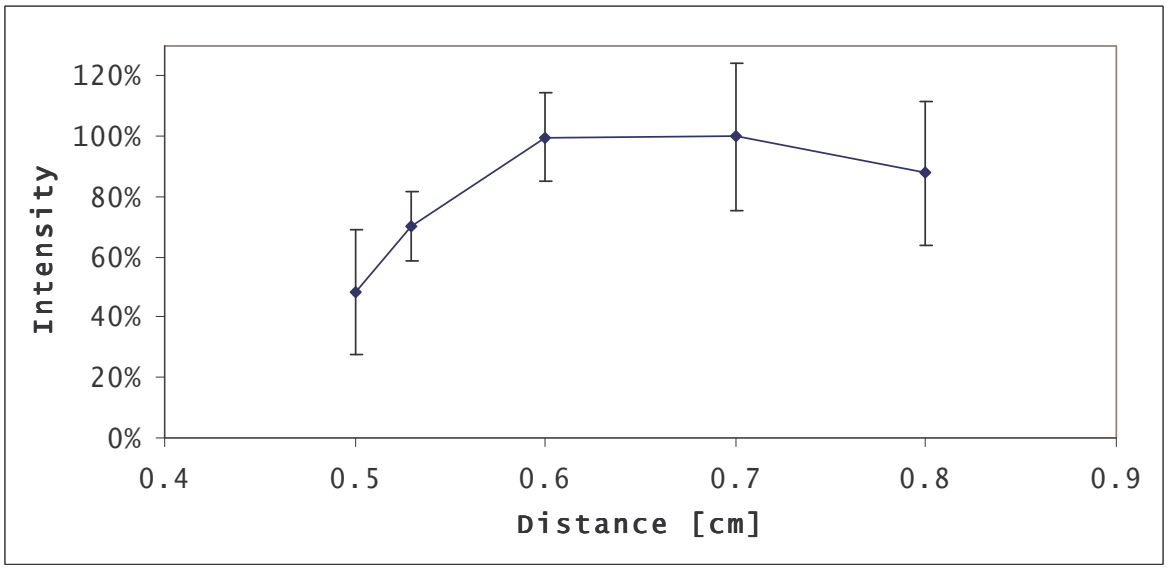


Figure 34: Dependency of the signal intensity of the distance of the dispenser nozzle to the heated capillary at 4 kV. Measurements were performed on the ion trap MS.

The Intensity of the signal was also examined in relation of the voltage applied and additionally in relation of the distance of the dispenser and the MS orifice on the FT-ICR MS (fig. 35). A distance of 4.45 mm seems to be only applicable, when high voltages are applied. For all other distances tested, a first optimum is observable at around 3,500 V. For the short distances, another higher maximum is observable at 5,500 V, shortly, before direct electrical discharge occurred at around 6,000 V in all cases. Nevertheless, quantitatively a clear trend is not observable and the results are found to be relatively unreproducible.

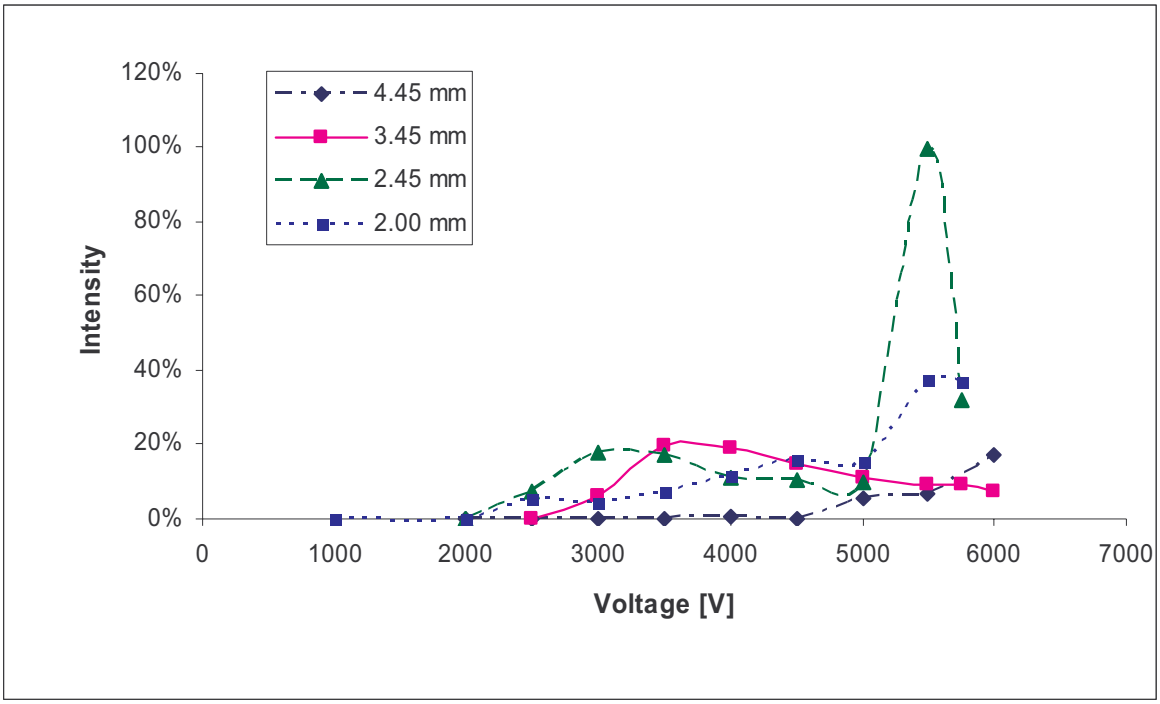


Figure 35: Examples for the intensities of the signal obtained by FT-ICR-MS by application of different voltages and different distances of the dispenser and the MS inlet. At around 6000 V, direct electrical discharge was observed in all experiments.

Applying the FT-ICR MS, also the dependency of the signal intensity from the dispenser frequency, respectively the time between the application of two pulses, was examined and the result is shown in figure 36. The pulse duration of 22.5 µs is negligible, so that the period is approximately inverse proportional to the frequency. It can be observed that at low frequencies the dependency is approximately linear, while at higher frequencies (shorter time between two pulses), a stronger increase is observable. This may be due to a higher efficiency of the desolvatation or ionisation process at higher frequencies. The function of the curve can not be derived from the graph due to the high RSDs up to 20 % and higher.

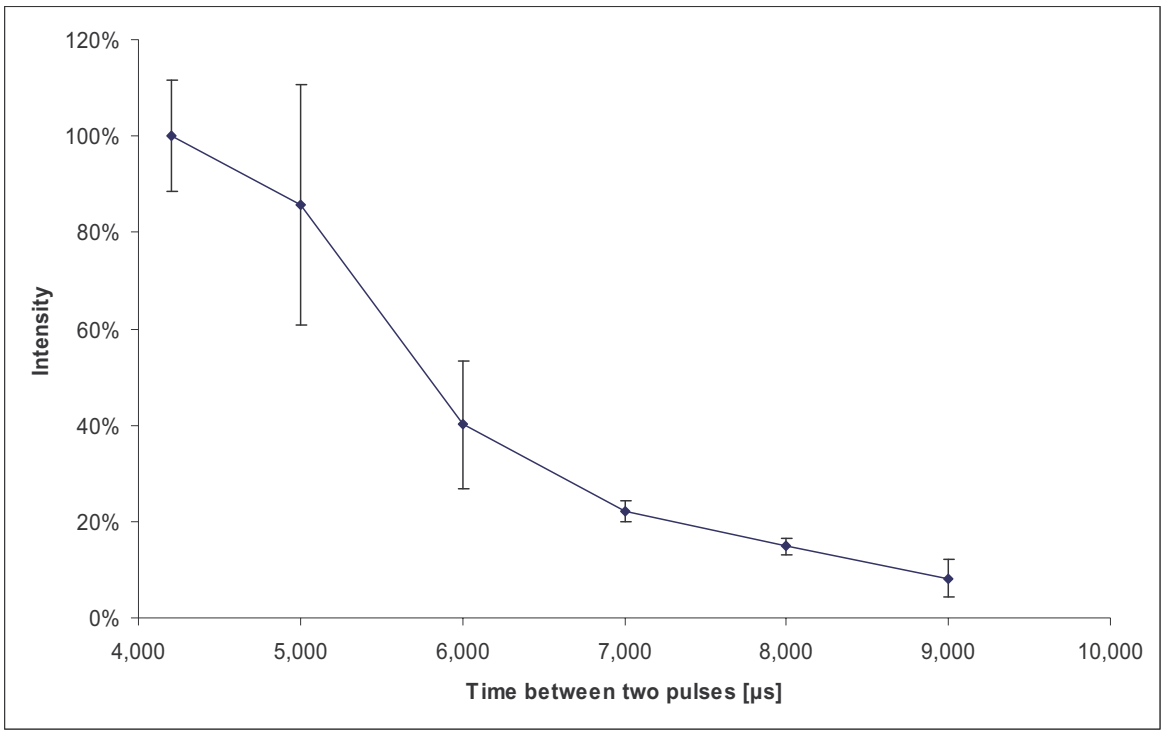
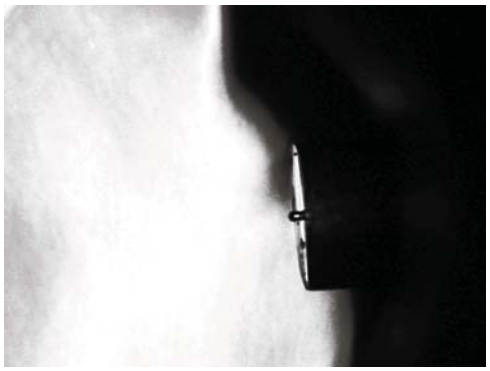
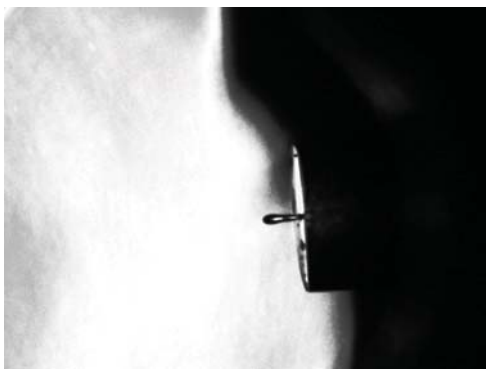
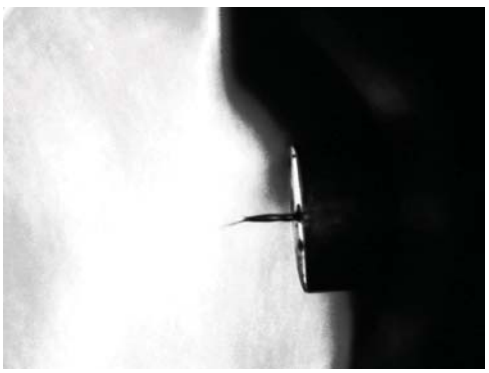
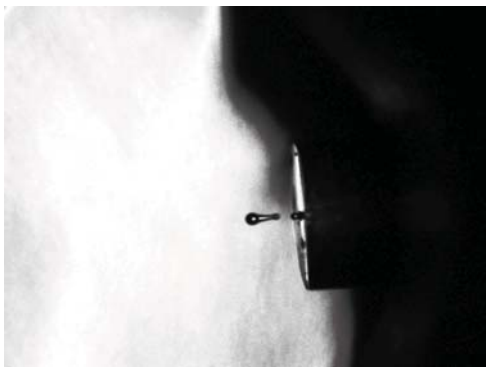
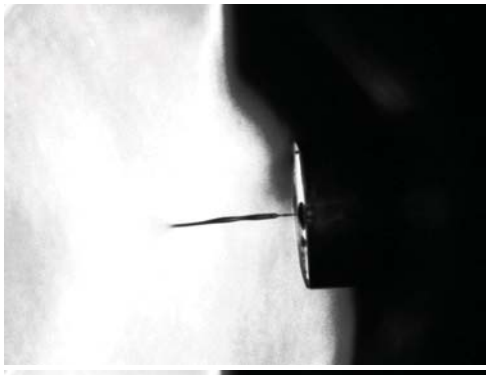
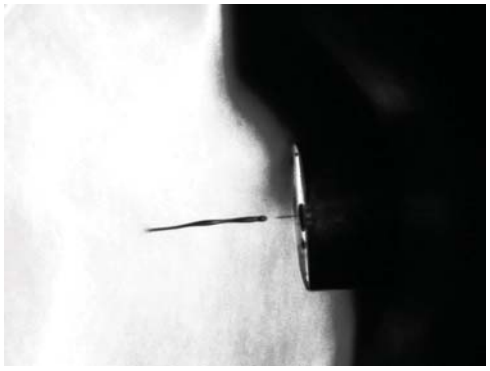


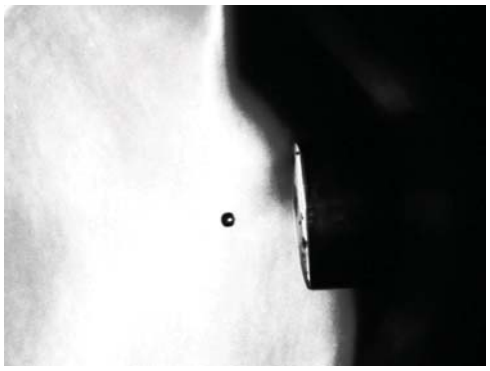
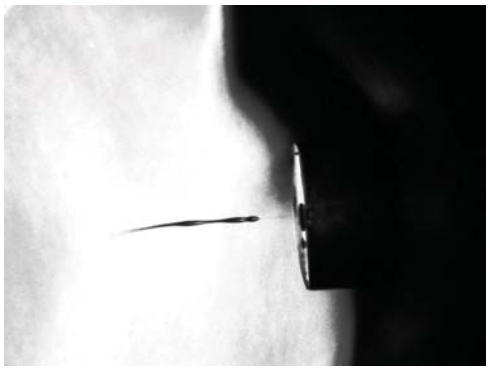
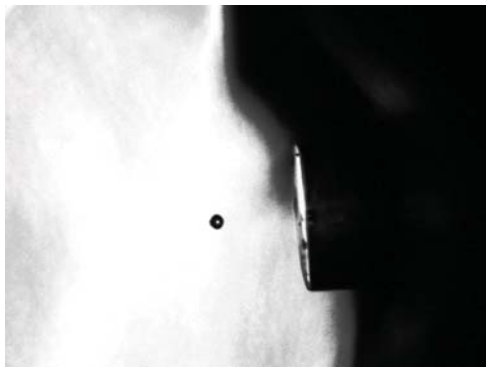
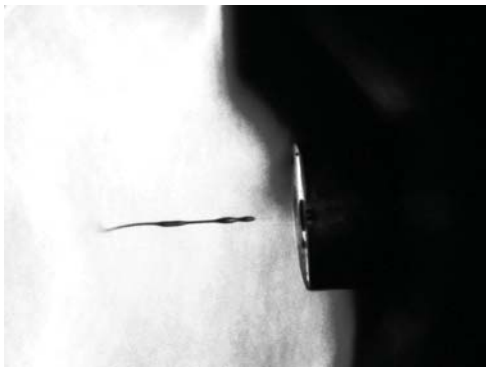
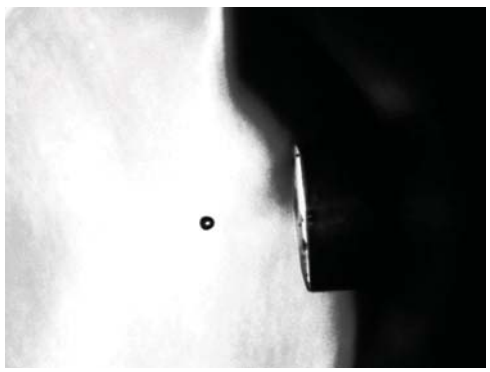
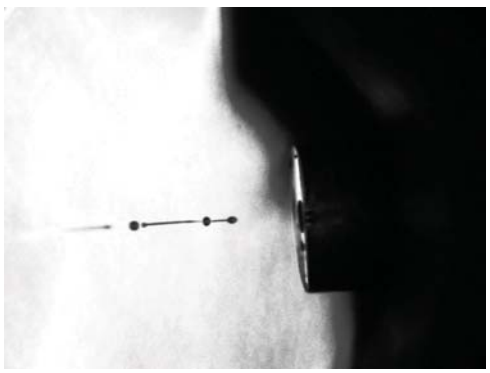
Figure 36: Dependency of the intensity of the FT-ICR MS signal from the frequency of the dispenser plus the standard deviation (N=3).

The high deviations in all experiments led to a closer examination of the process of droplet production under high voltage conditions. The determination of the RSD of the droplets produced under high voltage conditions resulted in 23 % RSD which is very high compared to RSDs around 1 % typically observed applying this dispenser without application of voltage (see chapter 6). Figure 37 shows photographs taken at different stages of droplet production with and without application of voltage. It was clearly observable that no proper droplet production is taking place in the case documented on the right side of the figure (high voltage conditions): A stream of liquid breaks up in several droplets of different sizes. Additionally one or several sprays are visible at the edges of the capillary nozzle. This state is not stable over a longer period of time. After several minutes, a change in the shape of the dispensed liquid stream was observed. This goes along with a change in the ionisation efficiency, which leads to a change in the signal intensities of several orders of magnitude. This instable state was observed at voltages down to around 1 kV. No signals were detected below this threshold. These observations may also explain the non-linear dependency of the frequency and the intensity displayed in figure 36, because the shape of the liquid stream may change depending on the dispenser frequency. The shape of the liquid stream did not change significantly when a grounded counter electrode was applied at a distance of around 0.5 cm. This may be due to the ground-like potential of the surrounding air.

The observed effect can therefore be seen as a sort of pulsed nanospray. The main advantage of the dispenser, the precise and reproducible dosage is in this setup lost nevertheless. For the given applications, the setup does not provide significant advantages compared to a conventional nanospray but has an irreproducible long-term performance. These drawbacks led to the application of different mechanisms for desolvatation and ionisation which were applied in the surface mediated thermodesolvatation and photoionisation approach.

Delay [µS]	a) No voltage	b) Voltage: 4.2 kV
10		
20		
30		
40		

Delay [µS]	a) No voltage	b) Voltage: 4.2 kV
50		
60		
70		
80		

Delay [µS]	a) No voltage	b) Voltage: 4.2 kV
90		
100		
110		
120		

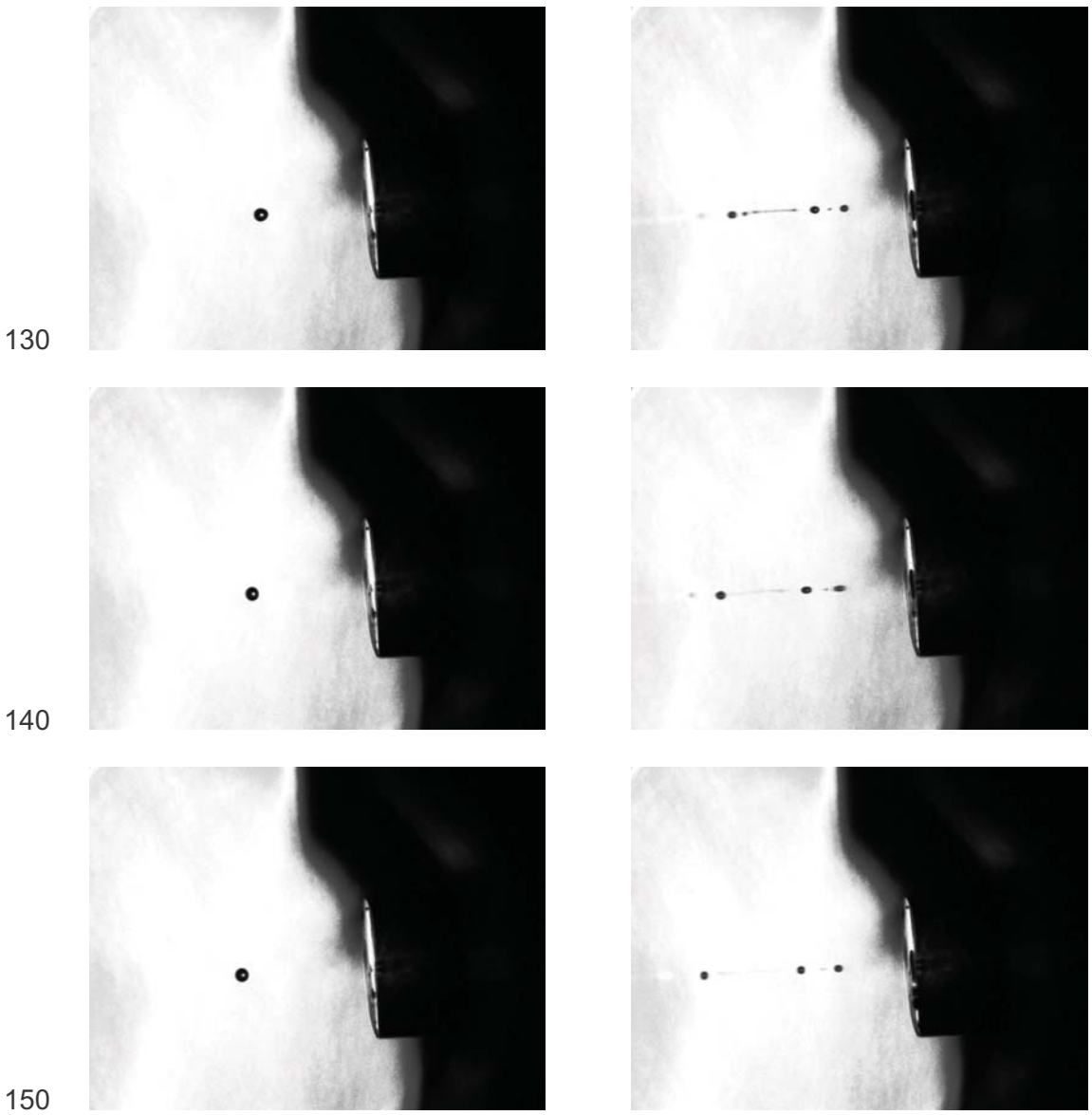


Figure 37 (page 93 to 96): Droplet production photographed at different delay times of the stroboscope diode with and without application of a voltage of 4.2 kV. The pulse width was 22.5 µS, the driver voltage was 80 V and the period between two pulses was 9 mS. The exposure time for the photos was 0.5 S which results in 56 pulses per picture.

7.2. Surface mediated thermodesolvatation and photoionisation (SMT-PI)

7.2.1. Introduction

Since electrochemical ionisation was shown to be not practicable for the ionisation of analytes in dispensed droplets, when the reproducibility and accuracy of the dispenser has to be preserved, a different method of desolvatation and ionisation had to be found. The dosage, the desolvatation and the ionisation was performed within one step in the single droplet electrospray approach. A separation of these three steps was aimed in order to optimise each step separately. The desolvatation was tested to be provided by heated air and on heated surfaces after the dosage. The ionisation was intended to be provided by photoionisation, which became popular in the last years. The ionisation takes place due to the emission of an UV emitting lamp (in most cases this is a krypton discharge lamp) in atmospheric pressure photoionosation (APPI) [121-123] or due to the emission of a laser of different wavelength, like in atmospheric pressure laser ionisation (APLI) [124-126]. Eventhough, the ionisation efficiency of APPI is more or less comparable to ESI, these photoionisation methods show clear advantages in the high apolar range of analytes. Another advantage of these methods compared to ESI or MALDI is that the desolvatation and the ionisation is decoupled so that these two processes can be optimized separately.
There are several ways how an analyte can be ionized by UV irradiation: One possibility is general direct photoionisation [122, 127]:

(15) $M + h\nu \rightarrow M^{\bullet +}$, where M is the analyte molecule.

Due to the often low concentrations of the analytes, the yield of ionized molecules can be increased by addition of a dopant which has a lower ionisation efficiency and is capable of transferring the charge to the analyte molecule:

(16) $D + h\nu \rightarrow D^{\bullet +}$

followed by

(17) $D^{\bullet +} + M \rightarrow D + M^{\bullet +}$

where D is the dopant molecule. In many cases also solvent molecules are involved in this process. According to Koster et al. [128], the reaction goes as follows:

(18) $D^{\bullet +} + S \rightarrow [D - H]^{\bullet} + [S + H]^{+}$,

followed by

(19) $[S + H]^{+} + M \rightarrow S + [M + H]^{+}$

where S is the solvent molecule. In this case, dopant molecules are depleted.

7.2.2. Setups

For the applications applying a krypton discharge lamp, a closed ionisation chamber was designed. There were two reasons to do so: first, this setup was applied to protect the operator from harmful UV irradiation. The second reason was that higher efficiency was expected, when a directed stream of air flows through the system, due to the vacuum in the MS. In an open setup, the risk of molecules and ions in the gas phase, drifted away may be higher. The centre of the apparatus is formed by a thermostatted aluminium block. The setup is given schematically in figure 38a and the construction elements are given in figure 39 assembled and dissembled (the desolvatation chamber, displayed on the pictures was not applied in this case). The temperature of the central chamber is provided by an inserted heating element run at around 50 W and controlled by a Pt100 sensor with a connected control element. The control accuracy is +/- 2° C in the heating block. The heating of all other parts is provided by the close contact of all elements. All of these are of aluminium. A deepening of the block provides the space for the ionisation-lamp housing which is also manufactured inhouse and is made of polyether ether ketone (PEEK). The lamp is a krypton discharge lamp. The window of the lamp has a diameter of 18 mm. The same size has the ionisation chamber which is around 2 mm high. In order to associate this apparatus with the ion trap mass spectrometer, an elongation of 4 cm is necessary. This is provided by two homemade 2 cm aluminium capillaries with 1 mm inner diameter. For the application on the FT-ICR MS, a reduction piece made of Teflon™ was applied to mount the chamber directly onto the heated capillary.

On the other side of the ionisation chamber, another capillary of 1 cm length is applied. The dispenser was positioned in line with the capillary at a distance of around 5 mm (fig. 38 a). The intention was, to desolvatate the droplets during their flight through the first capillary so that the analytes reach the ionisation chamber in the gas phase to be ionized there. It was found that this is not possible: A desolvatation and ionisation takes place, but

not in the gas phase as intended, but on the inner surface of the capillary. A change of the angle, at which the dispenser is located towards the capillary did not change the signal intensities. Because a desaolvatation on the inner surface of the capillary is not controllable and reproducible, the surface was provided in front of the capillary and at an angle of 90 degree as shown in figure 38b. To provide directed airflow through the system, a half-open desolvatation chamber was designed (see fig. 39). The desorbtion chamber was mounted on two 1 cm capillaries with 1 mm inner diameter (The capillary was elongated 1 cm compared to the first setup). The desorbtion chamber is closed except for the 1.5 mm hole for the application of the droplets. Due to the vacuum in the mass spectrometer, a slight underpressure in the whole system is to be expected causing gas flow in direction of the MS. The desorbtion surface is of aluminium. It was silanized by incubating the part in a 5% dichlorsilane solution in toluene for 15 minutes. After that, the metal part is rinsed with toluene, methanol and diethylether. This procedure was performed every day. The ion gauge was manually set to 30 ms in all experiments with the ion trap MS. The lamp was run at 0.88 mA. In case of an open setup, the solution was dispensed onto the inner surface of the elongation capillary. No silanisation was applied here.

In case of the indirect SMT-PI, 5 µL of sample was deposited on the desolvatation surface and after the evaporation of the solvent was complete, the desorption chamber was applied on the setup and the measurement was started after around one minute to heat the desorption chamber. Alternatively, an aluminium block, held at the same temperature as the ionisation chamber, was mounted in front of the capillary which in this case was only 1 cm long (see fig. 38c). To desorb the analytes, acetonitrile with 1% acetone as dopant was dosed continuously on one spot of the desorbtion surface. Acetonitrile was found to provide a slightly higher signal intensity than methanol (data not shown). The spectra resulting from at least 0.5 minutes of continuous run were integrated.

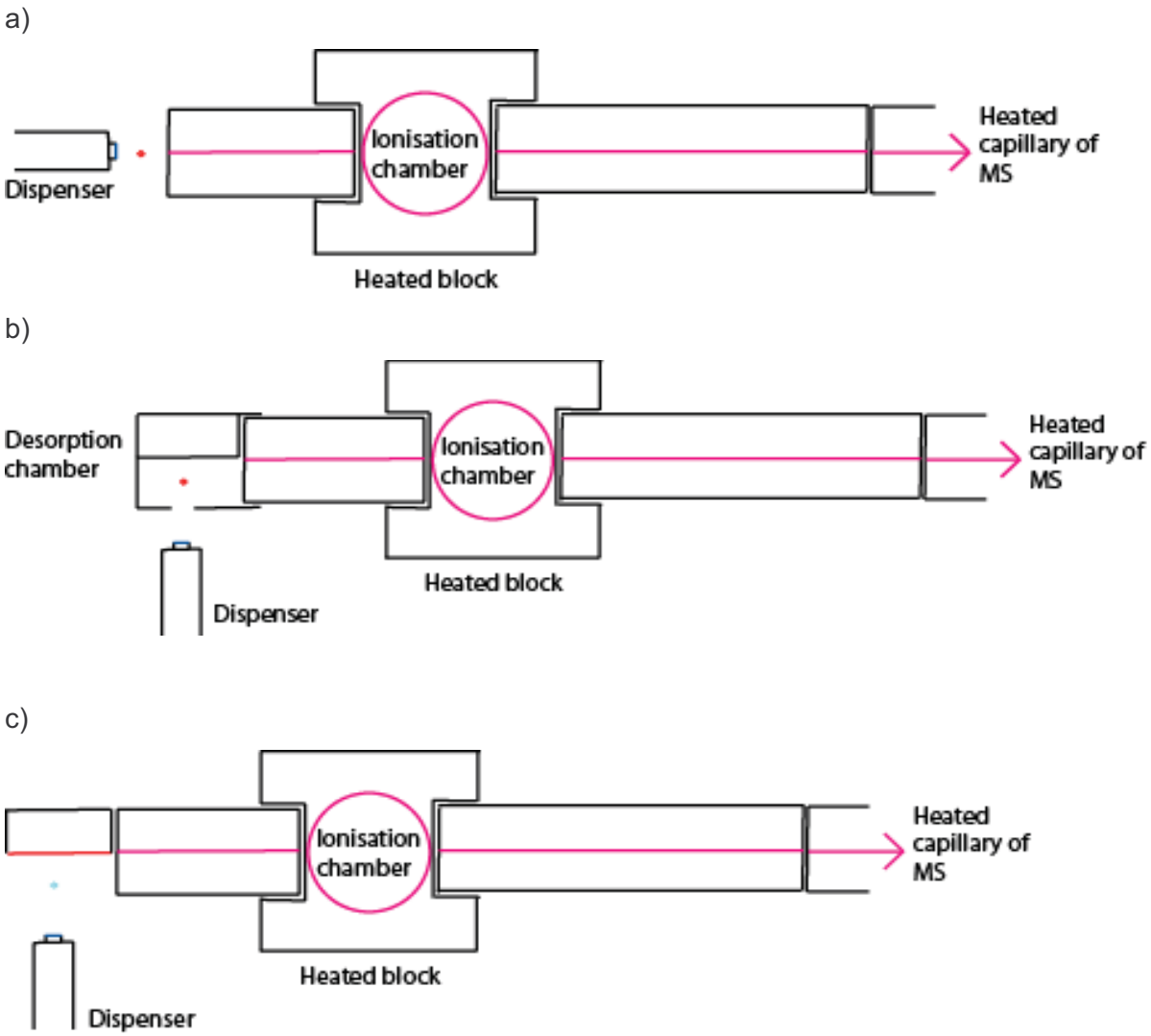
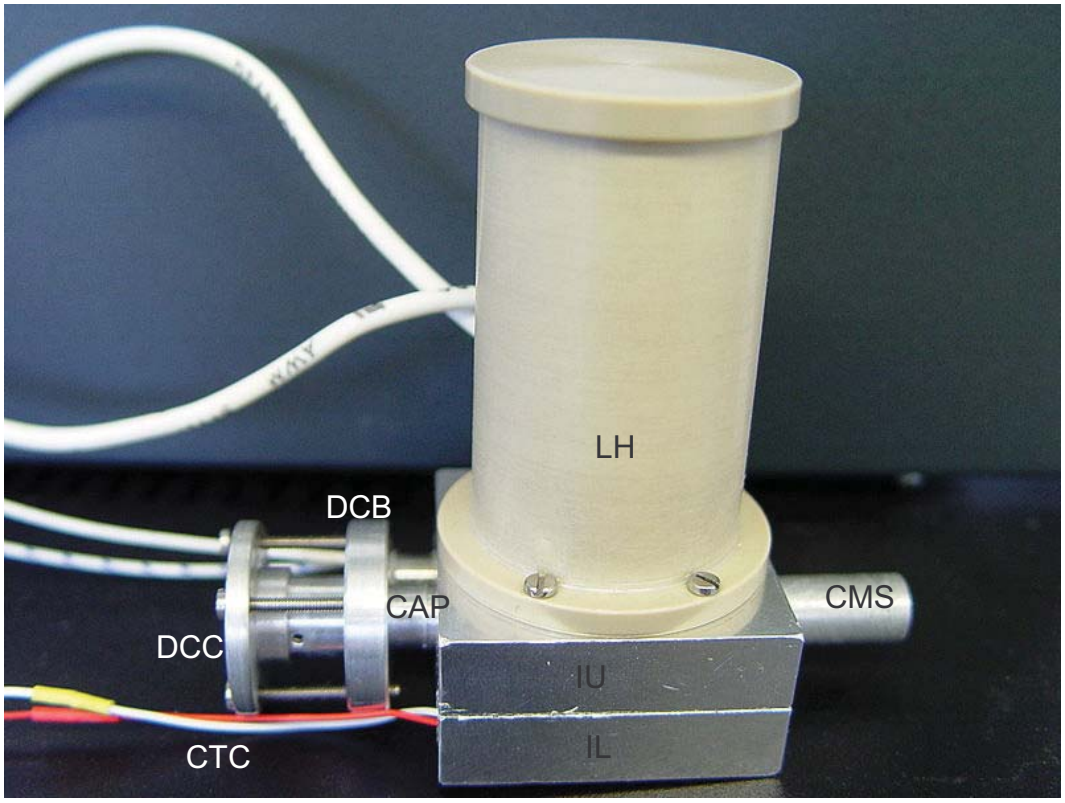


Figure 38: Schematic presentation of the different SMT-PI setups (here in case of application on the ion trap MS) a) direct application into the capillary: The sample is dispensed into the capillary by the dispenser. After a 2 cm distance piece with 1 mm inner diameter, the analytes enter the ionisation chamber with the Kr-lamp mounted in an angle of 90 degree on it. After passing another distance piece of 4 cm and 1 mm inner diameter (which is missing in case of the application on the FT-ICR MS), the ions enter the mass spectrometer. b) direct SMT-PI (here with a half-open setup): The droplet enters the desorption chamber through a 1.5 mm hole and hits the desorbtion surface. c) indirect SMT-PI (open setup): The sample is applied on the heated surface and desorbed by solvent plus dopant applied by the dispenser.

a)



b)

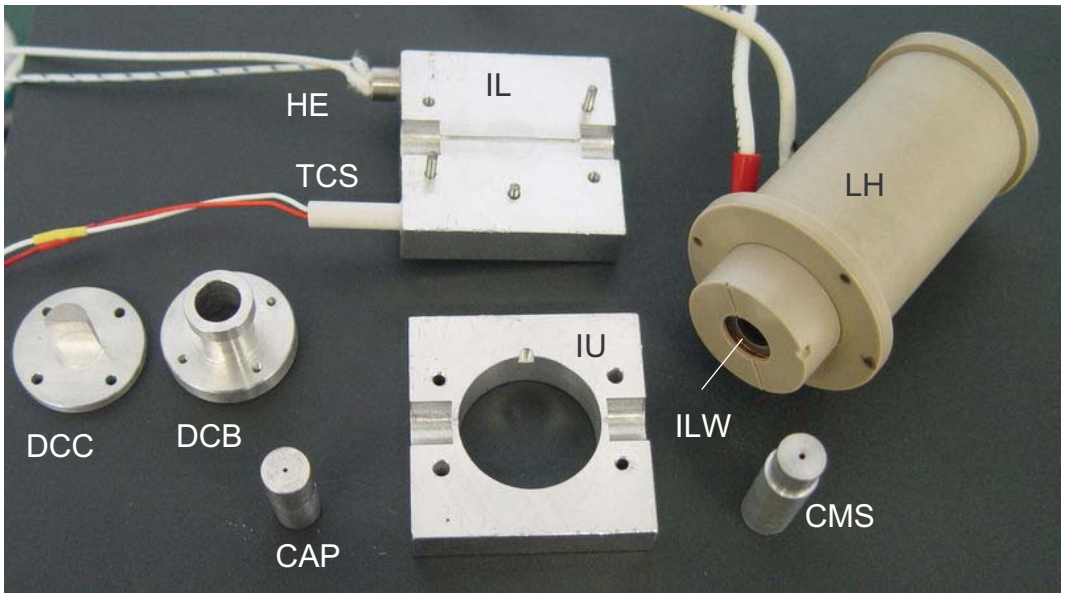


Figure 39: SMT-PI a) assembled and b) dissembled. CAP: capillary between desorption and ionisation chamber, CMS: capillary to MS, CTC: cable temperature control, DCB: desorbtion chamber body (with entrance hole), DCC: desorbtion chamber cover with desorbtion surface, HE: heating element, IL: ionisation chamber lower part, ILW: ionisation lamp window, IU: ionisation chamber upper part, LH: ionisation lamp housing, TCS: temperature control sensor (torn out a few mm in b)

7.2.3. Direct surface-mediated thermodesolvatation and photoionisation

To test direct SMT-PI with UV ionisation, unsubstituted N-acyl-homoserine lactones (HSLs) with a chainlength of 4, 6, 8, 10, 12, and 14 carbon atoms are applied as standards. Figure 40 shows the spectra resulting from direct SMT-PI in an open setup of a 10 mg/L standard mixture of six HSLs with different size and polarity at different temperatures. The analytes are detected in their protonated form in positive ion mode according to formula 18 and 19. It can be seen clearly that at with rising temperature, the maximum intensity shifts towards the larger and more polar analytes. This may be due to a low thermostability of the small analytes in this temperature range, while the larger and more polar analytes need higher temperatures to desolvate again from the surface. It can also be seen that all HSLs can be detected by this method and that the optimum temperature for the detection of all analytes is 100° C in this setup, while lower temperatures seem to be favourable to detect the small HSLs and higher temperatures for the detection of the larger HSLs. A further examination of the selectivity of the analysis resulting from the different temperatures applied may be worth considering for future studies. This effect could be made use of, when it is additionally taken into consideration for the identification of unknown analytes.

7.2.4. Indirect surface-mediated thermodesolvatation and photoionisation

Surface-mediated chemical analysis techniques became more and more important over the last years, especially in combination with mass spectrometric detection. The most prominent one is matrix assisted laser desorption ionisation (MALDI) [129, 130] which is only one representative of several laser desorption ionisation (LDI) techniques [131, 132]. Another new technique is desorption electrospray ionisation (DESI) [133, 134]. These techniques make use of several advantages: 1. The handling of the sample is advantageous: An immobilized sample on a surface is easy to handle, easy to store and easily accessible. 2. These methods are uninvasive and due to the fact that in many cases only a small part of the analytes are consumed during the analysis, the analysis time can be long which leads to an improved sensitivity and resolution, and in many cases, the immobilized sample can be stored and reanalyzed. 3. Like it is the case in MALDI, the properties of the surface may play an important role in the desolvatation process.

Because of this reasons, the SMT-PI setup was tested in indirect mode which means that the sample is deposited on the surface and desorbed by droplets of solvent plus dopant.

To test this, a supernatant of a *Burkholderia cepacia*, strain LA-3, culture, grown for 12 h in nutrient broth medium was used. The sample was extracted on a SPE-cartridge as described by Li et al. *[VII]*. This goes along with a 10fold concentration.

The result of the analysis of a *Burkholderia cepacia* culture supernatant is shown in figure 41. C8-HSL and C10-HSL could be clearly detected by application of the method on the Ion Trap. Both HSL could be detected in their protonated form as well as putatively in form of an ammonium-adduct. A detection and verification of the results was also possible with FT-ICR MS (see fig. 42). Here only the protonated form is detectable. The power and the necessity for the high resolution provided by FT-ICR MS becomes obvious, when having a closer look on the peak for the C8-HSL: The analyte peak is found in next neighbourhood to another peak resulting from the sample matrix. The m/z divergence of these two peaks is lower than 0.08 but a clear separation and distinct identification of the analyte is possible anyway.

The study of the processes leading to the putative ammonium adduct formation will be subject of further studies. HSLs are expected to be found as they were also found in previous examinations of cultures of this bacterium [47], *[II]*, *[VIII]*. This result shows the applicability of this method even for very complex real samples without much sample preparation. The small amount of sample needed (5 µL of extracted sample which could be lowered in further optimisation) is a clear advantage because these samples are typically not available in higher amounts. The analysis time took 6 minutes (the spectra from minute 2 to 6 were integrated) respectively 300 scans in the FT-ICR MS which can be raised to increase the sensitivity. The sample was spread over the desorbtion surface which is around 0.5 cm^2 in size. Only a small area of this surface is examined so that further examinations with different settings for example may be possible as well as a storage of the desorbtion surface for later verifications. A movable desorbtion surface may widen up this setup for applications in high-throughput approaches or for imaging. A special coating of the surface may influence the desorbtion behaviour of different analytes so that different analytes could be desorbed specifically.

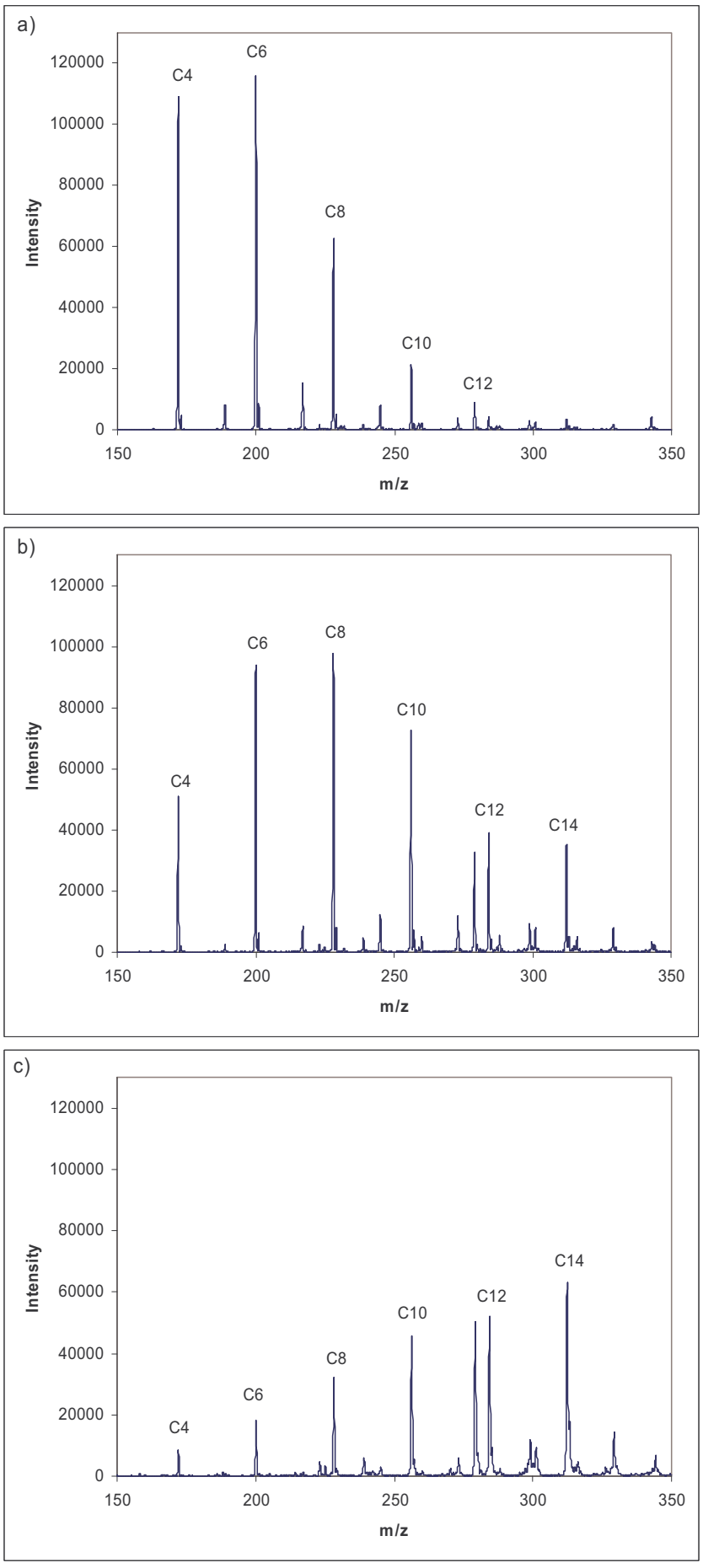


Figure 40: Direct SMT-PI with UV ionisation of a 10 mg/L HSL standard mixture solution of C4-, C6-, C8-, C10-, C12- and C14-HSL at
a) 80° C,
b) 100° C and
c) 120° C. All HSLs are found in their protonated from.
The signal at 279 is an impurity.

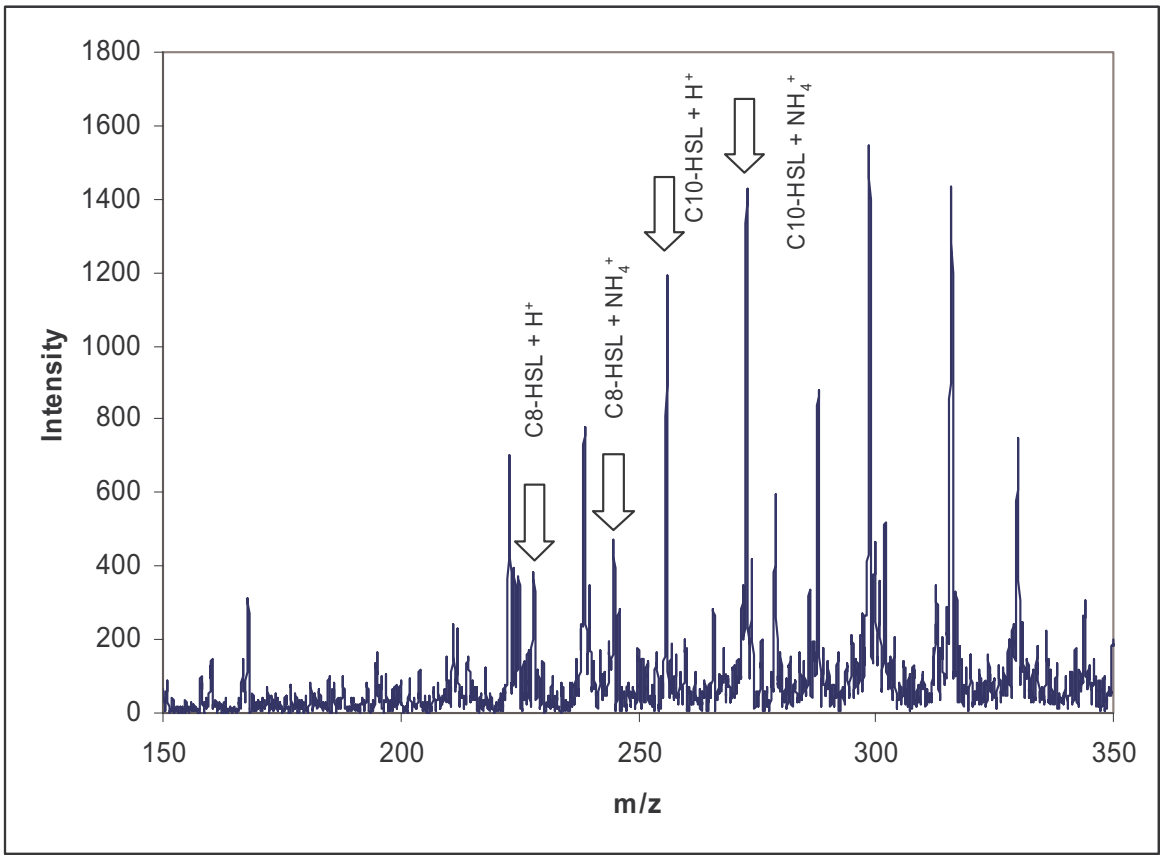


Figure 41: Spectrum resulting from the indirect SMT-PI analysis of the extracted supernatant of a *Burkholderia cepacia* culture. C8-HSL und C10-HSL could be determined in their protonated form as well as putatively in form of an ammonium adduct.

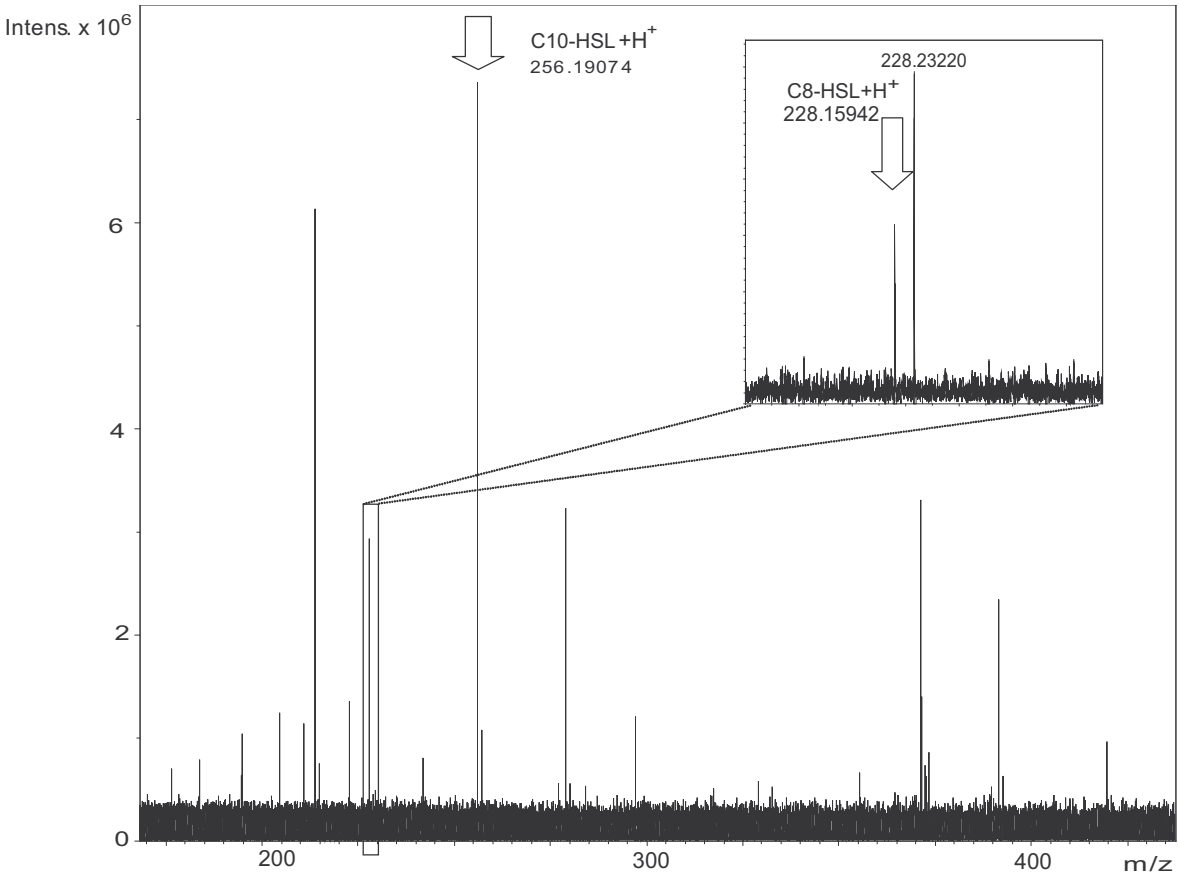


Figure 42: FT-ICR MS spectrum resulting from the indirect SMT-PI analysis of the extracted supernatant of a *Burkholderia cepacia* culture. C8-HSL und C10-HSL could be clearly assigned by their elemental compositions in their protonated form. 300 scans were accumulated to generate this spectrum.

7.3. Summary

An approach based on the production of single, charged droplets for sample introduction for MS analytics was shown to be applicable in principal but showed unavoidable irreproducibilities and a proper dosage is not possible. The principle of surface enhanced thermodesorbtion with photoionisation of the desorbed molecules was shown to be successfully applicable for HSL analytics. Eventhough the method is not optimized jet, HSLs could be successfully determined in real samples applying indirect SMT-PI. The fast and relatively simple analysis opens new perspectives in HSL analytics. Also, the small amount of sample needed offers the potential for at site analysis in the rhizosphere which is planned in the future. The special character of a physical process which is based on the desorbtion of the analytes from surfaces by a specific and highly controllable application of a solvent may open up new ways of influencing this process by changing parameters like the surface properties or the solvent composition. Further developments and

optimisations of this principle will result in additional advantages to be found in comparison to conventional methods and a further increase in the sensitivity, applicability and easiness of usage. The applicability of this new technique is not restricted to HSLs: The replacement of the photoionisation lamp by a laser revealed detection limits down to the low amol range for polycyclic aromatic hydrocarbons (PAHs) which is very sensitive keeping in mind that an open setup was applied and FT-ICR MS is not the most sensitive mass spectrometric detection method (data not shown in this work).

8. Conclusion and outlook

The existing analytical approaches for the analysis of N-acyl homoserines lactones could be complemented and improved in several ways. The implementation of an UPLC-PDA method for the analysis of unsubstituted and saturated HSLs from C6 to C14 besides all corresponding serines offers a solid basis for in depth hydrolysis studies which are important to be performed, since this reaction is crucial in the whole signalling process. The general possibility was proven and the results differed widely from the hydrolysis kinetics formulae known to date. Generally, the serines should always be kept in focus, whenever HSLs are studied, since the hydrolysation process is likely to occur either biologically or chemically. The possibility to engage PDA detection circumvents problems with a putative re-lactonisation in the different MS interfaces. On the other hand side, PDA detection widens up the spectrum of detection methods and allows cross validations.
The speed of the analysis is another step forward: The runtime for state-of-the art analytics was between 20 and 40 minutes. This could be reduced to around one minute which is a more than 90 % runtime reduction. The UPLC method is fully automatisable which is not the case in every earlier developed method. Even though the sensitivity is still high enough for real sample analytics, the UPLC method is less sensitive than comparable methods. This can be overcome by coupling the UPLC separation with higher sensitive detection methods, like MS. TOF-MS is generally fast enough to be coupled to UPLC and the UPLC method is generally MS compatible, so that a coupling of UPLC and TOF-MS may significantly increase selectivity and sensitivity. This is planned to be implemented in the future.

The employment of drop-on-demand dispenser technology was shown to be a reliable tool for quantifications in small volumes of sample. The quantification of HSLs in bacterial culture supernatants without extraction was not performed before. This opens the way for detailed studies of real life samples, for example from the rhizosphere which is a long-term goal of the project. Due to the automated dosage and analysis, the total analysis time per sample may lie around 3 to 4 minutes (not including the concentration step): each one minute for the two analyses (with and without standard addition), around one minute for the filtration and dosage of the sample. The dosage of the standard is performed within seconds. The analysis time by conventional methods lies at 20 minutes for the separation plus the time needed for an elaborate extraction. This provides the basis for a fast high-throughput scanning of many samples for HSLs.

SMT-PI was shown to be another promising principle for the fast and selective identification of HSLs in real samples. Also here, the high speed and easiness of the analysis, as well as the small sample volumes to be applied are the main advantages. A further optimisation of the setup will improve the performance characteristics significantly for the direct and indirect application. A possible integration of additional features like special surface properties may open up new analytical possibilities and is subject of further investigation.

All analytical methods presented in this work are freely combinable. This opens up the possibility to address specific analytical challenges by combining different analytical approaches. The examples given in chapter 4 show the possibilities of applying “combined forces”, like UPLC in combination with high resolution MS and bioassays. Another advantage of providing different analytical methods is the possibility for cross-validations as well as the insight in the possibilities and limitation of the different approaches compared to each other.

Even though the development and improvement of methods for the analytics of HSL was the goal of this work, the developed approaches are applicable to a wide range of analytes outside HSL analytics and may be advantageous in many fields. Drop-on-demand dispenser technology is a powerful tool and the possibility to dose quantitatively by application of an easy method for the determination of the average single droplet volume may opens possibilities in many fields of quantitative analytics. One application is the integration in the SMT-PI approach. This new technology will reveal its potential, when it is further optimised. The fundamental difference of this approach from conventional methods will certainly have advantages for specific applications in many fields.

9. Appendix

9.1. Chemicals and consumables

All chemicals except as stated otherwise were purchased from Sigma-Aldrich (Steinheim, Germany) and were at least of analytical grade. All HSL (see chapter 9.4 for full names) as well as ammonium formate and sodium hydroxide were purchased from Sigma Aldrich (Taufkirchen, Germany). Water was provided by a Milli-Q plus System by Millipore Corporation (Billerica, CA, USA), acetonitrile ("hypergrade" quality) was from Merck (Darmstadt, Germany), hexane from Riedel-de Haen (Honeywell GmbH, Seelze, Germany). Formic acid was provided by Merck (Darmstadt, Germany).
Caffeine and ammonium formiate were purchased from Sigma-Aldrich Chemie, Steinheim, Germany. N-Decanoyl homoserine is not commercially available. To prepare the standard solution, to a 1,000 mg/L solution of N-docanoyl homoserine lactone in acetonitrile, 5 % of 1 M NaOH (Sigma-Aldrich, Taufkirchen, Germany) in water was added to hydrolyze the lactone. After stirring, the suspension was dried under nitrogen and was ready for analysis. Dimethylsilane, Toluene and Dimethylether were from Merck, Darmstadt, Germany. Pyren D10 is from Dr. Ehrensdorfer (Augsburg, Germany).
Filters were 0.22-µm PTFE filter (VWR International, Darmstadt, Germany).

9.2. Instruments

9.2.1. UPLC

UPLC™ analysis was performed by an Acquity System (Waters Corporation, Milford, MA, USA) with a 2996 PDA detector. The system was equipped with an Acquity 2.1 x 100 mm BEH C_{18} column with 1.7 µm particles (Waters Corporation, Milford, MA, USA). The effective dwell volume of the system is 208 µL *[X]*. The sample manager was thermostated at 27° C.
The vials used were UPLC vials (12mmx32 mm, screw-neck glass vials, Waters)

9.2.2. Drop-on-demand dispenser

An MD-K-130 HV drop-on-demand system from Microdrop Technologies, Norderstedt, Germany for vertical dosage was used in combination with an MD-E-201 controller. For

monitoring, a model 7633 oscilloscope from Tektronix Holland (Heerenveen, The Netherlands) was used. The dispenser head was mounted on an XYZ micrometer stage and observations were made with a Zeiss Stemi 2000-C microscope (Carl Zeiss, Oberkochen, Germany). A medium frequency of around 200 Hz was chosen for the experiments (around 100 Hz, respectively 9000 µS period between two pulses for the single droplet direct ESI experiment).
In case a voltage was applied, this was provided by the ion trap MS source.

9.2.3. Ion trap MS

The ion trap mass spectrometer was a ThermoFinnigan (San José, CA, USA) LCQ Duo ion trap. It was run in positive mode. It was tuned to the protonated caffeine peak at m/z 195. The source was opened to provide direct access to the heated capillary. The ion gauge control was set off for the experiments and injection time was set to 30 ms. The capillary voltage was set to 15 V. 5 microscans were performed and the scan range was m/z 150 to 350. The temperature of the heated capillary was set to 300 ° C in case of the single droplet ESI experiments and to 5 °C above the temperature of the chamber in case of the surface enhanced desolvatisation photoionisation experiments. The high voltage for electrospray experiments is provided by the instrument and applied at the sprayer tip. In the single droplet electrospray experiments, this voltage supply was connected to the electrode in the dispenser. At least five single scans were taken into account for each datapoint and to evaluate its standard deviation.

9.2.4. FT-ICR MS

FT-ICR MS measurements were performed on a Bruker Daltonics (Bremen, Germany) Apex Qe 12 Tesla instrument equipped with an APOLLO II source. Spectra were acquired in positive ion mode and in broadband mode. Unless otherwise stated, the heated capillary was held at 200 °C. In electrospray mode, the voltage is applied on the capillary, while the counter electrode is grounded. Calibration was performed externally on clusters of arginine (ca. 10 mg L^{-1} in 1:1 (v/v) methanol/water with 0.1 % (v/v) formic acid. In case of the single droplet electrospray experiments on FT-ICR-MS, a dry gas flow of 2 L s^{-1} was found to be optimal. The source was opened to have free contact to the heated capillary.

9.2.5. Surface mediated thermodesolvatation and photoionisation (SMT-PI)

The temperature is provided by a heating element (model 654 by HS-Heizelemente, Fridingen, Germany) and controlled by a Pt100 sensor (Labfacility, Bognor Regis, UK) with a connected control unit (MPS4 by Schön Elektrotechnik, Klettgau, Germany). The Kr-lamp housing is also manufactured inhouse and is made of polyethet ether ketone (PEEK). The lamp is a PKS106 krypton discharge lamp by LOT-Oriel, Darmstadt, Germany. This apparatus was associated with the ion trap mass spectrometer and the FTICR-MS

9.3. Software

pKa, LogP and LogD values were performed with Pallas 3.1 for Windows with PrologP 7.0, pKalc 5.1 and PrologD 3.0 (CompuDrug , Budapest, Hungary).
UPLC results were processed using Waters Empower and Dionex (Dionex GmbH, Idstein, Germany) Chromeleon software. In peak processing the peak width was determined at half peak height. Obviously deficient peak integrations given by the processing software were corrected manually.
The fitting of the hydrolysis model to the experimental data was performed by a minimization procedure (least square method) of the software tool MATLAB (Vers. 7.3.0, The Mathworks Inc., Natick, Massachusetts, USA).
For the determination of the droplet size and distance from the nozzle on a photography, Adobe Photoshop 7 software (Adobe Systems, San Jose, USA) was used.

9.4. Methods

9.4.1. Preparation of standards for UPLC analysis

Standards were prepared starting from a mixture of seven HSL standard stock solutions each 1000 mg/L in acetonitrile. In case of the lactones, the mixture was diluted 1:2 by water and 0.2 % formic acid was added; in case of the homoserines, it was diluted in 0.07 M NaOH and after a reaction time of 15 min for the hydrolysis, 0.4 % formic acid was added *[VIII]*. This resulted in a pH of around 3 for the lactones 5, respectively, for the homoserines. A mixture of 1:1 (v/v) of these two solutions (HS and HSL) resulted in a concentration of 23.8 mg/L of the homoserines and of the lactones at a pH of around 4.

For the calibration curves, this solution was diluted with a 1:2 (v/v) acetonitrile/water-mixture.

9.4.2. Ultra performance liquid chromatography (UPLC) analysis of HSLs beside HSs

20 µL of sample were injected by full loop injection and repeated three times. Detection was performed at 195.4 nm (4.8 nm width) and a scan rate of 20 Hz.
The initial solvent composition of the mobile phase was 3/7 (v/v) acetonitrile / 10 mM ammonium formate buffer, adjusted to the given pH by titration with formic acid whereby the solvent was premixed and the pH adjustment was performed after the addition of acetonitrile. In case of the pH 3.0 and 3.25 solvents, the solution consisted only of water and acetonitrile, titrated to the end-pH with formic acid.
Before every sample set, the column was rinsed with the buffer solution at least five hours to condition the system according to Marchand et al. [135]. Linear solvent strength (LSS) gradients were applied to an end concentration of 100% acetonitrile. The optimal separation condition was a linear gradient from 30% acetonitrile and 70% 10 mM ammonium formate buffer adjusted to pH 4.25 (v/v) to 100% acetonitrile in 0.5 min after an isocratic pre-run of the initial composition for 0.2 min. The flow rate was 0.9 mL/min and the column temperature 60° C, resulting in a backpressure of around 800 to 900 bar.

9.4.3. Real sample analysis by UPLC

For the examination of the hydrolysis of C8 and C10-HSL, the analytes were spiked to final concentration of 20 mg/L onto a buffer prepared from sodium dihydrogen-phosphate and disodium dihydrogenphsphate at five different pHs (7.0, 7.5, 8.0, 8.5 and 9.0). The reaction solution was kept at room temperature. Sample was injected at once after the spiking through a time period of 13 h. The results were collected and used to put up a model for the kinetics.
For the analysis of a real sample, sample preparation was performed according to Li et al. *[VII]*. Briefly, bacterial supernatant of *Burkholderia cepacia*, strain LA-3 was used. 50 ml of Luria Bertani liquid medium (“LB-medium”) which contains 10 g Tryptone, 5 g yeast extract and 4 g NaCl (Sigma-Aldrich, Steinheim, Germany) was inoculated by the bacteria, grown at 30° C and stirred with 175 rpm overnight. The separation of the supernatant from the bacteria was performed by centrifugation at 5000 rpm and 4° C for 5

min. Subsequent solid phase extraction was made using C_{18} cartridges (1 g/6 mL MEGA BondElut, Varian, Palo Alto, CA, USA). The cartridges were conditioned with 2 ml of methanol and 2 ml of water. After application of 40 ml of sample, the columns were washed with 4 ml of methanol/water (15/85, v/v) and dried under vacuum. The analytes were eluted with 2 ml hexane/2-propanol (15/85, v/v). After evaporation to dryness under nitrogen, the analytes were dissolved in 4 ml acetonitrile/water (30/70, v/v) and filtered through a PTFE membrane filter with 13 mm diameter and a pore size of 0.2 µm (VWR International, Darmstadt, Germany). This procedure results in a 10-fold concentration for the subsequent analysis.

For the hydrolisis of HSLs in the samples, 20 µl of 1M NaOH was added on 400 µl of the extract, incubated for 15 min and 20 µl of 10% formic acid in acetonitrile/water (66/33, v/v) was added to acidify the solution before injection. On another aliquot of 400 µl extract, 40 µl 5% formic acid in acetonitrile/water (33/66, v/v) was added and used as a control.

9.4.4. Real sample preparation for the standard addition experiment

As a real sample, a supernatant of a *Burkholderia cepatia*, strain LA-3, culture, grown for 12 h in nutrient broth medium was used. To increase the concentration of the analyte, the sample was reduced to 25% of the original volume by drying it under nitrogen and redissolving it in 0.05 M NaOH in water. After 15 min, 0.4 % formic acid was added to an end volume of one fourth of the original sample volume. The solution was filtered through a 0.22-µm poly(tetrafluoroethylene) (PTFE) filter (VWR International, Darmstadt, Germany).

9.4.5. Droplet volume determination via photography

Photographs were taken with a Sony DSC-F717 camera (Sony Deutschland, Colone, Germany) mounted on the microscope. At least nine shots were taken within each measurement with different delay times of the diode. The diameter of the droplet was determined in relation to the diameter of the nozzle, as done by Wu et al. [91]. In this case, the diameter determined is independent of the zoom factors of the microscope and the camera. The diameter was scaled twice at angles of 90° to each other and averaged. The period between two pulses was 5,050 µs, corresponding to about 200-Hz dispensing frequency.

9.4.6. Droplet volume determination by weighing the reservoir

In this method, the running system is stopped and the reservoir is taken off the system, encapsulated and weighed on a Sartorius CP 225 D microbalance (Sartorius, Göttingen, Germany). After at least 500,000 droplets had been dispensed, the reservoir was weighed again. The weighing procedure did not exceed 2 min to prevent losses due to evaporation. The mass divergence is equal to the dispensed mass, so the volume can be determined by dividing the mass, corrected by the density of the liquid, through the number of droplets dispensed. The period between two pulses was 5,050 µs which corresponds to about 200-Hz dispensing frequency.

9.4.7. Droplet volume verification by UPLC analysis

The column was thermostated at 60 °C and the sample system was maintained at 15 °C. The system was run with 2:8 (v/v) acetonitrile/water in isocratic mode. The flow rate was set to 0.8 mL/min and 20 µL of sample was injected via full-loop injection. This resulted in a chromatographic runtime of 0.6 min and a total runtime of about 1.5 min per injection. Detection was performed at 273 nm and peak areas were calculated using Waters Empower software. Each injection was repeated five times and the mean value was taken into account.
For the comparison of the graphimetrical and the imaging approach, 200-mL graduated glass flasks (EM, In, class A from Hirschmann Laborgeräte, Eberstadt, Germany) and pipettes of the type “reference” (Eppendorf, Hamburg, Germany) were applied.

9.4.8. Sample preparation for the standard addition approach

The homoserine was dissolved in the same volume of water as the original lactone-solution had been. After filtration (0.22-µm PTFE filter; VWR International, Darmstadt Germany), an aliquot of the solution was dissolved 1:99 in water and the concentration of the serine was determined by the UPLC method described in the next section. The concentrations determined were 747 mg/L for the solution used for the standard addition to the spiked samples and 832 mg/L for the solution used for the analysis of the real sample.

9.4.9. UPLC analysis of the real samples for standard addition

The method for the analysis of N-acyl-homoserines is described in detail in chapter 3 *[II]*. For the preparation of the external standards, the 1,000 mg/L stock solution of N-decanoyl homoserine lactone in acetonitrile was diluted in a mixture of one part acetonitrile and two parts 0.07 M NaOH (v/v). After 15 min, 0.4 % formic acid was added. This standard solution was diluted in acetonitrile/water (1:2 v/v) to lower concentrations for the external calibration curve. A five-point calibration from 1.5 to 24 mg/L was performed every day.
The same UPLC system and column were used as for the droplet volume verification. In this case, the autosampler was thermostated at 27 °C and the column oven at 60 °C. A 20-µL aliquot of sample was injected by full-loop injection. The detection was performed at 195.4 nm and 20 Hz.
The initial composition of solvent was 3:7 (v/v) acetonitrile/10 mM ammonium formiate buffer, adjusted to pH 4.25 with formic acid. A gradient profile of 0.2 min of the initial composition followed by a gradient of 0.5 min to 100% acetonitrile was performed at a flow rate of 0.9 mL/min.

9.4.10. Experimental determination of the dispensed droplet speed

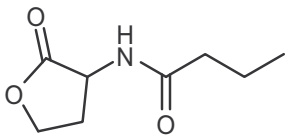
Photographs were taken with a Sony DSC-F717 camera (Sony Deutschland, Colone, Germany) mounted on the microscope Zeiss Stemi 2000-C (Carl Zeiss, Oberkochen, Germany). The distance of the droplet to the dispenser nozzle was measured on a photo in reference to the nozzle diameter, like it was done for the determination of the droplet diameter. Furthermore, the distance to the border of the picture was determined applying the same method. For droplets farer away from the nozzle, the distance was determined by moving the dispenser which is mounted on a xyz-micometer stage, while the camera remained at the same position. The distance was therefore the distance droplet-border of the photo (the zoom-factor was determined in the first measurement) plus the distance determined on the micrometer screw (which was aligned before). The distances were determined at different delay times of the stroboscope diode and the average speed was determined by the speed drop between two adjacent determinations.

9.4.11. Single droplet electrospray mass spectrometry

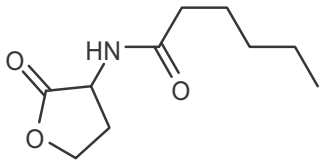
10 mg/L caffeine in methanol/water (1:1, v/v) plus 0.1% formic acid was chosen for the experiments as a test-solution.

9.5. Analytes

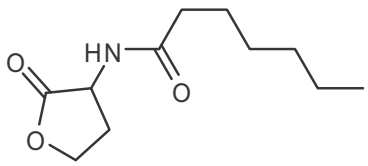
N-butanoyl-D/L-homoserine lactone
Short name: C4-HSL
LogP: 0.03
Mass: 170.081719



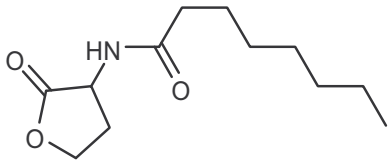
N-hexanoyl-D/L-homoserine lactone
Short name: C6-HSL
LogP: 1.02
Mass: 198.113019



N-heptanoyl-D/L-homoserine lactone
Short name: C7-HSL
LogP: 1.94
Mass: 212.128669



N-octanoyl-D/L-homoserine lactone
Short name: C8-HSL
LogP: 1.97
Mass: 226.144319

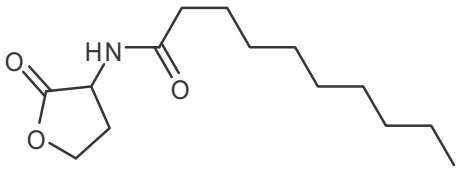


N-decanoyl-D/L-homoserine lactone

Short name: C10-HSL

LogP: 2.96

Mass: 254.17562

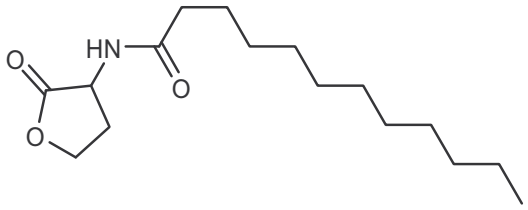


N-dodecanoyl-D/L-homoserine lactone

Short name: C12-HSL

LogP: 4.02

Mass: 282.20692

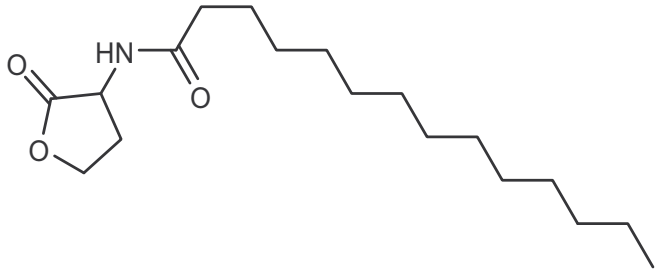


N-tetradecanoyl-D/L-homoserine lactone

Short name: C14-HSL

LogP: 5.09

Mass: 310.23822



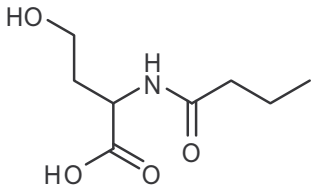
N-butanoyl-D/L-homoserine

Short name: C4-HS

LogP: 3.49

pK_a: -0.94

Mass: 188.09228



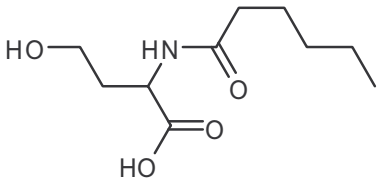
N-hexanoyl-D/L-homoserine

Short name: C6-HS

LogP: 3.23

pK_a: -0.43

Mass: 216.12358



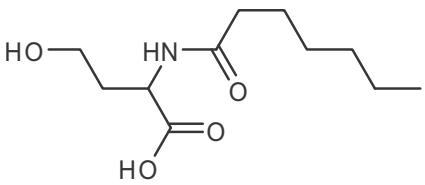
N-heptanoyl-D/L-homoserine

Short name: C7-HS

LogP: 3.23

pK_a: 0.04

Mass: 230.13923



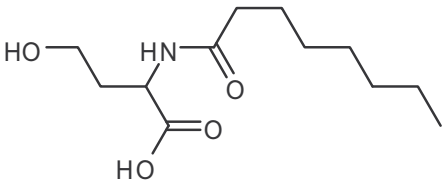
N-octanoyl-D/L-homoserine

Short name: C8-HS

LogP: 3.23

pK_a: 0.49

Mass: 244.15488



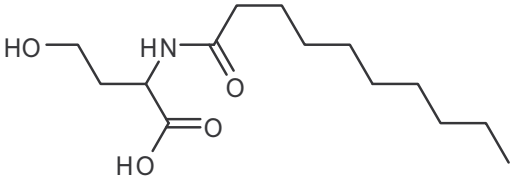
N-decanoyl-D/L-homoserine

Short name: C10-HS

LogP: 3.23

pK_a: 1.33

Mass: 272.18618



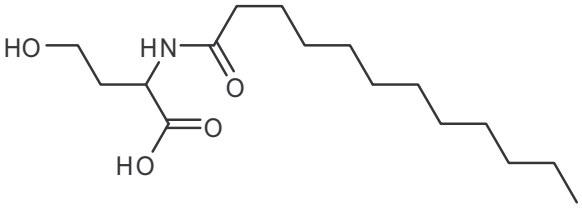
N-dodecanoyl-D/L-homoserine

Short name: C12-HS

LogP: 3.23

pK_a: 2.18

Mass: 300.21748



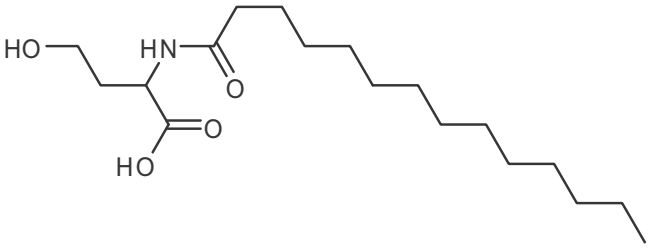
N-tetradecanoyl-D/L-homoserine

Short name: C14-HS

LogP: 3.23

pK_a: 3.11

Mass: 328.24878



References

See also page 4 for references *[I]* to *[X]*

1. Kempner ESH, F. E.: **Aspects of Light Production by Photobacterium fischeri**. Journal of Bacteriology 1968, **95**(3):975-979.
2. Visick KL, Foster J, Doino J, McFall-Ngai M, Ruby EG: **Vibrio fischeri lux genes play an important role in colonization and development of the host light organ**. Journal of Bacteriology 2000, **182**(16):4578-4586.
3. Visick KL, McFall-Ngai MJ: **An exclusive contract: Specificity in the Vibrio fischeri Euprymna scolopes partnership**. Journal of Bacteriology 2000, **182**(7):1779-1787.
4. Nealson KHP, t.; Hastings, J. W. : **Cellular control of the synthesis and activity of the bacterial luminescent system**. Journal of Bacteriology 1970, **104**:313-322.
5. Eberhard AB, A. L.; Eberhard, C.; Kenyon, L.; Nealson, K. H.; Oppenheimer, N. J.: **Structural Identification of Autoinducer of Photobacterium fischeri Luciferase**. Biochemistry 1981, **20**:2444-2449.
6. Fuqua C, Greenberg EP: **Listening in on bacteria: Acyl-homoserine lactone signalling**. Nat Rev Mol Cell Bio 2002, **3**(9):685-695.
7. Fuqua WCW, S. C.; Greenberg, E. P.: **Quorum Sensing in Bacteria: the LuxR-LuxI Family of Cell Density-Responsive Transcriptional Regulators**. Journal of Bacteriology 1994, **176**(2):269-275.
8. Lithgow JK, Wilkinson A, Hardman A, Rodelas B, Wisniewski-Dye F, Williams P, Downie JA: **The regulatory locus cinRI in Rhizobium leguminosarum controls a network of quorum-sensing loci**. Molecular Microbiology 2000, **37**(1):81-97.
9. Horng YT, Deng SC, Daykin M, Soo PC, Wei JR, Luh KT, Ho SW, Swift S, Lai HC, Williams P: **The LuxR family protein SpnR functions as a negative regulator of N-acylhomoserine lactone-dependent quorum sensing in Serratia marcescens**. Molecular Microbiology 2002, **45**(6):1655-1671.
10. Frommberger M: **Entwicklung von Methoden zur Analyse von N-Acyl-Homoserinlactonen durch Kapillartrenntechniken und Massenspektrometrie**. Freising: Technische Universität München; 2005.
11. Parsek MR, Greenberg EP: **Acyl-homoserine lactone quorum sensing in Gram-negative bacteria: A signaling mechanism involved in associations with higher organisms**. P Natl Acad Sci USA 2000, **97**(16):8789-8793.
12. Swift S, Karlyshev AV, Fish L, Durant EL, Winson MK, Chhabra SR, Williams P, MacIntyre S, Stewart GSAB: **Quorum sensing in Aeromonas hydrophila and Aeromonas salmonicida: Identification of the LuxRI homologs AhyRI and AsaRI and their cognate N-acylhomoserine lactone signal molecules**. Journal of Bacteriology 1997, **179**(17):5271-5281.
13. Flodgaard LR, Christensen AB, Molin S, Givskov M, Gram L: **Influence of food preservation parameters and associated microbiota on production rate, profile and stability of acylated homoserine lactones from food-derived Enterobacteriaceae**. International Journal of Food Microbiology 2003, **84**(2):145-156.
14. Laue RE, Jiang Y, Chhabra SR, Jacob S, Stewart GSAB, Hardman A, Downie JA, O'Gara F, Williams P: **The biocontrol strain Pseudomonas fluorescens F113 produces the Rhizobium small bacteriocin, N-(3-hydroxy-7-cis-tetradecenoyl)homoserine lactone, via HdtS, a putative novel N-acylhomoserine lactone synthase**. Microbiology-Uk 2000, **146**:2469-2480.
15. Whitehead NA, Barnard AML, Slater H, Simpson NJL, Salmond GPC: **Quorum-sensing in gram-negative bacteria**. Fems Microbiology Reviews 2001, **25**(4):365-404.

16. Redfield RJ: **Is quorum sensing a side effect of diffusion sensing?** Trends in Microbiology 2002, **10**(8):365-370.
17. Hense BA, Kuttler C, Mueller J, Rothballer M, Hartmann A, Kreft JU: **Opinion - Does efficiency sensing unify diffusion and quorum sensing?** Nature Reviews Microbiology 2007, **5**(3):230-239.
18. Schaefer AL, Hanzelka BL, Parsek MR, Greenberg EP: **Detection, purification, and structural elucidation of the acylhomoserine lactone inducer of Vibrio fischeri luminescence and other related molecules**. Bioluminescence and Chemiluminescence, Pt C 2000, **305**:288-301.
19. Dong YH, Wang LH, Xu JL, Zhang HB, Zhang XF, Zhang LH: **Quenching quorum-sensing-dependent bacterial infection by an N-acyl homoserine lactonase**. Nature 2001, **411**(6839):813-817.
20. Wang YJ, Leadbetter JR: **Rapid acyl-homoserine lactone quorum signal biodegradation in diverse soils**. Applied and Environmental Microbiology 2005, **71**(3):1291-1299.
21. Zhang LH: **Quorum quenching and proactive host defense**. Trends in Plant Science 2003, **8**(5):238-244.
22. Huang JJ, Han JI, Zhang LH, Leadbetter JR: **Utilization of acyl-homoserine lactone quorum signals for growth by a soil pseudomonad and Pseudomonas aeruginosa PAO1**. Applied and Environmental Microbiology 2003, **69**(10):5941-5949.
23. Michels JJ, Allain EJ, Borchardt SA, Hu PF, McCoy WF: **Degradation pathway of homoserine lactone bacterial signal molecules by halogen antimicrobials identified by liquid chromatography with photodiode array and mass spectrometric detection**. J Chromatogr A 2000, **898**(2):153-165.
24. Gonzalez JE, Keshavan ND: **Messing with bacterial quorum sensing**. Microbiology and Molecular Biology Reviews 2006, **70**(4):859-+.
25. Sperandio V, Torres AG, Giron JA, Kaper JB: **Quorum sensing is a global regulatory mechanism in enterohemorrhagic Escherichia coli O157 : H7**. Journal of Bacteriology 2001, **183**(17):5187-5197.
26. Schuhegger R, Ihring A, Gantner S, Bahnweg G, Knappe C, Vogg G, Hutzler P, Schmid M, Van Breusegem F, Eberl L et al: **Induction of systemic resistance in tomato by N-acyl-L-homoserine lactone-producing rhizosphere bacteria**. Plant Cell and Environment 2006, **29**(5):909-918.
27. Gao MS, Teplitski M, Robinson JB, Bauer WD: **Production of substances by Medicago truncatula that affect bacterial quorum sensing**. Molecular Plant-Microbe Interactions 2003, **16**(9):827-834.
28. Shaw PD, Ping G, Daly SL, Cha C, Cronan JE, Rinehart KL, Farrand SK: **Detecting and characterizing N-acyl-homoserine lactone signal molecules by thin-layer chromatography**. P Natl Acad Sci USA 1997, **94**(12):6036-6041.
29. Steidle A, Sigl K, Schuhegger R, Ihring A, Schmid M, Gantner S, Stoffels M, Riedel K, Givskov M, Hartmann A et al: **Visualization of N-acylhomoserine lactone-mediated cell-cell communication between bacteria colonizing the tomato rhizosphere**. Applied and Environmental Microbiology 2001, **67**(12):5761-5770.
30. Gould TA, Herman J, Krank J, Murphy RC, Churchill MEA: **Specificity of acyl-homoserine lactone synthases examined by mass spectrometry**. Journal of Bacteriology 2006, **188**(2):773-783.
31. Middleton B, Rodgers HC, Camara M, Knox AJ, Williams P, Hardman A: **Direct detection of N-acylhomoserine lactones in cystic fibrosis sputum**. Fems Microbiology Letters 2002, **207**(1):1-7.
32. Chambers CE, Visser MB, Schwab U, Sokol PA: **Identification of N-acylhomoserine lactones in mucopurulent respiratory secretions from cystic fibrosis patients**. Fems Microbiology Letters 2005, **244**(2):297-304.
33. Milton DL, Hardman A, Camara M, Chhabra SR, Bycroft BW, Stewart GSAB, Williams P: **Quorum sensing in Vibrio anguillarum: Characterization of the**

vanI/vanR locus and identification of the autoinducer N-(3-oxodecanoyl)-L-homoserine lactone. Journal of Bacteriology 1997, **179**(9):3004-3012.
34. Milton DL, Chalker VJ, Kirke D, Hardman A, Camara M, Williams P: **The luxM Homologue vanM from Vibrio anguillanrum directs the synthesis of N-(3-hydroxyhexanoyl)homoserine lactone and N-hexanoylhomoserine lactone**. Journal of Bacteriology 2001, **183**(12):3537-3547.
35. Teplitski M, Eberhard A, Gronquist MR, Gao M, Robinson JB, Bauer WD: **Chemical identification of N-acyl homoserine lactone quorum-sensing signals produced by Sinorhizobium meliloti strains in defined medium**. Archives of Microbiology 2003, **180**(6):494-497.
36. Llamas I, Quesada E, Martinez-Canovas M, Gronquist M, Eberhard A, Gonzalez JE: **Quorum sensing in halophilic bacteria: detection of N-acyl-homoserine lactones in the exopolysaccharide-producing species of Halomonas**. Extremophiles 2005, **9**(4):333-341.
37. Pomini AM, Manfio GP, Araujo WL, Marsaioli AJ: **Acyl-homoserine lactones from Erwinia psidii R. IBSBF 435(T), a guava phytopathogen (Psidium guajava L.)**. Journal of Agricultural and Food Chemistry 2005, **53**(16):6262-6265.
38. Jiang Y, Camara M, Chhabra SR, Hardie KR, Bycroft BW, Lazdunski A, Salmond GPC, Stewart GSAB, Williams P: **In vitro biosynthesis of the Pseudomonas aeruginosa quorum-sensing signal molecule N-butanoyl-L-homoserine lactone**. Molecular Microbiology 1998, **28**(1):193-203.
39. Schupp PJ, Charlton TS, Taylor MW, Kjelleberg S, Steinberg PD: **Use of solid-phase extraction to enable enhanced detection of acyl homoserine lactones (AHLs) in environmental samples**. Anal Bioanal Chem 2005, **383**(1):132-137.
40. Cataldi TRI, Bianco G, Frommberger M, Schmitt-Kopplin P: **Direct analysis of selected N-acyl-L-homoserine lactones by gas chromatography/mass spectrometry**. Rapid Commun Mass Sp 2004, **18**(12):1341-1344.
41. Wagner-Dobler I, Thiel V, Eberl L, Allgaier M, Bodor A, Meyer S, Ebner S, Hennig A, Pukall R, Schulz S: **Discovery of complex mixtures of novel long-chain quorum sensing signals in free-living and host-associated marine alphaproteobacteria**. Chembiochem 2005, **6**(12):2195-2206.
42. Charlton TS, de Nys R, Netting A, Kumar N, Hentzer M, Givskov M, Kjelleberg S: **A novel and sensitive method for the quantification of N-3-oxoacyl homoserine lactones using gas chromatography-mass spectrometry: application ito a model bacterial biofilm**. Environmental Microbiology 2000, **2**(5):530-541.
43. Morin D, Grasland B, Vallee-Rehel K, Dufau C, Haras D: **On-line high-performance liquid chromatography-mass spectrometric detection and quantification of N-acylhomoserine lactones, quorum sensing signal molecules, in the presence of biological matrices**. J Chromatogr A 2003, **1002**(1-2):79-92.
44. Flodgaard LR, Dalgaard P, Andersen JB, Nielsen KF, Givskov M, Gram L: **Nonbioluminescent strains of Photobacterium phosphoreum produce the cell-to-cell communication signal N-(3-hydroxyoctanoyl)homoserine lactone**. Applied and Environmental Microbiology 2005, **71**(4):2113-2120.
45. Bruhn JB, Christensen AB, Flodgaard LR, Nielsen KF, Larsen TO, Givskov M, Gram L: **Presence of acylated homoserine lactones (AHLs) and AHL-producing bacteria in meat and potential role of AHL in spoilage of meat**. Applied and Environmental Microbiology 2004, **70**(7):4293-4302.
46. Lin YH, Xu JL, Hu JY, Wang LH, Ong SL, Leadbetter JR, Zhang LH: **Acyl-homoserine lactone acylase from Ralstonia strain XJ12B represents a novel and potent class of quorum-quenching enzymes**. Molecular Microbiology 2003, **47**(3):849-860.
47. Frommberger M, Schmitt-Kopplin P, Ping G, Frisch H, Schmid M, Zhang Y, Hartmann A, Kettrup A: **A simple and robust set-up for on-column sample preconcentration - nano-liquid chromatography - electrospray ionization**

mass spectrometry for the analysis of N-acylhomoserine lactones. Anal Bioanal Chem 2004, **378**(4):1014-1020.
48. Delalande L, Faure D, Raffoux A, Uroz S, D'Angelo-Picard C, Elasri M, Carlier A, Berruyer R, Petit A, Williams P et al: **N-hexanoyl-L-homoserine lactone, a mediator of bacterial quorum-sensing regulation, exhibits plant-dependent stability and may be inactivated by germinating Lotus corniculatus seedlings**. Fems Microbiology Ecology 2005, **52**(1):13-20.
49. Frommberger M, Schmitt-Kopplin P, Menzinger F, Albrecht V, Schmid M, Eberl L, Hartmann A, Kettrup A: **Analysis of N-acyl-L-homoserine lactones produced by Burkholderia cepacia with partial filling micellar electrokinetic chromatography - electrospray ionization-ion trap mass spectrometry**. Electrophoresis 2003, **24**(17):3067-3074.
50. Moon HS: **Identification of homoserine lactone derivatives using the methionine functionalized solid phase synthesis by gas chromatography/mass spectrometry**. Archives of Pharmacal Research 2004, **27**(1):25-30.
51. Rasch M, Andersen JB, Nielsen KF, Flodgaard LR, Christensen H, Givskov M, Gram L: **Involvement of bacterial quorum-sensing signals in spoilage of bean sprouts**. Applied and Environmental Microbiology 2005, **71**(6):3321-3330.
52. Cataldi TRI, Blanco G, Palazzo L, Quaranta V: **Occurrence of N-acyl-L-homoserine lactones in extracts of some Gram-negative bacteria evaluated by gas chromatography-mass spectrometry**. Analytical Biochemistry 2007, **361**(2):226-235.
53. Schmitt-Kopplin P, Frommberger M: **Capillary electrophoresis - mass spectrometry: 15 years of developments and applications**. Electrophoresis 2003, **24**(22-23):3837-3867.
54. Garcia-Campana AM, Taverna M, Fabre H: **LIF detection of peptides and proteins in CE**. Electrophoresis 2007, **28**(1-2):208-232.
55. Couderc F, Causse E, Bayle C: **Drug analysis by capillary electrophoresis and laser-induced fluorescence**. Electrophoresis 1998, **19**(16-17):2777-2790.
56. Smith RD, Shen YF, Tang KQ: **Ultrasensitive and quantitative analyses from combined separations-mass spectrometry for the characterization of proteomes**. Accounts Chem Res 2004, **37**(4):269-278.
57. van de Merbel NC, Giegold S, Teutenberg T: **Practical comparison of different approaches to speed up LC separations**. Lc Gc Eur 2007, **20**(1):32-+.
58. Citova I, Havlikova L, Urbanek L, Solichova D, Novakova L, Solich P: **Comparison of a novel ultra-performance liquid chromatographic method for determination of retinol and alpha-tocopherol in human serum with conventional HPLC using monolithic and particulate columns**. Anal Bioanal Chem 2007, **388**(3):675-681.
59. Snyder LR, Kirkland JJ, Glajch JL: **Practical HPLC Method Development**, 2nd edn. Hoboken: John Wiley & Sons; 1997.
60. Novakova L, Solichova D, Solich P: **Advantages of ultra performance liquid chromatography over high-performance liquid chromatography: Comparison of different analytical 2 approaches during analysis of diclofenac gel**. Journal of Separation Science 2006, **29**(16):2433-2443.
61. Majors RE: **Fast and ultrafast HPLC on sub-2 mu m porous particles - Where do we go from here?** Lc Gc Eur 2006, **19**(6):352-+.
62. Swartz ME: **UPLC (TM): An introduction and review**. J Liq Chromatogr R T 2005, **28**(7-8):1253-1263.
63. Sherma J, Larkin JD, Larkin FH: **UPLC: Ultra-performance liquid chromatography**. J Aoac Int 2005, **88**(3):63a-67a.
64. Swartz ME: **Ultra performance liquid chromatography (UPLC): An introduction**. Lc Gc N Am 2005:8-14.
65. Wren SAC: **Peak capacity in gradient ultra performance liquid chromatography (UPLC)**. J Pharmaceut Biomed 2005, **38**(2):337-343.

66. Yang Y, Hodges CC: **Assay transfer from HPLC to UPLC for higher analysis throughput**. Lc Gc N Am 2005:31-35.
67. Grumbach ES, Wheat TE, Kele M, Mazzeo JR: **Developing columns for UPLC: Design considerations and recent developments**. Lc Gc N Am 2005:40-44.
68. Churchwell MI, Twaddle NC, Meeker LR, Doerge DR: **Improving LC-MS sensitivity through increases in chromatographic performance: Comparisons of UPLC-ES/MS/MS to HPLC-ES/MS/MS**. J Chromatogr B 2005, **825**(2):134-143.
69. Wilson ID, Plumb R, Granger J, Major H, Williams R, Lenz EA: **HPLC-MS-based methods for the study of metabonomics**. J Chromatogr B 2005, **817**(1):67-76.
70. Plumb R: **UPLC detects more metabolites than HPLC**. Trac-Trend Anal Chem 2004, **23**(10-11):V-V.
71. [Anon]: **UPLC reaches levels that HPLC never did**. Trac-Trend Anal Chem 2005, **24**(2):Iv-V.
72. Yu K, Little D, Plumb R, Smith B: **High-throughput quantification for a drug mixture in rat plasma - a comparison of Ultra Performance(TM) liquid chromatography/tandem mass spectrometry with high-performance liquid chromatography/tandem mass spectrometry**. Rapid Commun Mass Sp 2006, **20**(4):544-552.
73. Olsovska J, Jelinkova M, Man P, Koberska M, Janata J, Flieger M: **High-throughput quantification of lincomycin traces in fermentation broth of genetically modified Streptomyces spp. Comparison of ultra-performance liquid chromatography and high-performance liquid chromatography with UV detection**. J Chromatogr A 2007, **1139**(2):214-220.
74. Chesnut SM, Salisbury JJ: **The role of UHPLC in pharmaceutical development**. Journal of Separation Science 2007, **30**(8):1183-1190.
75. Wyndham KD, O'Gara JE, Walter TH, Glose KH, Lawrence NL, Alden BA, Izzo GS, Hudalla CJ, Iraneta PC: **Characterization and evaluation of C18HPLC stationary phases based on ethyl-bridged hybrid organic/inorganic particles**. Anal Chem 2003, **75**(24):6781-6788.
76. Wilson ID, Nicholson JK, Castro-Perez J, Granger JH, Johnson KA, Smith BW, Plumb RS: **High resolution "Ultra performance" liquid chromatography coupled to oa-TOF mass spectrometry as a tool for differential metabolic pathway profiling in functional genomic studies**. J Proteome Res 2005, **4**(2):591-598.
77. Plumb RS, Wilson ID: **High throughput and high sensitivity LC/MS-OA-TOF and UPLC/TOF-MS for the identification of biomarkers of toxicity and disease using a metabonomics approach.** Abstr Pap Am Chem S 2004, **228**:U164-U164.
78. Plumb RS, Granger JH, Stumpf CL, Johnson KA, Smith BW, Gaulitz S, Wilson ID, Castro-Perez J: **A rapid screening approach to metabonomics using UPLC and oa-TOF mass spectrometry: application to age, gender and diurnal variation in normal/Zucker obese rats and black, white and nude mice**. Analyst 2005, **130**(6):844-849.
79. Plumb R, Castro-Perez J, Granger J, Beattie I, Joncour K, Wright A: **Ultra-performance liquid chromatography coupled to quadrupole-orthogonal time-of-flight mass spectrometry**. Rapid Commun Mass Sp 2004, **18**(19):2331-2337.
80. Swartz ME, Hazell B, Sievers D: **Photodiodenarray-Detektion in der UPLC**. LaborPraxis 2006(April 2006):64-66.
81. Martin A: **Some theoretical aspects of partition chromatography**. Biochemical Society Symposia 1949, **3**:4.
82. Lee E: **Microdrop Generation**. Boca Raton, London, New York, Washington, D.C.: CRC Press; 2003.
83. Beulen B, de Jong J, Reinten H, van den Berg M, Wijshoff H, van Dongen R: **Flows on the nozzle plate of an inkjet printhead**. Experiments in Fluids 2007, **42**(2):217-224.

84. Onnerfjord P, Nilsson J, Wallman L, Laurell T, Marko-Varga G: **Picoliter sample preparation in MALDI-TOF MS using a micromachined silicon flow-through dispenser**. Anal Chem 1998, **70**(22):4755-4760.
85. Berggren WT, Westphall MS, Smith LM: **Single-pulse nanoelectrospray ionization**. Anal Chem 2002, **74**(14):3443-3448.
86. Tseng F-G, Kim C-J, Ho C-M: **A Microinjector free of satellite drops and characterisation of the ejected droplets**. In: 1998 ASME International Mechanical Engineering Congress and expositions. 1998.
87. Bruns A, Hoffelner H, Overmann J: **A novel approach for high throughput cultivation assays and the isolation of planktonic bacteria**. Fems Microbiology Ecology 2003, **45**(2):161-171.
88. Eberhardt R, Neidhart B: **Acoustic levitation device for sample pretreatment in microanalysis and trace analysis**. Fresenius Journal of Analytical Chemistry 1999, **365**(6):475-479.
89. Niles WD, Coassin PJ: **Piezo- and solenoid valve-based liquid dispensing for miniaturized assays**. Assay Drug Dev Techn 2005, **3**(2):189-202.
90. Frohn A, Roth N: **Dynamics of Droplets**. Berlin, Heidelberg, New York: Springer; 2000.
91. Wu HC, Hwang WS, Lin HJ: **Development of a three-dimensional simulation system for micro-inkjet and its experimental verification**. Mat Sci Eng a-Struct 2004, **373**(1-2):268-278.
92. Rieber M, Graf F, Hase M, Roth N, Weigand B: **Numerical Simulations of Moving Spherical and Strongly Deformed Droplets**. ILASS-Europe 2000 2000.
93. de Jong J, de Bruin G, Reinten H, van den Berg M, Wijshoff H, Versluis M, Lohse D: **Air entrapment in piezo-driven inkjet printheads**. Journal of the Acoustical Society of America 2006, **120**(3):1257-1265.
94. de Jong J, Jeurissen R, Borel H, van den Berg M, Wijshoff H, Reinten H, Versluis M, Prosperetti A, Lohse D: **Entrapped air bubbles in piezo-driven inkjet printing: Their effect on the droplet velocity**. Physics of Fluids 2006, **18**(12):-.
95. Schober A, Günther R, Schwienhorst A, Döring M, Lindemann BF: **Accurate High-Speed Liquid Handling of Very Small Biological Samples**. Biotechniques 1993, **15**(2):324-329.
96. Cech NB, Enke CG: **Practical implications of some recent studies in electrospray ionization fundamentals**. Mass Spectrom Rev 2001, **20**(6):362-387.
97. Aderogba S, Meacham JM, Degertekin FL, Fedorov AG, Fernandez FM: **Nanoelectrospray ion generation for high-throughput mass spectrometry using a micromachined ultrasonic ejector array**. Applied Physics Letters 2005, **86**(20):-.
98. Meacham JM, Ejimofor C, Kumar S, Degertekin FL, Fedorov AG: **Micromachined ultrasonic droplet generator based on a liquid horn structure**. Review of Scientific Instruments 2004, **75**(5):1347-1352.
99. Fernandez FM, Hampton CY, Meacham JM, Degertekin FL, Fedorov AG: **Venturi-assisted Nanospray Protein Ion Generation by a Micromachined Ultrasonic Electrospray Array**. 17th International Mass Spectrometry Conference, Prague, 2006 2006.
100. Allmaier G: **Picoliter to nanoliter deposition of peptide and protein solutions for matrix-assisted laser desorption ionization mass spectrometry**. Rapid Commun Mass Sp 1997, **11**(14):1567-1569.
101. Little DP, Cornish TJ, ODonnell MJ, Braun A, Cotter RJ, Koster H: **MALDI on a chip: Analysis of arrays of low femtomole to subfemtomole quantities of synthetic oligonucleotides and DNA diagnostic products dispensed by a piezoelectric pipet**. Anal Chem 1997, **69**(22):4540-4546.
102. Laurell T, Wallman L, Nilsson J: **Design and development of a silicon microfabricated flow-through dispenser for on-line picolitre sample handling**. J Micromech Microeng 1999, **9**(4):369-376.

103. Ekstrom S, Onnerfjord P, Nilsson J, Bengtsson M, Laurell T, Marko-Varga G: **Integrated microanalytical technology enabling rapid and automated protein identification**. Anal Chem 2000, **72**(2):286-293.
104. Ekstrom S, Ericsson D, Onnerfjord P, Bengtsson M, Nilsson J, Marko-Varga G, Laurell T: **Signal amplification using "spot on-a-chip" technology for the identification of proteins via MALDI-TOF MS**. Anal Chem 2001, **73**(2):214-219.
105. Santesson S, Nilsson S: **Airborne chemistry: acoustic levitation in chemical analysis**. Anal Bioanal Chem 2004, **378**(7):1704-1709.
106. Tuckermann R, Bauerecker S, Neidhart B: **Schwebende Tröpfchen**. Physik in unserer Zeit 2001, **32**(2):69-75.
107. Petersson M, Nilsson J, Wallman L, Laurell T, Johansson J, Nilsson S: **Sample enrichment in a single levitated droplet for capillary electrophoresis**. Journal of Chromatography B 1998, **714**(1):39-46.
108. Welter E, Neidhart B: **Acoustically levitated droplets - A new tool for micro and trace analysis**. Fresenius Journal of Analytical Chemistry 1997, **357**(3):345-350.
109. Bogan MJ, Agnes GR: **MALDI-TOF-MS analysis of droplets prepared in an electrodynamic balance: "Wall-less" sample preparation**. Anal Chem 2002, **74**(3):489-496.
110. Bogan MJ, Agnes GR: **Wall-less sample preparation of mu m-sized sample spots for femtomole detection limits of proteins from liquid based UV-MALDI matrices**. J Am Soc Mass Spectr 2004, **15**(4):486-495.
111. Litborn E, Stjernstrom M, Roeraade J: **Nanoliter titration based on piezoelectric drop-on-demand technology and laser-induced fluorescence detection**. Anal Chem 1998, **70**(22):4847-4852.
112. Sziele D, Brüggemann O, Döring M, Freitag R, Schügerl K: **Adaptation of a microdrop injector to sampling in capillary electrophoresis**. J Chromatogr A 1994, **669**:254-258.
113. Stimpson DI, Cooley PW, Knepper SM, Wallace DB: **Parallel production of oligonucleotide arrays using membranes and reagent jet printing**. Biotechniques 1998, **25**(5):886-890.
114. Luginbuhl P, Indermuhle PF, Gretillat MA, Willemin F, de Rooij NF, Gerber D, Gervasio G, Vuilleumier JL, Twerenbold D, Duggelin M et al: **Femtoliter injector for DNA mass spectrometry**. Sensor Actuat B-Chem 2000, **63**(3):167-177.
115. Jacob P, Stockhaus A, Hergenroder R, Klockow D: **Phase transfer and freezing processes investigated on acoustically levitated aqueous droplets**. Fresenius Journal of Analytical Chemistry 2001, **371**(6):726-733.
116. Rompp A, Taban IM, Mihalca R, Duursma MC, Mize TH, McDonnell LA, Heeren RMA: **Examples of Fourier transform ion cyclotron resonance mass spectrometry developments: from ion physics to remote access biochemical mass spectrometry**. European Journal of Mass Spectrometry 2005, **11**(5):443-456.
117. Heeren RMA, Kleinnijenhuis AJ, McDonnell LA, Mize TH: **A mini-review of mass spectrometry using high-performance FTICR-MS methods**. Anal Bioanal Chem 2004, **378**(4):1048-1058.
118. Schmid DG, Grosche P, Bandel H, Jung G: **FTICR-Mass spectrometry for high-resolution analysis in combinatorial chemistry**. Biotechnology and Bioengineering 2000, **71**(2):149-161.
119. Bogdanov B, Smith RD: **Proteomics by FTICR mass spectrometry: Top down and bottom up**. Mass Spectrom Rev 2005, **24**(2):168-200.
120. Hofstadler SA, Sannes-Lowery KA, Hannis JC: **Analysis of nucleic acids by FTICR MS**. Mass Spectrom Rev 2005, **24**(2):265-285.
121. Marotta E, Seraglia R, Fabris F, Traldi P: **Atmospheric pressure photoionization mechanisms - 1. The case of acetonitrile**. International Journal of Mass Spectrometry 2003, **228**(2-3):841-849.

122. Raffaelli A, Saba A: **Atmospheric pressure photoionization mass spectrometry**. Mass Spectrom Rev 2003, **22**(5):318-331.
123. Tubaro M, Marotta E, Seraglia R, Traldi P: **Atmospheric pressure photoionization mechanisms. 2. The case of benzene and toluene**. Rapid Commun Mass Sp 2003, **17**(21):2423-2429.
124. Benter T, Appel MF, Garnica RM, Schmidt S, Schindler RN: **Atmospheric pressure laser ionization mass spectrometry (APLI MS): Potential analytical applications in medical diagnostics and environmental chemistry.** Abstr Pap Am Chem S 1999, **218**:U174-U175.
125. Constapel M, Schellentrager M, Schmitz OJ, Gab S, Brockmann KJ, Giese R, Benter T: **Atmospheric-pressure laser ionization: a novel ionization method for liquid chromatography/mass spectrometry**. Rapid Commun Mass Sp 2005, **19**(3):326-336.
126. Schmidt S, Appel MF, Garnica RM, Schindler RN, Benter T: **Atmospheric pressure laser ionization. An analytical technique for highly selective detection of ultralow concentrations in the gas phase**. Anal Chem 1999, **71**(17):3721-3729.
127. Bos SJ, van Leeuwen SM, Karst U: **From fundamentals to applications: recent developments in atmospheric pressure photoionization mass spectrometry**. Anal Bioanal Chem 2006, **384**(1):85-99.
128. Koster G, Bruins A: **Mechanisms for ion formation in LC/MS by athmospheric pressure photo-ionization**. In: Proceedings of the 49th ASMS Conference on Mass Spectrometry and Allied Topics: May 27–31, 2001 2001; Chicago, IL; 2001.
129. Creaser CS, Ratcliffe L: **Atmospheric pressure matrix-assisted laser desorption/ionisation mass spectrometry: A review**. Current Analytical Chemistry 2006, **2**(1):9-15.
130. Stump MJ, Fleming RC, Gong WH, Jaber AJ, Jones JJ, Surber CW, Wilkins CL: **Matrix-assisted laser desorption mass spectrometry**. Applied Spectroscopy Reviews 2002, **37**(3):275-303.
131. Dattelbaum AM, Iyer S: **Surface-assisted laser desorption/ionization mass spectrometry**. Expert Review of Proteomics 2006, **3**(1):153-161.
132. Peterson DS: **Matrix-free methods for laser desorption/ionization mass spectrometry**. Mass Spectrom Rev 2007, **26**(1):19-34.
133. Cooks RG, Ouyang Z, Takats Z, Wiseman JM: **Ambient mass spectrometry**. Science 2006, **311**(5767):1566-1570.
134. Takats Z, Wiseman JM, Gologan B, Cooks RG: **Mass spectrometry sampling under ambient conditions with desorption electrospray ionization**. Science 2004, **306**(5695):471-473.
135. Marchand DH, Williams LA, Dolan JW, Snyder LR: **Slow equilibration of reversed-phase columns for the separation of ionized solutes**. J Chromatogr A 2003, **1015**(1-2):53-64.